Integrated expansion and cardiac differentiation of human induced pluripotent stem cells in 2D and 3D conditions

Mariana Martins Barardo dos Santos Pina

Thesis to obtain the Master of Science Degree in

Biomedical Engineering

Supervisors: Professor Tiago Paulo Gonçalves Fernandes

Professor Maria Margarida Fonseca Rodrigues Diogo

Examination Committee

Chairperson: Professor Cláudia Alexandra Martins Lobato da Silva

Supervisor: Professor Tiago Paulo Gonçalves Fernandes

Member of the Committee: Doctor Carlos André Vitorino Rodrigues

October 2017

Acknowledgments

The work developed in this thesis was only possible due to the incredible help and support of many intervenients and who I would like to thank.

Firstly, I would like to thank Professor Joaquim Sampaio Cabral for giving me the opportunity to work with the SCERG team. Also, I would like to thank my supervisors Professor Tiago Fernandes and Professor Margarida Diogo. Professor Tiago, thank you for all the availability since the beginning, for discussing results with me, for all the insight, good ideas and mostly thank you for all the patience. Professor Margarida, thank you for all the enthusiasm and good mood. I would also like to thank you, all the availability to discuss results, for presenting innovative ideas and for supporting me when things were not going so well. It was a pleasure and an honor to be orientated by both of you.

Cláudia Miranda, my “third supervisor”, I could not thank you enough all you have done for me. Thank you for all the patience, the advices, the sympathy, the knowledge shared and the good mood. You taught me pretty much everything in the laboratory, helped me with all my doubts and cheered me up when I got bad results (and it happened relatively often!). Thank you for being always there, even on weekends.

I would also like to thank Ana Rita Gomes and Teresa Silva. Ana Rita, I am very grateful for all the time you spent helping me, giving me innovative ideas and support. Thank you for all the help with the statistics and with all my thesis in general. In addition, thank you for all the friendship in all the rollercoaster of emotions that was this master thesis. Teresa, thank you so much for all the availability and help in several laboratory techniques and for being the happiest person I know, before 10 AM. Also, I would like to acknowledge Doctor Carlos Rodrigues, that helped me solve several problems in the laboratory. Ana Carina Manjua, thank you for all the support in the laboratory.

All my master colleagues, Ana Filipa, João, André and Leonor. Ana Filipa, thank you for all the support in the lab, for all the hours that you spent helping me and for all the laughs and good mood. It would not be the same without you! João and André, thank you for all the help in the lab and for all the funny moments. Leonor, thank you for being so nice since the beginning and for all the help with my doubts!

Finally, I would like to thank all my SCERG colleagues that in one way or another helped me through this months. It was awesome to be part of such a friendly and happy work group.

In addition, I would like to thank my university friends, for being always there for me, in the good and bad moments through this thesis and through the last five years. Patrícia G., Patrícia R., Maria, Catarina, Miguel, Joana, João Pedro, Gonçalo C. and Gonçalo G. you will always be my partners in crime! A special thank you for João Mário, for all the love, support and for believing in me even when I did not believe.

Lastly, I would like to thank my family, specially my parents and grandparents, that were always there for me with their unconditional support. Without all your efforts my master thesis and all my academical course would never had happened. Thank you for never let me give up on anything and for being by my side since day one!

Abstract

Pluripotent stem cells (PSC) more precisely human induced pluripotent stem cells (hiPSC) turn into reality the establishment of platforms for disease modelling, drug screening or even regenerative medicine. However, to achieve that, there is a need to establish a reliable and prone to scale up system, for their expansion and differentiation. One area of interest is the cardiovascular differentiation, due to the high morbidity and mortality associated with cardiovascular diseases (CVD). This work aimed to expand and differentiate hiPSC into cardiomyocytes using newly developed media in two culture systems, 2D as adherent culture and 3D as suspension aggregates. Cells were expanded in monolayer and as suspension aggregates being their pluripotency confirmed, after the expansion by immunocytochemistry, embryoid bodies formation and flow cytometry. After expansion, the percentage of OCT4 obtained was up to 99.6%, in 2D and up to 97.6%, in 3D. hiPSC were differentiated through the temporal modulation of the canonical Wnt signaling pathway for 12 days. The cells differentiated in 2D started to demonstrate spontaneous contraction at day 8 and in 3D at day 7 of differentiation. The expression of the pluripotency marker (Nanog) gradually decreased over time, while the expression of the cardiac marker (TNNT2) gradually increased. Flow cytometry analysis performed at day 12 revealed up to 42.2% cTnT positive cardiomyocytes in 2D and up to 78.2% in the differentiation performed in 3D. Despite being necessary further optimization, the results suggest that the protocol could be used to the expansion of hiPSC and posterior differentiation into cardiomyocytes.

Keywords: Human induced pluripotent stem cells, expansion, cardiac differentiation, cardiomyocytes

Resumo

As células estaminais pluripotentes, mais concretamente as células estaminais humanas pluripotentes induzidas (hiPSC) podem ser usadas para a criação de plataformas para modular doenças, testar fármacos ou até para medicina regenerativa. Todavia para ser possível alcançar estas aplicações é imperativo estabelecer um sistema fidedigno para a expansão e a diferenciação de hiPSC. Uma área de interesse é a da diferenciação cardiovascular, devido à grande taxa de morbilidade e mortalidade associada às doenças cardiovasculares. O objetivo deste trabalho foi a expansão e diferenciação de hiPSC em cardiomiócitos, em 2D (sob forma de monocamada) e 3D (através de agregados em suspensão), usando novos meios de cultura e de diferenciação. Posteriormente à expansão, obteve-se um valor máximo de 99.6% de OCT4, em 2D e de 97.6%, em 3D. hiPSC foram diferenciadas em cardiomiócitos através da modulação temporal da via de sinalização Wnt canónica. As células diferenciadas em monocamada demonstraram contração espontânea a partir do dia 8 e as células diferenciadas em agregados a partir do dia 7 de diferenciação, A expressão de um marcador de pluripotência (Nanog) diminuiu progressivamente ao longo do tempo, enquanto que a do marcador cardíaco (TNNT2) aumentou. As análises de citometria de fluxo, realizadas no dia 12 de diferenciação revelaram um máximo de 42.2% de cTnT para a diferenciação em monocamada e 78.2% para a diferenciação em agregados. Apesar de ser necessário aplicar algumas otimizações ao protocolo, os resultados obtidos sugerem que este pode ser utilizado para a expansão e posterior diferenciação de hiPSC em cardiomiócitos.

Palavras chave: células estaminais pluripotentes induzidas, expansão, diferenciação cardíaca, cardiomiócitos

List of Contents

List of figures

List of Tables

List of Acronyms

2D	Two-dimensional
3D	Three- dimensional
APC	Adenomatous polyposis coli gene
ATP	Adenosine triphosphate
BSA	Bovine serum albumine
BMP	Bone morphogenetic protein
CHIR	CHIR99021
CHD	Coronary heart disease
CK	Casein kinase
Cv	Coefficient of variation
CMM	Cardiomyocyte maintenance medium
cTnT	Cardiac troponin T
CVD	Cardiovascular diseases
CVPC	Cardiovascular progenitor cells
DMEM	Dulbeccos's Modified Eagle Medium
DMSO	Dimethylsulfoxide
DNA	Deoxyribonucleic acid
EB	Embryoid bodies
EDTA	Ethylenediamine tetraacetic acid
ESC	Embryonic stem cells
ESC-CM	Embryonic stem cells derived cardiomyocytes
ECM	Extracellular matrix
FACS	Fluorescence-activated cell sorting
FBS	Fetal bovine serum
FCB	Flow cytometry buffer
FHF	First heart field
FGF	Fibroblast growth factor
FLK	Fetal liver kinase
GSK	Glycogen synthase kinase
HCN 4	Hyperpolarization-activated cyclic nucleotide-gated channel
hESC	Human embryonic stem cells
hESC-CM	Human embryonic stem cell derived cardiomyocytes
hiPSC	Human induced pluripotent stem cells
hiPSC-CM	Human induced pluripotent stem cells derived cardiomyocytes
hPSC-CM	Human pluripotent stem cell derived cardiomyocytes
hPSC	Human pluripotent stem cells

ICD	Implanted cardioverter defibrillator
ICM	Inner cell mass
ISL	LIM-homebox transcription factor islet
iPSC	Induced pluripotent stem cells
iPSC-CM	Induced pluripotent stem cells derived cardiomyocytes
IWP	Inhibitor of Wnt production
KDR	Kinase insert domain
KLF	Kruppel-like factor
LA	Left atrium
LPR	Low-density lipoprotein receptor-related protein
LV	Left ventricle
MACS	Magnetic-activated cell sorting
MEF	Mouse embryonic fibroblasts
MEF2C	Myocyte enhancer factor 2 C
MEM-NEAA	Minimum essential medium non-essential amino acids
MESP	Mesoderm Posterior transcription factor
MI	Myocardial infarction
miRNA	Micro ribonucleic acid
MLC	Myosin light chain
$NaHCO_3$	Sodium bicarbonate
NGS	Normal goat serum
RNA	Ribonucleic acid
RPMI	Roswell Park Memorial Institute
OCT	Octamer-binding transcription factor
PSC	Pluripotent stem cells
PSC-CM	Pluripotent stem cells derived cardiomyocytes
PFA	Paraformaldehyde
PBS	Phosphate-Buffered Saline
qRT-PCR	Quantitative real-time polymerase chain reaction
RA	Right atrium
ROCK	Rho-associated protein kinase
RV	Right ventricle
SEM	Standard error of the mean
SHF	Second heart field
SIRPA	Signal-regulatory protein
Sox	Sex determining region Y-box
SSEA	Stage specific embryonic antigen
TCLab	Tecnologias Celulares para Aplicação Médica
TCF/LEF	T cell factor/lymphoid enhancer factor
TNNT	Troponin T

TGF	Transforming growth factor
TRA	Tumour rejection antigen
VCAM	Vascular cell adhesion molecule
VEGF	Vascular endothelial growth factor
VEGFR	Vascular endothelial growth factor receptor
Wnt	Wingless-type mouse mammary tumor virus integration site

1 Introduction

1.1 Stem Cells

1.1.1 General concepts

Stem cells are a widely discussed topic in biology that draws attention from researchers and general public, as well. The spotlight in this topic is due to all their possible usage that can go from drug screening to regenerative medicine. The term “stem cell” first appeared in the scientific literature in the 19th century, namely in the work of Ernst Haeckel [1]. Firstly, Haeckel used the term stem cell to describe the unicellular ancestor from which all the multicellular organisms evolved. Nevertheless, the official discovery of stem cells only took place in the 20th century (1963), when Becker et all discovered hematopoietic stem cells in mice bone marrow [2].

Currently, stem cells are functionally defined as cells that have the capacity to self-renew (can be divided and maintain the undifferentiated state) and to differentiate originating specialized cells [3]. Stem cells gradually differentiate into more specialized cells losing their differentiation potential (**Figure 1.1**). Consequently, stem cells are classified according to their differentiation potential as: totipotent, pluripotent, multipotent and unipotent. Totipotent stem cells can generate a complete organism (e.g. a fertilized egg) [3]. Pluripotent stem cells (PSC) can generate cells from the three embryonic germ layers (endoderm, mesoderm and ectoderm), but do not have the potential to generate the extraembryonic tissue [1, 3, 4]. Multipotent stem cells are adult or neonatal stem cells and originate a limited number of cell types, being tissue-specific (e.g. mesenchymal stem cells, that can differentiate into cells with mesodermal origin, such as chondrocytes and adipocytes) [1, 3, 4]. Finally, unipotent stem cells only have the capacity to differentiate along one lineage [1, 4].

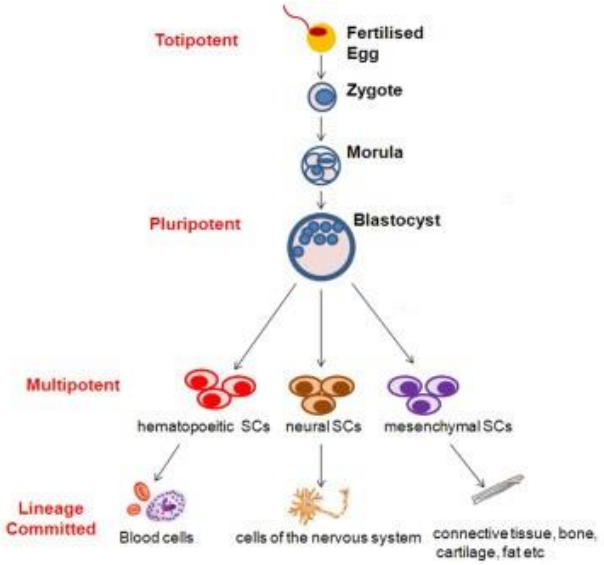

Figure 1.1 Stem cell differentiation potential. Stem Cells gradually differentiate in more specialized cells. The fertilised egg is totipotent and can originate a complete organism. Pluripotent stem cells can generate the three germ layers. Multipotent have a restricted ability to differentiate, being tissue specific. *Adapted from reference [4]*

Moreover, cells can be classified accordingly to their tissue of origin as: embryonic, fetal, neonatal and adult stem cells. Embryonic stem cells (ESC) have origin in one of the first stages of the embryonic development, namely the blastocyst. Fetal Stem Cells can be isolated from fetal blood, bone marrow and other fetal tissues. Also, neonatal stem cells can be isolated from the umbilical cord blood and from Wharton's jelly substance within the umbilical cord. On the other hand, the adult stem cells are derived from a differentiated tissue and have the potential to differentiate in all the cellular subtypes of the tissue from where they were isolated [3, 5-7].

1.1.2 Human Pluripotent Stem Cells

As previously mentioned, pluripotent stem cells have the capacity to self-renew and the potential to differentiate in the three germ layers (endoderm, mesoderm and ectoderm). PSC and consequently, human pluripotent stem cells (hPSC) are derived from several sources from which I will highlight: embryonic tissues (typically derived from the inner cell mass of pre-implantation embryos) or can be induced due to the reprogramming of differentiated cells [8, 9].

1.1.2.1 Human Embryonic Stem Cells

The first ESC were described in 1981, when were isolated from the murine inner cell mass of the developing blastocyst by Martin Evans and co-workers [10] and Gail Martin [11]. Since that date, ESC had been widely studied and in 1998, a team lead by James Thomson and Jeffrey Jones, obtained, for the first time, human embryonic stem cells (hESC) [12].

These cells have the capacity to differentiate into the three germ layers (ectoderm, mesoderm and endoderm) and consequently in all the different cells of the human body. This characteristic made them perfect to study the mechanisms underlying lineage commitment and made tissue engineering and regenerative medicine a faraway, but a real future possibility. The initial hESC lines were derived from "spare" embryos produced by *in vitro* fertilization. However, the generation of hESC has awaken some

ethical issues, since would imply the use of human embryos for scientific research, making their use very restricted and non-consensual [1, 13].

For hESC the gold standard to test pluripotency consists in the demonstration that the cells can form teratomas, *in vivo*, when implanted in immunodeficient mice. Additionally, other pluripotency assays could be performed, namely *in vitro*, using some differentiation protocols. Also, the pluripotency of these cells can be assessed through the expression of some pluripotency markers. hPSC express the intracellular markers: Oct-3/4 (octamer-binding transcription factor), Sox 2 (Sex determining region Y-box 2) and Nanog. Likewise, the surface markers Stage Specific Embryonic Antigen (SSEA3 and SSEA4) and tumour rejection antigens (TRA): Tra-1-60 and Tra-1-8 should also be expressed by these cells [1, 14, 15].

1.1.2.2 Human Induced Pluripotent Stem Cells

In 2006, Takahashi and Yamanaka made one of the most promising discoveries of the century by successfully obtaining PSC from mouse embryonic and adult fibroblasts [16]. The induction of PSC was accomplished by means of retroviral insertion of four transcription factors: Oct3/4, Sox2, c-Myc and Kruppel-like factor 4 (KLF4). One year later, the same team obtained PSC from human adult fibroblasts [9]. Also, in 2007, another group of researchers have reported the induction of PSC from human somatic cells using different transcription factors (Oct3/4, Sox2, Nanog and Lin28) and lentiviruses [17]. The capacity to produce PSC from the reprogramming of differentiated cells was a breakthrough that opened, once again, the road through regenerative medicine, drug screening and personalized medicine. Besides being obtained from fibroblasts, induced pluripotent stem cells (iPSC) were induced from other types of differentiated cells such as neural, stomach and liver cells [5]. The general process of obtaining iPSC is represented in **Figure 1.2**.

Researchers were thrilled with the fact that iPSC had all the key characteristics of ESC, namely the expression of the same pluripotency markers (SSEA-3, SSEA-4, TRA-1-60 and TRA-1-81), the formation of teratomas *in vivo* and the same morphology [5, 18]. Besides, hiPSC do not have associated the two major problems of hESC: most of the ethical issues and the possible immune rejection from the host after transplantation [5, 18]. However, after 2009 some researchers work suggested that there are some differences between iPSC and ESC, specifically in the DNA methylation or gene expression, mentioning that the cells retained gene expression from donor cells, as well [19-21]. On the other hand, some researchers remain to conclude that is very difficult to distinguish ESC and iPSC due to different gene expression or DNA methylation, arguing that the differences, or at least some part of them, are due to different culture conditions, different methods of passaging, different operator-specific procedures and different reprogramming methods [22, 23].

Initially the reprogramming was achieved by using retroviruses or lentiviruses. However, the use of these viruses might cause insertional mutagenesis, which raises concerns regarding the use of the reprogrammed cells in cellular therapy. Therefore, many techniques that did not involve vector integration into the host genome had emerged through the years. These techniques comprised: adenovirus, Sendai virus, synthesized proteins and RNAs, transposon PiggyBac, minicircle vectors,

episomal plasmids and small molecules [24]. Despite the development of so many different reprogramming methods none of them combines the perfect characteristics: absence of footprint (meaning that the reprogramming method does not lead to genome alterations of the cells), robustness across different types of cells, a good efficiency and not being excessively time-consuming [24, 25].

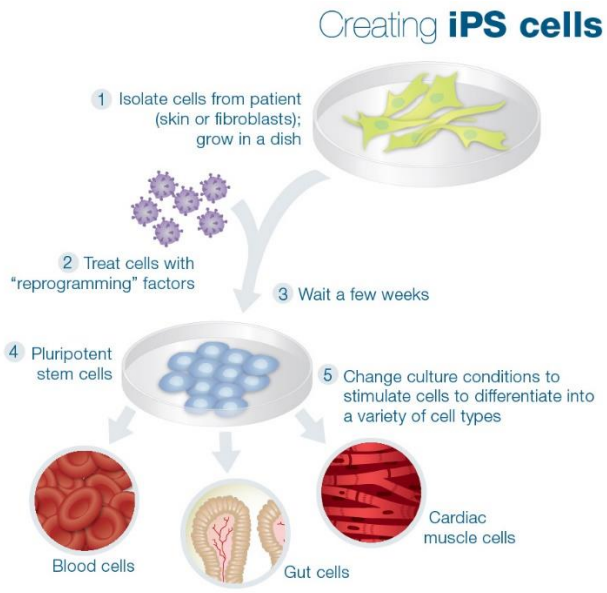

Figure 1.2 General process of generation of patient-specific hiPSC. Firstly, somatic cells are isolated from a patient. Afterwards, the cells are treated with "reprogramming factors" that can be "delivered" using different approaches. iPSC are created and can be differentiated into any desired cell type. *Adapted from: http://learn.genetics.utah.edu/content/stemcells/quickref/*

1.1.3 Culture platforms for human pluripotent stem cells

When expanding hPSC in culture, there are essentially two requirements that need to be assured: their pluripotency and their proliferative potential. So, throughout the years, protocols were developed with the silver lining of establishing a robust, scalable, chemically-defined, xeno-free protocol for expansion of these cells, in order to turn possible their use for regenerative medicine, drug development or disease modelling. Regarding the expansion of hPSC *in vitro* the cells can be produced by traditional 2D culture as adherent colonies or can be produced as suspension aggregates in 3D culture.

In the case of 2D culture, pluripotent stem cells are cultured as a monolayer on the top of an adhesion substrate. Initially, it was used as feeder layer mouse embryonic fibroblasts (MEF), providing a source of extracellular matrix (ECM) molecules and soluble signaling molecules [12]. However, the use of non-human feeder layers was not desirable, since it represented a source of pathogens for hPSC and due to the inconsistency of factors secreted by MEF [26, 27]. This leaded to research of new substrates and molecules for hPSC expansion. In 2001, was first reported the culture of hESC on Matrigel using feeder-free conditions [28]. Matrigel is a complex mixture harvested from Engelberth-Holm-Swarm mouse sarcoma cells and is mainly composed by laminin, collagen IV, heparin sulphate proteoglycans, entactin/nidogen and growth factors [29]. Matrigel is widely used *in vitro* but there are several possible adhesion substrates using human recombinant proteins, such as human recombinant vitronectin [30] and human recombinant Laminin [31]. Also, it was already developed biological and synthetic polymeric

substrates for hiPSC culture, such as Synthemax ® [32] and StemAdhere ® [33]. Since these growth substrates are defined, synthetic and xeno-free, the combination of these characteristics with the usage of chemically defined medium represents an important step in the production of clinically compliant culture systems for hPSC culture. Conversely, Matrigel is prone to batch-to-batch variability and can lead to xenogeneic contaminations. However, these new substrates are very expansive, leading to cost and scalability issues [26, 27]. Concerning the cell passaging, initially cells were detached and individualized using enzymes, such as Accutase. However, it was always required the usage of small chemicals, such as Rho-associated protein kinase (ROCK) inhibitors, to improve the survival rate. The ROCK pathway is responsible for the cellular apoptosis, when the cells are individualized, being used inhibitors of this pathway to avoid the cellular apoptosis induced by the single cell state, since hPSC survival relies on cell-cell and cell-matrix interaction [34, 35]. Y-2763 and Thiazovivin are examples of ROCK inhibitors molecules [34]. Also, the success of enzymatic methods was affected by the enzyme quality that varies from batch-to-batch. Nowadays, the most used protocol is enzymatic-free and relies on the usage of EDTA (ethylenediamine tetraacetic acid) that achieves high cell survival rates. EDTA binds with ions, such as calcium and magnesium, removing them from the medium. Without these divalent cations the integrin-ligand binding is inhibited and since integrins are responsible for cell-to-cell and cell-to-matrix interactions, without calcium and magnesium occurs the cellular detachment from the surface [36, 37]. The monolayer culture has the advantage that all the cells in culture receive the same amount of nutrients and signalling molecules. During the expansion process dead cells are easily removed, since they detach the surface and are removed upon medium change. However, the 2D culture does not accurately mimics the 3D environment of cells, misleading data for *in vivo* responses. Besides, cells are morphologically different from cells *in vivo* and the production of a large quantity of hPSC in monolayer is very restricted due to the low surface-to-volume ratio [38].

In the case of 3D culture, the hESC and hiPSC are expanded as aggregates that can be in a certain type of scaffold/matrix or floating as scaffold-free aggregates [39]. The aggregates for 3D cultured can be formed by several techniques, such as: hanging drop, suspension culture with random aggregation and microwells [39]. The hanging drop method allows the reliable generation of uniform aggregates when used at small scale. The suspension culture method is very simple and allows the creation of a large number of aggregates, but usually the aggregates present a heterogeneity in size and also in shape [39]. Finally, the aggregates formation in microwells allows the production of large quantities of homogenous aggregates, despite of being relatively costly [39]. To overcome the fact of being costly, it had already been developed protocols to produce “homemade” agarose microwells through soft lithography processes [40]. In this alternative it is used reusable silicon masters to produce the agarose microwells, being only needed to buy one commercially available microwell plate to design the masters [40]. The 3D culture sustains many advantages: cells grow in a 3D environment, allowing cells to interact with each other and with the surrounding environment, representing a robust and, scalable way to obtain large amounts of hPSC. Suspension cultures make possible the regular sampling, allowing a close monitoring of cell number counts, and aggregates proprieties leading to a well-monitored and reproducible process [38, 41]. Also, their morphology resembles the one that can be found *in vivo,* and it is possible to develop the progressive scale-up of the culture. On the other hand, the main

disadvantage leads with different transfer rates of oxygen, nutrients and growth factors through the aggregates. In consequence of that, outer layers are proliferative while the inner layers are quiescent and hypoxic [38]. The first attempts to culture hPSC in suspension culture have used coated microcarriers [42]. In the first studies, the specific coating used was Matrigel, that allowed the growth of anchorage dependent cells. Through the years were developed several types of microcarriers with different coatings with successful results. Nowadays are already developed sterile microcarriers specialized with synthetic polymeric substrates (e.g. Synthemax II) that allow the cellular culture in xeno-free conditions [42, 43]. However, this kind of system usually implies the seeding and harvesting of the cells from the microcarriers, which in some cases is not especially prone to scale-up [44]. Since 2010, the expansion of hPSC as floating aggregates have been researched by several groups, that establish similar and highly reproducible cultures systems for several hESC and hiPSC lines. In these 3D cultures, the medium is always supplemented with a ROCK inhibitor molecule through the aggregation process (first 24-48 hours), to avoid the cellular death when in single cell state [42, 45-47]. The 3D culture systems can be static (e.g. in ultra-low-attachment plates) or dynamic (e.g. spinner flasks). Comparing the static culture with the dynamic, in dynamic it is possible to form aggregates with smaller diameters and with lower heterogeneity regarding their size. Also, dynamic culture ensures the environmental homogeneity, improves the mass transfer of gases/nutrients into the cells and allows a straightforward culture scaling up [46, 48, 49].

1.1.4 Human Stem Cells applications

As briefly mentioned before, stem cells have a myriad of potential applications, such as: drug screening, disease modelling, cellular therapy and tissue engineering.

Possible applications of stem cells are cellular therapy and tissue engineering, to repair damaged tissues. In the case of cellular therapy, the cells could be transplanted into the damaged tissue and help to recover the injury. For example, mesenchymal stem cells (MSC) appear to deliver some paracrine trophic factors into the damaged heart that helps the infarcted heart muscle recovery [50]. On the case of tissue engineering, cells are differentiated into the cells of the damaged tissue, *in vivo* or *in vitro* before being transplanted. Bone marrow stromal cells due their capacity to differentiate into cells of mesodermal origin, have been used in the field of tissue engineering, for reconstructing damaged tissues, such as bone and cartilage [51].

Despite the cells that were already used in the previous mentioned applications not being pluripotent, it has been developed several studies to evaluate the possibility of using PSC derivatives for a number of applications. With the silver lining of disease modelling and drug screening, several groups of researchers and of pharmacological industry have been creating banks of healthy and genetically defective embryos (identified in pre-implantation tests) [52]. Although, hESC are not the most indicate cells for disease modelling, since the usage of these cells generates a considerable ethical debate and, also, a few single gene disorders are represented in the ESC lines of defective embryos [52]. On the other side, the somatic cells of a patient suffering from a specific disease can be reprogrammed into hiPSC and then differentiated in somatic cells that are affected by the disease. These cells have the disease phenotype and can be studied, in order to unveil the cellular mechanisms behind the disease.

There were already been modulated some diseases, such as: Leopard syndrome [53], Rett syndrome [54] and long QT syndrome [55]. Also, it is possible to perform the drug screening of new pharmacological compounds, being the indicated platform to assess efficacy and toxicology of new drugs. This is very important, since many of the drugs withdrawals are due to toxicity problems and the majority of drug attrition occurs in the late stages of the drug development, when great investment was already made [56]. Some researchers, already worked on the development of *in vitro* models that used differentiated cells from hiPSC that could be later used to perform toxicity assays. For example, Beauchamp and co-workers had developed a cardiac microtissue that demonstrate long term functionality and respond to pharmacological, electrical and physical stimuli [56]. Besides, this platform allows performing drug screening tests to develop personalized medicine, using patient cells to test several drugs with different dosages, in order to discover which one is the most suitable drug for treating a certain patient [5, 18, 52]. Finally, there are several clinical trials using hPSC. Most of the clinical trials use hESC and only one is being performed with cells derived from hiPSC. One possible explanation to this fact is that the discovery of hESC was a decade before hiPSC, therefore hESC are better characterized. At the same time, the possible epigenetic memory of the cells and the teratoma formation are reasons of concern. The clinical trial with hiPSC, uses derived retinal pigment epithelium (RPE) cells, derived from hiPSC, in order to treat macular degeneration [57, 58].

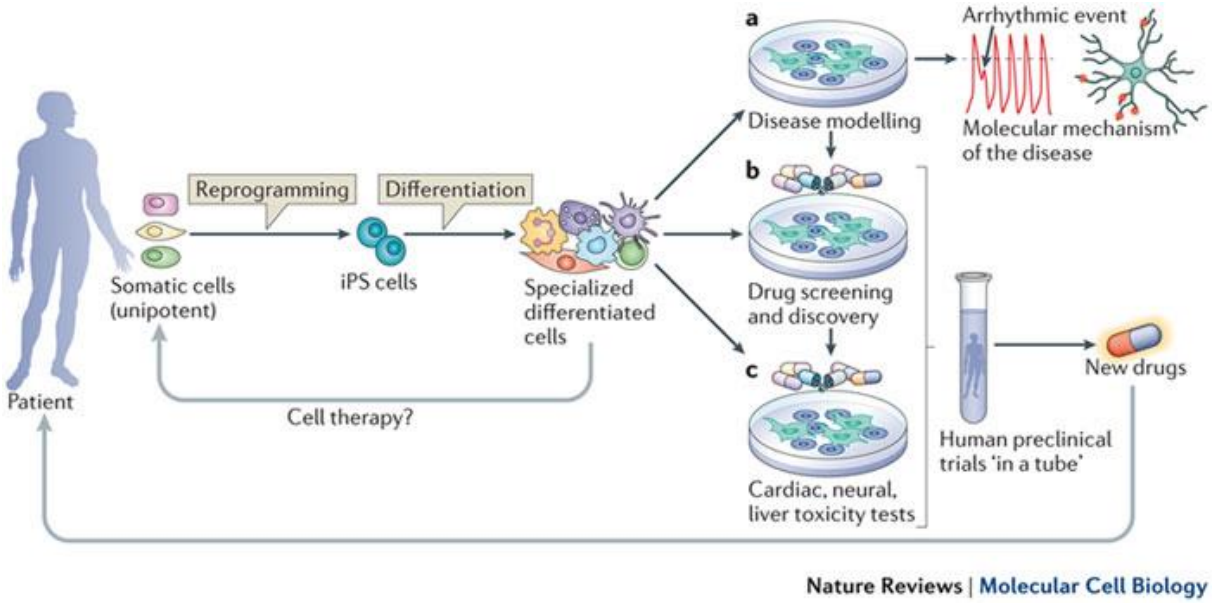

Figure 1.3 Applications of hiPSC. hiPSC are induced from human somatic cells. After *in vitro* induction, hiPSC can be differentiated in specialized cells that have several applications. **A** hiPSC can be used for disease modelling in order to understand the mechanisms that lead to disease phenotypes, such as cardiac arrhythmia or defects in neurons. **B** hiPSC can also be used in drug screening and discovery, being possible to access the effects of new compounds and drugs and at the same time, to identify some target pathways. **C** hiPSC can be used for toxicity tests. **B and C** together represent human preclinical trials "in a tube". *Adapted from reference [59]*

1.2 The human heart

The heart is the first organ to be fully formed and functional during the embryonic development [60]. It is developed from the mesoderm germ layer and is composed by different types of cells: cardiomyocytes, smooth muscle cells, endothelial cells and fibroblasts [61]. This organ is a muscular pump, that integrates the cardiovascular system, and has two major functions: collect blood from the different tissues in the body and pump it to the lungs (in which CO_2 will be exchanged for O_2) and collect blood from the lungs and pump it to all tissues in the body (to oxygenate them) [62]. It is important to mention, that in the blood not only circulates O_2 and CO_2, but also nutrients, hormones and waste, such as salts and excess water [62]. The human heart is divided in four chambers, two upper chambers called atria and two lower chambers called ventricles [62]. The atria function primarily as collecting chambers and the ventricles function to pump blood [62]. On one hand, the right atrium and ventricle collect blood from the body tissues and pump it to the lungs [62]. On the other hand, the left atrium and ventricle receive the blood from the lungs and distributes throughout the body [62]. It is important to note, that blood circulates unidirectionally through the heart due to the presence of four valves: tricuspid, bicuspid, pulmonary and aortic [62].

1.2.1 Development of the heart *in vivo*

In the last two decades, several studies tried to unveil the processes that lead to the heart formation. Much of the knowledge concerning the cardiac development is based on mammalian models (e.g. mouse), because of ethical and technical problems of any form of study in the human fetus. Despite the existence of some differences between mouse and humans in the heart formation (e.g. contrasting times for occurring the same stages of development – the human heart starts to beat at day 22 after fertilization, but the mouse heart starts at day 9) it is considered that mouse models represent with relatively accuracy the human cardiac development [61, 63].

First of all, after the egg fertilization, several cellular divisions occur, and the differentiation process starts, creating a structure called blastocyst [64-66]. This structure comprises a cavity filled with blastocel and an inner cell mass (ICM) that is surrounded by trophectoderm [64]. Afterwards, the blastocyst is implanted in the uterus and the ICM becomes divided into epiblast and hypoblast (primitive endoderm) [64-66]. The trophectoderm and the hypoblast will produce non-embryonic tissues, such as the placenta [64-66]. After that, the epiblast undergoes a differentiation process called gastrulation, in which the primitive streak (transient structure consisting in an epiblast derived cell mass) will induce the epithelial to mesenchymal transition (EMT), being firstly formed the definitive endoderm with cells from the hypoblast, after that is formed the mesoderm, using cells from de epiblast. Lastly, the remaining cells in the epiblast give origin to the ectoderm [64-66].

The heart induction from mesoderm is a result of interactions of inductive and inhibitory signals from the adjacent endoderm and ectoderm. These signals include: wingless-type mouse mammary tumor virus integration site (Wnt), fibroblast growth factor (FGF) and transforming growth factor β (TGF – β) signaling pathways that lead to the activation of early cardiomyocyte transcriptional programs [67, 68].

One of the first mesodermal transcription factor is T (Brachyury) and it induces cells from the primitive streak to express MESP1 (Mesoderm Posterior transcription factor 1) [61]. These cells migrate to the anterior lateral site of the embryo (where the heart will be located) and generate the two sources of mesoderm cardiac progenitors: the first heart field (FHF) and the second heart field (SHF) [61]. These cells provide different regional contributions to the heart in development. The FHF cells will form a crescent shape (cardiac crescent) and eventually will adhere along the ventral midline to form a primitive heart tube, consisting of an inner layer of endocardial cells and an outer layer of myocardial cells [61, 67, 69, 70]. The two layers communicate through the extracellular matrix between them [69]. Afterwards, the SHF cells migrate to the primitive heart tube in order to build the four cardiac chambers [61, 67, 69, 70]. The SHF cells remain in undifferentiated state until they incorporate the heart [61]. The FHF are mostly responsible for the construction of the left ventricle and the SHF are the mainly responsible for the construction of the right ventricle, outflow tract and atria [61, 67, 69, 70]. The heart also receives important contributions from two additional sources: the cardiac neural crest cells and the proepicardium [69, 70]. The cardiac neural crest cells contribute to the development of the outflow tract and great vessels, being essential to the cardiac autonomic nervous system, as well [70]. Proepicardial cells give rise to the epicardium, contribute to the development of the coronary smooth muscle and to the surrounding cardiac fibroblasts [70]. It also has been shown that that the epicardium is a source of cardiomyocytes [70]. This organ is fully formed at embryonic day 14.5, in mice, and day at 50 in humans [61]. The heart development is represented in **Figure 1.4**.

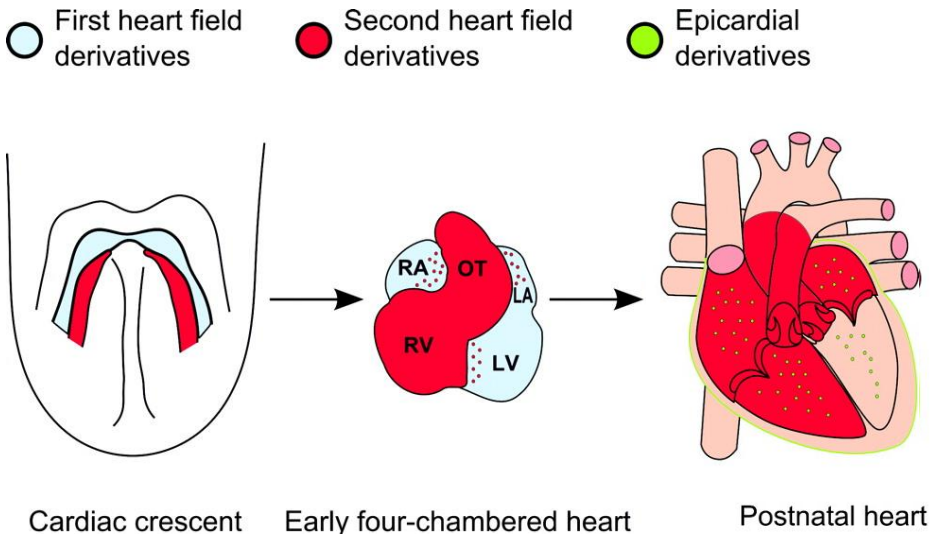

Figure 1.4 The embryological mammalian heart development. The heart initially if formed by a cardiac crescent shape **(left)**, a structure that is derived from FHF cardiogenic precursors, represented in **blue**. The cells from the cardiac crescent begin to adhere along the ventral midline to form a primitive heart tube, which originates the primitive chambers of the mammalian heart (**middle**). At this time, precursor cells that form the SHF migrate to the developing heart, represented in **red**. Finally, in the postnatal heart (**right**) progenitors from the FHF contribute primarily to the left ventricle (LV). SHF derivatives contribute mainly to the right ventricle (RV), to the atria (left atrium – LA and right atrium – RA) and outflow tract (OT). Epicardial progenitors (**green**) also contribute to a very diminish portion of cardiomyocytes. *Adapted from reference [70].*

1.2.2 Cardiovascular diseases and most used therapies

Cardiovascular diseases (CVD) are the leading cause of death worldwide accounting for more than 17.3 million deaths per year [71]. Besides that, it is expected that in 2030 CVD will be responsible for more than 24.6 million deaths [71]. In the United States of America, Coronary heart disease (CHD) is the leading cause of deaths, followed by stroke, heart failure, high blood pressure, diseases of the arteries and others CVD. CHD includes stable and unstable angina, myocardial infarction (MI) and sudden cardiac death [18, 61, 71-73].

In some CVD, patients are prescribed with drugs, that can have different goals: slow the cardiac rate, prevent arrhythmias or prevent and destroy blood clots. However, in many cases, the therapy based on drugs in not enough [74]. For example, when an artery near the heart is obstructed and the patient's life is at risk, it is performed a bypass surgery (to supply blood to the cardiac tissue) or is performed surgery to implant a balloon or a stent [75]. These surgeries help to reduce mortality and morbidity rates [74, 75].

Because of CHD, the blood circulation is compromised and in some cases the cardiomyocytes do not receive the necessary amount of O_2 for their correct function. MI occurs when heart muscle cells die due to the lack of O_2. After the necrosis of the cardiomyocytes and a long inflammatory phase, the ischemic zone is replaced by non-contractile fibrotic tissue. Afterwards, the heart can become unable to supply blood for the body resulting in heart failure and, ultimately in dead [72, 76, 77].

When a MI occurs, the endogenous cardiac stem cells are not sufficient to repair the damaged heart [78]. Sometimes after the MI, patients suffer from life threatening ventricular arrhythmias. In one of the current therapies, patients receive a pacemaker or an implanted cardioverter defibrillator (ICD). A pacemaker delivers electrical pulses to prompt the synchronized cardiac beating. A ICD monitors the heart rhythms and if senses life-threating rhythms, delivers shocks to the heart. Currently, the majority of ICD acts as pacemakers and defibrillators at the same time. These therapies have been extensively evaluated and clinical trials demonstrate that they improve the survival rate of patients after MI and are also therapies used in patients with abnormal heart rates, non-caused by MI [78].

Other devices have been developed to overcome heart failure (due to MI or other CVD) for mechanical circulatory support for the failing ventricle. These biomedical devices rely on pulsatile, volume displacements left ventricular assist device, and deliver a stroke volume analogous to ventricular systole. These devices have an average life expectancy of 15 to 24 months [79, 80].

Despite the advances in medical and device therapy for heart failure, in cases of end-stage, the more viable solution is heart transplantation [77, 79, 80]. However, the transplantation is limited by donor availability, many patients are not even eligible and the patient has an average survival of 10 years [79]. After transplantation, patients need to take immunosuppressive drugs in order to avoid immune rejection [77, 79, 80]. This is very important, because immune rejection is the number one cause of death in the first year after cardiac transplantation [80]. Long term survival following cardiac transplantation appears to be limited, primarily because of transplant vasculopathy and side effects related to the long term immunosuppressive therapy [77, 79, 80].

1.2.3 Cardiovascular progenitor cells

Progenitor cells are conventionally distinguished from stem cells by their limited differentiation potential and ability to replicate (*in vivo* or *in vitro*). Cardiovascular progenitor cells (CVPC) have their origin in mesoderm and can differentiate into cardiac cells culminating into fully differentiated cardiomyocytes [81]. CVPC can be obtained in two separate ways: derived *in vitro* from hPSC (hESC and hiPSC) or isolated from cardiac tissue collected at the different stages of development of the heart [81].

For decades, it was thought that the heart was a terminally differentiated organ without regenerative capacity [67]. The discovery of endogenous cardiac progenitor cells has changed the mindset and opened horizons in the field [67, 68, 81]. Although, studies show that in the human heart a minimal quantity of cardiomyocytes are replaced (<1% per year) during an entire life span and the rate of replacement declines with age [67, 77]. It is important to note that the CVPC are not identified with very specific markers, since some these markers can be used for a relatively vast group of cells [67, 68, 81].

A commonly primordial cardiovascular progenitor, already mentioned in section **1.2.1 Development of the heart in vivo**, is characterized by the expression of the transcription factor T (brachyury), that has been shown to be critical for the mesoderm formation [67]. This progenitor gives rise to FHF and SHF progenitors, as well [67].

Cells expressing the stem cell factor c-Kit, at least at the neonatal stage encompasses a population with some evidence of cardiomyogenic potential [67, 68, 82]. C-Kit$^+$ are indicated as contributors to the developing myocardium of the heart and some researches indicate that they exist in the adult heart, in diminished quantities [81]. *In vitro*, c-Kit$^+$ differentiate into cells that are biochemically similar to mature cardiomyocytes, although functionally different, rarely demonstrating spontaneous beating [81]. The assumption of c-Kit$^+$ as CVPC is controversial, not being largely accepted in the scientific community [67, 68, 82].

Also, vascular endothelial growth factor 2 (VEGFR 2), that results from the expression of kinase insert domain (KDR), in humans, and fetal liver kinase (FLK 1), in mice, together with T, makes it possible to identify cells that generate colonies capable to differentiate in cardiomyocytes, endothelial cells and smooth muscle cells [67, 83].

Other marker, MESP1, may identify an initially progenitor population that precedes the separations between FHF and SHF [67]. Cells expressing MESP1 contribute broadly to all cell types in the heart and this factor seems to be relevant for the posterior activation of other cardiogenic transcription factors: NKX2.5, GATA-binding protein 4 (GATA4), myocyte enhancer factor 2 C (MEF2C) and Islet 1 (ISL1) [67, 84].

Recently, a specific FHF marker was identified: hyperpolarization-activated cyclic nucleotide-gated channel 4 (HCN4) that marks the voltage-gated ion channel [67, 85]. This channel is a marker of the conduction system and appears to be specific mainly for cells that will form the cardiac cavities [67, 85].

ISL1 was identified as a SHF marker, since ISL1$^+$ cells were found in SHF derived structures [67]. However, ISL1 protein was detected already in the crescent shape stage of the cardiac development,

implying that ISL1 is expressed in FHF in an early stage [67]. ISL1 expression possibly identifies a progenitor state that originates myocardial cells, vascular endothelial cells and the conduction system [84, 86]. $ISL1^{+}$ cells are detectable in human neonates, but this marker is absent in adult hearts [84].

Other transcription factor expressed in CVPC is NKX2.5. NKX2.5 is extremely important for the growth of ventricular cardiomyocytes and characterizes FHF^{-} and SHF^{-} commitment to the cardiomyogenic fate [81]. The expression of NKX2.5 is so important, that NKX2.5 deficient mice develop an abnormal heart with reduced expression of many myocardial genes [81].

Already differentiated cardiomyocytes are recognized by cTnT (cardiac troponin T) [87]. Troponin T 2 (TNNT 2) is the gene that encodes cTnT and it is specific for cardiomyocytes [87].

1.3 Cardiac induction from hPSC

1.3.1 Differentiation of hPSC into cardiomyocytes

After the first derivation of PSC, several researchers tried to develop protocols for the differentiation of PSC into numerous cellular types, such as neurons or cardiomyocytes. The differentiation of PSC into cardiomyocytes has been particularly explored and several protocols have been described, with different approaches and consequent reliability and efficiency.

The three major approaches for the differentiation of hPCS into cardiomyocytes are: aggregates/Embryoid bodies (EB), monolayer culture and inductive co-culture [68].

Initially, after the derivation of hESC, scientists tried to differentiate these cells into cardiomyocytes through EB/aggregates formation [68]. Aggregates are spheroids of cells that can differentiate into derivatives of the three germ layers and these structures were firstly formed with non-human cells. Initially, the cells were expanded in monolayer, using MEF, Matrigel or other adhesion substrates. Afterwards the cells were dissociated and aggregated typically in hanging drops [68]. The first successful differentiation of hESC into cardiomyocytes used collagenase IV to separate hESC colonies, (H9 line) into small clumps that were later grown in suspension in non-adherent petri dishes [88]. Later, the EB were plated and beating areas were observed after 4 days [88]. The differentiation medium used was Dulbeccos's Modified Eagle Medium (DMEM)/F12 supplemented with fetal bovine serum (FBS). The colonies were separated into small clumps and not in single cells because hPSC tend to have a very low survival rate as single cell, due to anoikis. This problem can be solved by adding a ROCK inhibitor to the culture medium, since ROCK signaling pathways is crucial in cellular anoikis. Similar protocols were later developed that used other hESC and hiPSC lines [34, 68, 89]. The further developed protocols tried to accomplish serum and feeder free based culture, despite of the serum be an important element for the mesoderm induction and, early endoderm induction (that delivers important factors for the cardiac differentiation) [90]. One commercially available serum-free medium that was used in differentiation protocols was StemPro-34 (ThermoFisher Scientific ™). This medium that does not contain growth factors and was specially formulated for hematopoietic stem cell culture [91]. However, without serum included in the medium, the new protocols had to use growth factors to induce the cardiac

differentiation, such as bone morphogenetic protein 4 (BMP4), Activin A, FGF2, Wnt agonist and antagonist and vascular endothelial growth factor (VEGF) and small molecules, such as CHIR99021 (CHIR) [68]. Afterwards, the methods of differentiation focused in generating a differentiated population, almost only composed by cardiac cells, instead of cells from the three germ layers. For example, developed a system to differentiate hESC into cardiomyocytes relying in the usage of activin A and BMP4 originating more than 30% of cTnT positive cells [92]. At the time, this protocol was revolutionary because previous protocols originated less than 1% of cardiomyocytes [92]. Other problem that needed to be addressed was the heterogeneity of the aggregate size that consequently affected the reproducibility and the synchronicity of the differentiation, as well. Hence, to form aggregates with similar size, other approaches started to be used as microwells (such as AggreWells -Stem Cell Technologies™) or stirred bioreactors, as spinner flasks or Erlenmeyer flasks [41]. A well-known work was developed by Kempf and co-workers [41] that obtained up to 85% of cTnT positive cells through the cardiac differentiation in bioreactors at day 10 of differentiation. Also, a microcontact printer could be used for the creation of a micropatterned substrate (such as Matrigel) that will subsequently form cellular islands and each island will be used to form an aggregate [68].

Other system for hPSC cardiac differentiation is in 2D adherent culture. The approaches used for cardiac differentiation in monolayer are very similar to the ones used in aggregates, having the advantage of being more accurate, thus more reproducible [68]. This is due to the cellular arrangement in monolayer, which allows an even application of growth factors and other molecules [68]. One slightly different differentiation protocol in 2D was developed by Zhang and associated investigators, developed a protocol based on the application of Activin A, BMP4 and bFGF, in which the cells were cultured in a Matrigel sandwich [93]. In this protocol, hPSC were cultured in Matrigel and subsequently covered in Matrigel. This culture method was based in the fact that during the gastrulation process, cells experience epithelial to mesenchymal transition and enter in the primitive streak, generating mesodermal cells that give origin to the heart muscle [93]. This method could generate ~80% of cTnT positive cells [93].

Differentiation of hPSC into cardiomyocytes by coculture with visceral endoderm-like cells was demonstrated to be effective [68]. Visceral endoderm has a significant role in the *in vivo* differentiation of cardiac progenitor cells [68]. *In vitro* inductive coculture showed the formation of beating colonies in monolayer culture [68] .This type of culture is especially relevant when the researchers only need to demonstrate the ability to form functional cardiomyocytes [68].

Nowadays, one of the most efficient protocol were developed by Lian and co-workers [94, 95] relying on the basal medium Roswell Park Memorial Institute (RPMI) 1640, supplemented with B27, and in the modulation of the Wnt signaling pathway [94]. RPMI 1640 medium is chemically defined and B27 is a complex mixture of 21 components (with many having animal origin). Despite of that, a new protocol using a chemically defined medium far cardiac differentiation was proposed by Burridge and his co-workers [96]. This medium consists on only three components: the basal medium RPMI 1640, L-ascorbic acid 2-phosphate and rice-derived recombinant albumin (an alternative for bovine serum albumin) and has achieved up to 95% TNNT2+ cells with 11 different linages [96].

It is important to highlight that the cardiomyocytes obtained through these differentiation protocols are not in a mature state. In fact, analysis performed at day 60 of human pluripotent stem cell-derived cardiomyocytes (hPSC-CM) of by Lian and co-workers revealed expression of immature cardiomyocytes [94]. This mature/immature state of cardiomyocytes was assessed through the expression of myosin light chain *a* and *v* (MLC *a* and *v*) that labels atrial/immature ventricular cardiomyocytes and mature ventricular cardiomyocytes, respectively [94]. Day 60 analysis, revealed that more than 80% of all the cTnT positive cells expressed MLC a, despite more than 50% express MLC v.

1.3.2 hPSC derived cardiomyocytes by modulation of the canonical Wnt signaling pathway

Although the existence of innumerous protocols for the differentiation of hPSC into cardiomyocytes, the differentiation via temporal modulation of canonical Wnt signaling (also called Wnt/β-catenin) is one of the most widely used [94]. Wnt signaling, via the transcriptional coactivator β-catenin controls embryonic development and adult homeostasis [97].

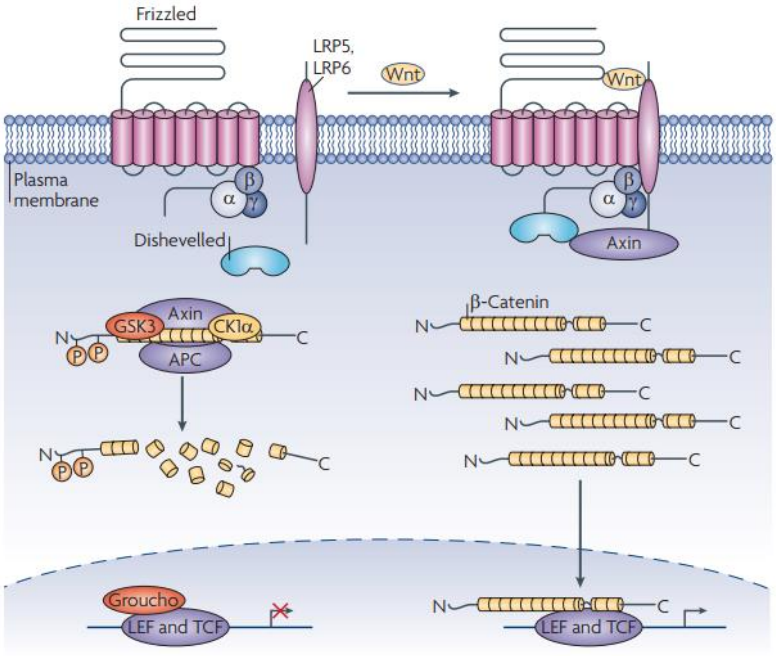

Figure 1.5 β catenin-dependent Wnt signalling. Inhibition (**left**) and activation (**right**) of the pathway. Adenomatous polyposis coli (APC), Axin protein, casein kinase 1α (CK1 α), and glycogen synthase kinase 3 (GSK3) form a complex that eliminates the β-catenin. Therefore, Wnt target genes are repressed by Groucho family of transcriptional receptors that binds to the factor/lymphoid enhancer factor (TCF/LEF) family of proteins. On the other hand, the Wnt pathway is activated when the Frizzled receptors, low-density lipoprotein receptor-related protein 5 (LPR5) or LPR6 lead to the recruitment of Axin to the LPR5 and 6 co-receptors. The degradation complex is inhibited, and β-catenin accumulates being translocated to the nucleus. In the nucleus β-catenin works as activator of LEF/TCF and consequently leads to the expression of Wnt target genes. *Adapted from reference* [98]

When Wnt signaling is inhibited, cytoplasmic β-catenin protein is constantly degraded by the action of the Axin complex, composed by two scaffold proteins; the axin protein, the tumor suppressor

adenomatous polyposis coli gene product (APC) and also by casein kinase 1α (CK1 α), and glycogen synthase kinase 3 (GSK3) [97, 98]. The elimination of β-catenin prevents it from reaching the nucleus and Wnt target genes are repressed by the Groucho family of transcriptional repressors, that binds to the DNA-bound T cell factor/lymphoid enhancer factor (TCF/LEF) family of proteins. On the other hand, Wnt pathway is activated when a Wnt ligand binds to the transmembrane Frizzled receptor: low-density lipoprotein receptor-related protein 5 (LPR5) or LPR6. Heterotrimeric G proteins (composed by α, β and γ subunits) and Dishevelled proteins are activated and lead to the recruitment of Axin to the LPR5 or LPR6 co-receptor. As a result, the degradation complex is inhibited, and β-catenin accumulates and travels to the nucleus to form complexes with TCF/LEF, activating Wnt target gene expression [97, 98].

Lian and co-workers developed a defined and growth factor-free differentiation protocol, that only relies on the temporal modulation of this signaling pathway [94]. In this protocol of cardiac differentiation, it occurs the early induction of Wnt/β-catenin (to induce the differentiation towards mesoderm) followed by the suppressing of the signaling pathway at later states of differentiation (to direct mesoderm progenitor cells to a cardiac fate). In order to activate the signaling pathway a GSK3 inhibitor – CHIR is used, allowing the accumulation of β-catenin in the cytoplasm, being activated the TCF/LEF promoter activity. CHIR-induced cells express early mesoderm markers, such as T after incubating the cells during 24 hours with CHIR. Afterwards, canonical Wnt is inhibited using an inhibitor of Wnt production (IWP), allowing for the specification into cardiovascular cells. Cells were incubated with IWP for 48 hours (between day 3 and day 5 of differentiation). Afterwards, the cells were differentiated in RPMI/B27 medium, changed every 3 days. After 12 days of differentiation, cells showed spontaneous contraction and, after day 15, up to 98% of the cells express cTnT. This protocol, relies only on the use of small molecules, being reproducible under chemically defined conditions and thus, simplifying translation for cellular therapies that need a high number of cells [94, 95].

Burridge et al. described some modifications to the previous presented protocol. [96] Namely, they assessed if all the 21 components of the B27 were necessary to obtain cardiomyocytes. It was discovered that only L-ascorbic acid 2-phosphate and bovine serum albumin (BSA) were essential. Later, BSA was replaced for rice-derived recombinant human albumin to rule out the presence of mammalian albumin-associated proteins. This new protocol produced contractile sheets containing up to 85% $cTnT^+$ cells [96].

Lian and co-workers more recently developed new investigations that indicate that albumin is not necessary for cardiomyocyte differentiation, and its presence diminishes the activity of small molecules agonists/antagonist of the Wnt canonical pathway, as well [99]. This albumin-free protocol produced ~90% $cTnT^+$ cells [99].

However, it is important to note that the efficiency of the generation of cardiomyocyte populations varies considerably accordingly to the hPSC line used, being some cells lines much more prone to cardiac differentiation than others, maybe due to endogenous levels of activations of some signaling pathways caused by epigenetic memory [100, 101]. Therefore, existing cardiac differentiation protocols developed using selected hPSC lines, probably will not be successfully applied to patient specific hiPSC [100].

1.3.3 CVPC derived from hPSC

As already mentioned in **1.3.2 Cardiovascular progenitor cells**, CVPC can be obtained in two separate ways: derived *in vitro* from hPSC (hESC and hiPSC) or isolated from cardiac tissue collected at the different stages of development of the heart [81].

The studies in CVPC derived from PSC are a novel way to test hypotheses that have emerged from research in model organisms and represents a unique opportunity to work with human cells. These studies are mostly focused on the markers: VEGFR2, ISL1 or NKX2.5 [81]. As already mentioned in **1.3.2 Cardiovascular progenitor cells**, VEGFR2 results in the expression of KDR. A population of cells isolated at day 6 of embryoid bodies mediated differentiation, which expressed KDR, gave rise to cardiomyocytes, smooth muscle cells and endothelial cells. Nevertheless, a disadvantage of using KDR as cell surface marker to recognize CVPC is that it also marks undifferentiated hPSC [68].

One early marker that could be used to sort early cardiac progenitors from hPSC culture is SSEA-1 [67, 68]. This marker identifies loss of pluripotency and can be used to isolate CVPC from cells in pluripotent state, although this is only viable if trying to separate CVPC from hPSC without other differentiated cells present [67, 68].

During human PSC differentiation, the cell-surface protein signal-regulatory protein (SIRPA) has been shown to be expressed almost at the same time of NKX2.5, giving origin to cardiomyocytes. Although, this protein's expression *in vivo* is unknown, because it is not expressed in the developing mouse heart [68, 81, 102].

1.3.4 Cardiomyocyte purification

The capacity to obtain relatively pure populations of cardiomyocytes is important for multiple applications of these cells. Studies of global gene expression are more reliable if the study is performed in a purified population [68, 103]. Besides, in order to perform cardiac drug assays, there is a need to generate a purified cardiomyocyte population, to be possible to attribute the measured alterations to direct effects on cardiomyocytes. Also, for the differentiation of cardiomyocytes from hPSC to be a reliable system to obtain cardiomyocytes for cellular therapy, researchers need to ensure that an efficient purification method is developed. The tumorigenic potential of the residual undifferentiated cells raises safety concerns for the application of hPSC-derived cardiovascular cells, due the possible formation of teratomas. However, it is important to note that the heart is formed by different cellular types, and for some cellular applications, such as the recovery of the damaged heart, it will be beneficial to use a "mixed" population instead of one solely constituted by cardiomyocytes [68, 103].

The purification of cardiomyocytes can be achieved using genetically engineered stem cell lines that express a certain drug resistance, or a reporter protein gene controlled by a cardiac-specific promoter. Klug and colleagues originally described this strategy [104]. A murine ESC line was engineered in order to a cardiac promoter express an antibiotic resistance gene, which enabled the generation of moderately pure cultures of cardiomyocytes on the presence of neomycin [104]. These kinds of purification rely on drug selection (eliminating cells that are not drug resistant) or on fluorescence-activated cell sorting

(FACS) for cells expressing fluorescent reporter proteins [68]. However, these strategies suffer major drawback since they use genetically modified cardiomyocytes [105].

Methods not relying in the genetic alteration of cells have been also developed and might be more promptly applied across various cells lines with efficiency. Methods based on cell surface markers proteins have been developed relying on FACS or magnetic- activated cell sorting (MACS). Cardiomyocytes were isolated by FACS based on their high mitochondrial content [106]. Hattori and co-workers, developed a protocol in which a fluorescent dye that labels mitochondria were used to selectively mark rat, mouse, marmoset and human PSC-derived cardiomyocytes [106]. This method is efficient, but only allows the isolation of mature cardiomyocytes that possess a high quantity of mitochondria [106]. Dubois and co-workers, reported that a cell surface protein called SIRPA is present in cardiac progenitors and it also expressed in hPSC derived cardiomyocytes [68, 105]. Using a cell sorting method relying on the use of an antibody against SIRPA, it was possible to isolate populations consisting of up to 98% cardiomyocytes [68, 105]. Uosaki and colleagues, identified that the Vascular cell adhesion molecule 1 (VCAM 1) antibody, specifically marked cardiomyocytes and by using MACS it was possible to isolate populations of cells with 95% of cardiomyocytes [107].

Nguyen and other investigators, develop a method for cardiomyocyte purification of cells in adherent culture [108]. The 2D cultures were dissociated and seeded into microwells. Afterwards, the aggregates were transferred into suspension culture. The culture as 3D cardiospheres increase the cardiomyocyte percentages from ~10-40% to levels of ~90% [108].

Tohyama and co-workers develop a protocol for a purification method that is based on the marked biochemical differences in glucose and lactate metabolism between cardiomyocytes on non-cardiomyocytes, including undifferentiated cells [109]. In this protocol, cells undergoing cardiac differentiation were exposed to Glucose-free DMEM, that does not contain glucose, or pyruvate, and is supplemented with lactate medium. Cardiomyocytes can uptake and use lactate to maintain adenosine triphosphate (ATP) levels and non-cardiomyocytes do not survive. The previously described purification is called the “lactate method”. Using this simple method, it was obtained cardiomyocytes with up to 95% of purity and with high proliferative capacity, that did not form tumors after transplantation [109].

Miki *et al.*, described an efficient method to purify cell populations with cardiomyocytes based on endogenous miRNA activity [110]. miRNA are non-coding ribonucleic acids that control gene expression. Thus, miRNA switches can induce the apoptosis of non-cardiomyocytes, allowing the population purification without cell sorting. miRNA switches are a valid option to purify cell populations in which there are not known many surface markers, being possible to use this methods in many types of cells and resulted in cells populations with ~90% of cardiomyocytes [110].

More recently, due to the advances in biomedical engineering it was developed a microfluidic system by Xin and co-workers that “traps” undifferentiated hPSC (in surfaces functionalized with anti-human TRA-1 antibody) allowing the cardiomyocytes to flow through [111]. This method is very fast and characterized by a low cost. Although, this method did not represent accurately the *in vitro*

cardiomyocytes differentiation, because it was only used two cells population: hiPSC and hiPSC-CM, not being represented all the intermediate cellular stages between them [111].

1.3.5 Pre-clinical and clinical studies using CVPC and cardiomyocytes derived from hPSC

CVPC derived from hPSC and hPSC-CM hold the potential for: drug screening, disease modelling and regenerative medicine [84].

The development of CVPC from hPSC approaches the challenge of obtaining sufficient quantities of cells needed for the CVPC to play a significant role in the field of regenerative medicine [70]. In the first clinical case report, using hESC derived cardiac progenitors, Menasché and co-workers derived cardiac progenitors from hESC and embedded them into a fibrin scaffold. The cardiac progenitors were $CD105^{+}$, which reveals their mesenchymal phenotype and $ISL1^{+}$ being able to differentiate in three main cell lineages of the heart (cardiomyocytes, smooth muscle cells and endothelial cells) [103, 112]. This patch was surgically delivered onto the infracted area in a patient suffering from severe heart failure. After 3 months, the patient had new-onset contractility in the previous patch-treated area. This was the first clinical application of cardiac progenitors derived from hESC instead of cells collected in adult tissues and, for the first time, cells were delivered in a patch and not injected as single cells in suspension. It is compelling that the mechanisms underpinning this functional improvement involve the cell induced paracrine stimulations of repair pathways. Also, this intervention was only performed in one patient being necessary to be performed more tests in other patients to be possible to establish more accurate conclusions. The clinical trial concerning this fibrin scaffold with cardiac progenitors is currently on going, in France, being extremely important to achieve more statistically significant results [103, 112].

At the same time, hPSC-CM are without a doubt a promising tool for cardiac cellular therapy and tissue engineering. In consequence, several animal models have been developed throughout the years. Funakoshi and co-workers, aimed to identify the optimal differentiation stage of cardiomyocytes in order to use these cells in cellular therapy [113]. To achieve this goal the researchers expanded iPSC and induced their differentiation towards cardiomyocytes. Afterwards, the undifferentiated cells and the cells in different days of differentiation were injected into rat hearts that have suffered MI. The best result was obtained for the transplantation of day 20 cardiomyocytes, showing good engraftment and functional improvement of the infracted heart. However, the engrafted iPSC derived cardiomyocytes only proliferate during the first month [113].

It was also tested other ways of deliver iPSC-CM, such as a patch. Wendel *et al*, produced an engineered cardiac patch made from hiPSC derived cardiomyocytes entrapped in a fibrin gel. The pericyte cells were the vascular support chosen for the present study to induce compaction of the fibrin gel, which is essential for concentrate and align cardiomyocytes [114, 115]. The patches were implanted into infarcted rat heart and the results revealed that the patch remained viable for at least 4 weeks, reducing the infarct sized and improving the cardiac function [114, 115]. Also, Masumoto and co-workers had developed a cardiac tissue sheet that was constituted not only by cardiomyocytes but also by endothelial cells and vascular mural cells, originating a vascularized cardiac tissue [116]. These sheets

were transplanted into rat hearts. A considerable number of cells survived 4 weeks after the transplantation and during the follow up period of 8 weeks did not occur any tumor formation. This work suggests that the pre-vascularization of the graft may improve the vascular connection between the graft and the host hence leading to better long-term results [116].

Many of the animal models used in trials, rely on mice or rats but the heart of these animals displays several differences from the human heart. These differences concern the size of the heart, the cardiac rate and variations at cellular and molecular level [117]. So, there is a need to support the results obtained in rodent in large animal models more closely resembling the human heart. Chong and Murray developed the first large animal studies using hPSC for cardiac regeneration [117]. Namely, they used hESC derived cardiomyocytes (hESC-CM) in a non-human primate model of ischemic cardiac injury. The results were very promising since it was obtained an extensive evidence of engraftment, remuscularization and electromechanical synchronization, 2 to 7 weeks after transplantation. However, electrocardiographic analysis revealed some arrhythmias in treated monkeys [117].

Also, Ye and co-workers, developed a patch containing cardiomyocytes, smooth muscle cells and endothelial cells that were transplanted to pigs in which it was induced MI [118]. The animals showed a functional improvement of the heart after transplantation of the fibrin patch embedded with cells and did not show cardiac arrhythmias during the 4 weeks follow-up period. Moreover, cells had an engraftment rate of almost 10% [118].

2 Aim of studies

The rise of hiPSC was one of the major steps in biomedical research, drug screening, disease modeling and regenerative medicine. These cells are obtained through the reprogramming of human somatic cells, having the capacity to differentiate in any cellular type of the three germ layers (ectoderm, mesoderm and endoderm). This discovery was a breakthrough in the field of stem cells, since they were very similar to hESC and can be manipulated without all ethical setbacks. Thereby, several research groups worked towards the development of several culture systems in order to enhance the proliferation rates and consequently the yield obtained.

Cardiovascular diseases are the number one cause of death worldwide, namely myocardial infarction and heart failure [119]. The regenerative capacity of the heart is extremely limited, therefore hiPSC induced cardiomyocytes are an important source of cardiovascular cells, that could be used for disease modeling, cardiotoxicity assays, personalized and regenerative medicine. Several research groups have tried to create a platform for differentiation of hiPSC in cardiomyocytes and other cardiac cells. However, it is extremely difficult to establish a successful protocol for the different cell lines, different culture systems and prone to scale-up. Recently, Burridge and co-workers established a protocol for the differentiation of hiPSC in cardiomyocytes, in which it was used a chemically defined medium to induce the cardiac differentiation consisting of only three components. This protocol was based in the modulation of the Wnt signaling pathway that had obtained reliable results for some hiPSC lines tested [96]. In this thesis work an adaptation of this protocol was applied.

Overall, the objective of this work was to expand hiPSC and generate hiPSC-CM in 2D and 3D systems, using chemically defined media.

In this context, the main specific objectives of this thesis were:

1. Characterize hiPSC expanded on adherent culture and as suspension aggregates in StemFlex medium, ensuring the maintenance of the cellular pluripotent state after the expansion.
2. To establish the best approximate confluence to initiate the cardiac induction, in the case of adherent culture, and in the case of suspension aggregates to establish a range of average aggregates diameters to initiate the cardiac induction after hiPSC expansion. It was also an objective to characterize cells during the process of cardiac differentiation through the modulation of the Wnt signaling pathway, to obtain spontaneously beating cTnT positive cells.

It is important to note, that the media used in monolayer and aggregate culture had the same components and concentrations, therefore we tested the possibility of using a transversal protocol to 2D and 3D culture systems.

3 Materials and Methods

3.1 Maintenance and Expansion of human induced pluripotent stem cells

3.1.1 Cell lines

In this work were used two hiPSC cell lines: F002.1A.13 (TCLab- Tecnologias Celulares para Aplicação Médica, Unipessoal, Lda) and Gibco ® Human Episomal iPSC Line Gibco (Life Technologies – Thermo Fisher Scientific). The first one was obtained through the reprogramming of fibroblast samples collected from an adult female. The reprogramming was performed through the ectopic expression of four reprogramming factors (OCT4, SOX2, KLF4 and c-MYC) using a retroviral system. The second one was obtained from CD34+ cord blood cells of healthy donors using a three-plasmid, seven reprogramming factors (SOKMNLT; SOX2, OCT4, KLF4, c-MYC, NANOG, LIN28, and SV40L T antigen) episomal system (https://www.thermofisher.com/order/catalog/product/A18945 Acceded: 02/10/17).

3.1.2 Adhesion substrate

3.1.2.1 Matrigel

In this work, it was only used one adhesion substrate: Matrigel® (Corning®). Matrigel is harvested from Engelberth-Holm-Swarm mouse sarcoma cells and is a complex mixture, manly composed by laminin, collagen IV, heparin sulphate proteoglycans, entactin/nidogen and growth factors. [29]

Matrigel was stored in aliquots at -20ºC. Afterwards, aliquots were diluted 100x in cold DMEM/F12 (Gibco®). This diluted solution is used to coat multiwell tissue culture plates (Falcon ®). These plates should be left at least for 2 hours at room temperature before being used or stored at +4ºC for a maximum of two weeks.

3.1.3 Culture Media

3.1.3.1 StemFlex™ Medium

StemFlex™ (ThermoFisher Scientific™) is a feeder-free medium used for the expansion of PSCs that is optimized to enhance recent applications of hPSC, such as single-cell passaging, gene editing and reprogramming. (https://www.thermofisher.com/pt/en/home/life-science/stem-cell-research/induced-pluripotent-stem-cells/medium-robust-feeder-free-psc-culture.html Acceded: 14/08/17). The composition of StemFlex™ medium is not fully known but is acknowledged that DMEM/F12 is the basal medium (Gibco®), which is supplemented with HEPES at 16.702 mM, L-Glutamine, Sodium Bicarbonate at 1.937 g/L ($NaHCO_3$) and BSA. HEPES and $NAHCO_3$ are buffers used to control the pH and L-Glutamine is an amino acid required for hPSC culture. This medium was used for hiPSC expansion both in monolayer and as 3D aggregates.

StemFlex™ Supplement (10x) was thawed for approximately 2 hours or overnight at 4ºC. The supplement was mixed with the basal medium to originate the complete medium. Afterwards, the complete medium was supplemented with 0.5% (v/v) Penicilin/Streptomycin (PenStrep, Gibco®), in order to avoid bacterial contaminations of cell cultures. The complete medium was stored at 4ºC for up to two weeks.

3.1.3.2 Washing Medium

Washing medium was used whenever the cells were processed in suspension or to inactivate enzymatic activity. This solution was composed by 12.0 g/L of DMEM/F12 powder (Gibco®) with L-Glutamine, 2.44 g/L of sodium bicarbonate (Sigma-Aldrich®), supplemented with 10% (v/v) of KnockOut-Serum (Gibco®), 1% of minimum essential medium non-essential amino acids – MEM-NEAA (Gibco®) and 1% (v/v) Penicilin/Streptomycin (PenStrep, Gibco®). Additionally, the prepared solution was filtrated through filters with pores of 0.5 µm (VWR®), in order to be sterile. The filtered solution was protected from light, stored at 4ºC and always pre-warmed at room temperature before being used.

3.1.4 Cell Thawing

Cryovials (ThermoFisher Scientific™) containing hiPSC are cryopreserved in liquid nitrogen (Statebourne Biorack 3000). Firstly, 4 mL of washing medium is added to a 15 mL Falcon ® tube and warmed in a 37ºC water bath. In order to thaw the cryovials, they must be placed briefly a 37ºC water bath (maximum 10-15 seconds and always stirring). After that, 1 mL of the pre-warmed washing medium was slowly added to the cryovial and mixed with the cells, until they were fully thawed. The cell suspension was added to the remaining 3 mL of washing medium in the Falcon ® tube. Afterwards the tube was centrifuged (Hemle Labortechnik GmbH, model Z 400 K) for 3 minutes at 1000 rpm. The supernatant was discarded, and the cells were resuspended in 1 mL of StemFlex™. Then, the cells were equally distributed in the previous Matrigel-coated wells of a multiwell tissue culture plate (Falcon ®) containing 0.5 mL of StemFlex™. Finally, the culture plated was incubated in a humidified incubator (Memmert), at 37ºC with 5% of CO_2 and 20% of O_2. The cells were fed in the day after the seeding followed by every-other-day feeding thereafter.

3.1.5 Cell passaging with EDTA

The regular cell passaging was performed using EDTA (0.5mM -Invitogen ™)). The cell passaging with EDTA is an enzyme-free method that allows the hiPSCs colonies detachment as small aggregates. This method is associated with higher cellular yield, lower contaminations and higher survival rates, than the conventional enzymatic methods (e.g.: TrypLE, Accutase and Trypsin-EDTA) [36].

Firstly, the culture medium was aspirated from the wells. After that, the cells were washed twice with 1mL/well of EDTA, and then were incubated with 1.5 mL/well of EDTA for 5 minutes at room temperature. After the aspiration of the EDTA solution, the cells were collected as small clumps with culture medium using a 1000 µL pipette and placed in a Falcon ® tube. The final volume in the Falcon tube should allow the placement of 1 mL/well of cell suspension. Afterwards, the cells were distributed equally in Matrigel- coated wells, that already had 0.5 mL/well of culture medium. Finally, the newly

plated cells were placed in a humidified incubator, at 37ºC with 5% of CO_2 and 20% of O_2. It is important to note that the previously mentioned volumes were used for 6 well tissue culture plates (Corning®).

3.1.6 Cell cryopreservation

Firstly, the culture medium was aspirated from the wells. After that, the cells were washed twice with 1mL/well of EDTA, and then were incubated with 1 mL/well of EDTA for 5 minutes at room temperature. Afterwards, cells were flushed with washing medium using a 1000 µL pipette. The cells were collected in a Falcon ® tube and centrifuged during 5 minutes at 1000 rpm. The supernatant was discarded, and the pellet was resuspended in StemFlex ™ medium with 10% (v/v) of Dimethylsulfoxide (DMSO, Gibco®). The mixture was transferred to cryovials (250 µL/cryovial) and stored at -80ºC, in a freezing container (Nalgene ®) before being transferred to the liquid nitrogen refrigerator (Statebourne Biorack 3000).

3.1.7 Cell counting

In order to generate aggregates and to plate cells with different seeding densities (cells/mL, in the case of the aggregates and cells/cm^2, in the case of the monolayer) and to check the cellular viability, it was necessary to perform cell counting. To distinguish between dead and viable cells it was used as stain the Trypan Blue (Gibco®). This stain, only penetrates dead cell membranes, given them a blue color, not interfering with the viable cells.

Firstly, the cells were collected using washing medium or the medium in which they were cultured, after being washed and incubated with EDTA. Afterwards, cells received a certain enzymatic treatment (e.g. Accutase (Sigma – Aldrich®) or, in the case of aggregates, 0.5% Trypsin – EDTA (Gibco®)). A representative sample of 10 µL was diluted with Trypan Blue (Gibco®) in a round bottom 96 well plate. The dilution of cells in Trypan Blue (Gibco®) was 1:2, 1:5 or 1:10 depending on the pellet size. Afterwards, the mixture was carefully homogenized, 10 µL sample was taken, placed in a hemocytometer (Marienfeld-Superior), and visualized on an inverted optical microscope (Olympus, model CKX31).

After performing the cell count, the quantity of cells in the original sample was calculated with the following equation:

$$Total\ number\ of\ cells\ = Number\ of\ cells\ counted\ \times \frac{Factor\ of\ diluition}{Number\ of\ squares} \times 10^4 \times V_T \quad (1)$$

In which V_T corresponds to the total volume of the original sample. It is important to mention that one hemocytometer square comprises a total volume of 10^{-4} cm^3.

3.1.8 hPSC aggregate formation and expansion

For hPSC aggregate formation, we used cells previously growth in monolayer, after reaching an approximate confluency of 85%. First of all, the cells were washed twice with 1mL/well of EDTA. After that, were incubated with 1 mL/well of EDTA for 5 minutes. Afterwards, the cells were flushed with StemFlex™ containing 1x (v/v) of Revitacell™ Supplement (ThermoFisher Scientific™) using a 1000 µL

pipette. The cells were collected in a Falcon tube and cell number was assessed in order to be possible to obtain aggregates with different seeding densities. Finally, the calculated volume of cell suspension and StemFlex™ supplemented with Revitacell™ were both transferred to a 6 well Ultra Low Attachment Multiwell plate (Corning® Costar®) making a total volume of 2 mL/well. The mixture of cells and medium was carefully homogenised, and the newly formed aggregates were incubated in a humidified incubator at 37ºC with 5% of CO_2 and 20% of O_2. The aggregates were expanded between 2-7 days and 80% of the culture medium was changed daily. It was performed a cell counting in the last day of expansion to calculate the fold increase. The fold increase was calculated according to equation (2).

$$Fold\ increase\ = \frac{Number\ of\ cells\ in\ the\ end\ of\ expansion}{Number\ of\ cells\ seeded} \quad (2)$$

Also, during the expansion, it was measured the evolution of the average aggregate diameter for each initial condition. Fiji software for ImageJ [120] was used to measure aggregate area and Microsoft ® Excel to calculate the average diameter. It was also calculated the coefficient of variation concerning the aggregates diameters for each day and seeding density. It was used the following equation [121]:

$$Coefficient\ of\ variation\ = \frac{Standard\ deviation\ of\ aggregates\ diameter}{Average\ value\ of\ aggregates\ diameter} \quad (3)$$

The different seeding densities for the aggregates that were used during this work are depicted in **Table 3.1**.

Table 3.1 Different seeding densities for aggregates formation. To obtain aggregates with different number of cells (from 2×10^5 to 4×10^6 cells) and consequently different seeding densities (from 1×10^5 to 2×10^6 cells/mL), it was performed a cell counting followed by aggregates formation in suspension culture.

Seeding density (cells/mL)	Number of cells per well
1×10^5	2×10^5
1.5×10^5	3×10^5
2.5×10^5	5×10^5
5×10^5	1×10^6
7.5×10^5	1.5×10^6
1×10^6	2×10^6
1.5×10^6	3×10^6
2×10^6	4×10^6

In order to evaluate the efficiency of the aggregation process, aggregates were formed as mentioned before and after 24 hours, the aggregates were selectively separated using a 37 µm Reversible Strainer (Stemcell Technologies™) from waste and single cells. The aggregates were singularized by incubation with Accutase for 7 minutes. Accutase was inactivated by the addition of washing medium. A sample of

the dissociated aggregates was collected for cell counting, as well, as a sample from the cells that remained in single cell.

3.1.9 hPSC Monolayer formation and expansion

In this part of the work, we wanted to obtain hPSC cultured in monolayer with different seeding densities. The method used was very similar to the method described in **3.1.8 hPSC Aggregates formation and expansion**. However, in this case the calculated volume of cell suspension and StemFlex supplemented with Revitacell 100x (v/v) were both transferred to a 12-well tissue culture plate with Matrigel– coated wells, making a total volume of 1 mL/well. The cells were expanded between 1-4 days and the culture medium was changed daily. The fold increase was also calculated with the equation (2), mentioned in **3.1.8 hPSC Monolayer formation and expansion**.

The different seeding densities for the monolayer that were used during this work are depicted in **Table 3.2**. It was considered that a 12 well tissue culture plate has approximately an area of 4 cm^2.

Table 3.2 Different seeding densities for monolayer formation. To obtain monolayers with different number of cells (from 1×10^4 to 1×10^5 cells) and consequently different seeding densities (from 4×10^4 to 4×10^5 cells/cm^2), it was performed a cell counting followed by monolayer formation.

Seeding density (cells/cm^2)	Number of cells per well
1×10^4	4×10^4
2.5×10^4	1×10^5
5×10^4	2×10^5
1×10^5	4×10^5

3.1.10 Embryoid bodies culture

The protocol for differentiation in embryoid bodies is schematically represented in **Figure 3.1**.

After the aggregates formation, they were expanded during 2 days in StemFlex™ in 24 wells ultra-low attachment plate with 1 mL/well of medium. 80% of the medium was daily changed.

Afterwards, to obtain embryoid bodies, the aggregates were differentiated 26 days using Embryoid bodies medium. This medium was composed by KnockOut™ DMEM supplemented with 25% (v/v) Heat Inactivate - FBS (Gibco®), 1% (v/v) of MEM-NEAA (Gibco®), Penicilin/Streptomycin (PenStrep, Gibco®) and L-Glutamine 200 mM (Invitrogen ™ Gibco®). 80% of the medium was changed every-other-day. At day 26 of differentiation, the aggregates were dissociated using 0.5% Trypsin – EDTA and replated in 24 well tissue culture plates (Falcon®). The wells were previously coated with Poly-ornithine (15 µg/mL - Sigma Aldrich®) and Laminin (20 µg/mL – Sigma Aldrich®). Afterwards, the cells were expanded for 7 days in EB medium. The success of the Embryoid bodies differentiation was assessed by intracellular immunocytochemistry by using confocal Zeiss Laser Scanning Microscope 710.

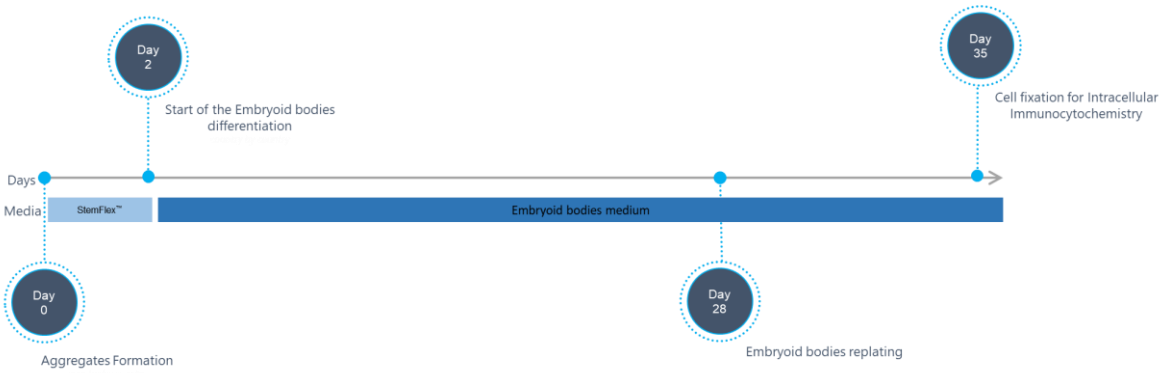

Figure 3.1 Schematic view of EB culture. The aggregates were formed and expanded during 2 days in StemFlex™ During the first 24 hours the medium was supplemented with Revitacell ™ 100x (v/v). Afterwards, the aggregates were expanded during 26 days in EB medium. At day 26 of differentiation the EB were dissociated and replated in 24 well tissue culture plates. The replated cells were expanded 7 days. Finally, the EB differentiation success was assessed by intracellular immunocytochemistry.

3.2 Cardiac induction of hPSC

The protocol for cardiac induction developed was adapted from the work by Burridge and co-workers. [96]. It was used a Pluripotent Stem Cells Cardiomyocyte Differentiation Kit (Gibco ® ThermoFisher Scientific™), that consists in a set of three different serum-free and xeno-free media that allow the differentiation of pluripotent stem cells into cardiomyocytes. The adapted protocol was used to perform the differentiation in monolayer and in aggregates, as well. Both protocols are schematically represented in **Figure 3.2** and **Figure 3.3**, respectively.

The medium used for the cardiac induction is chemically defined consisting in just three components: the basal medium RPMI 1640, L-ascorbic acid 2-phosphate and rice-derived recombinant human albumin. The three media only differ in two small molecules. Cardiomyocyte Differentiation Medium A (Gibco ® ThermoFisher Scientific™) contains 6 µM CHIR99021, in order to activate Wnt signaling pathway. On the other hand, Cardiomyocyte Differentiation Medium B (Gibco ® ThermoFisher Scientific™) is supplemented with 2 µM Wnt-C59 to inhibit the referred pathway. Finally, Cardiomyocyte Maintenance Medium (CMM - Gibco ® ThermoFisher Scientific™)) only has the three major components, not being supplemented with small molecules. [96]

The success of the differentiation was evaluated by the exhibition of spontaneous contraction (registered the first day of spontaneous contraction), by immunocytochemistry (expression of NKX2.5 and cTnT), by flow cytometry (expression of cTnT) and by cardiomyocyte yield. The cardiomyocyte yield was calculated using equation (4).

$$Cardiomyocyte\ Yield\ = \frac{Number\ of\ cells\ in\ the\ end\ of differentiation}{Number\ of\ cells\ seeded} \times \%\ cTnT\ positive\ cells \quad (4)$$

3.2.1 Cardiac induction of hPSC in monolayer

In monolayer, the cells plated in 12 wells Matrigel-coated plates with different seeding densities were expanded in StemFlex™ for up to 4 days. Afterwards, the approximate percentage of confluency of cells before the cardiac induction was registered and the medium was changed to Cardiomyocyte Differentiation Medium A. After 2 days, the medium was changed to Cardiomyocyte Differentiation Medium B. At day 4, the medium was changed to Cardiomyocyte Maintenance Medium and changed every-other-day until the end of the experiment at day 12 of differentiation. At day 12, cells were replated and collected in order to be qualitatively and quantitively analysed.

To perform the replating of the cells in monolayer, cells were washed twice with EDTA and then were incubated with 1 mL/well of EDTA for 7 minutes at room temperature. After the aspiration of the EDTA solution, the cells were collected with Cardiomyocyte Maintenance Medium using a 1000 µL pipette and placed in a 15 mL tube. A sample of cells was plated in previous Matrigel - coated 24 wells plate (Falcon ®) and expanded between 2 and 3 days, being later used for immunocytochemistry. The remaining cells were centrifuged for 5 minutes at 1000 rpm and the supernatant was discarded. The pellet was resuspended in 1 mL of 0.5% Trypsin – EDTA. Afterwards, the cells were placed in the water bath at 37ºC for 15 minutes. After the first 10 minutes were performed “up and downs” in the cell mixture using a 1000 µL pipette, in order to improve the cells dissociation. Then, it was added 3 mL of washing medium to the cells. Afterwards, cells were centrifuged during 5 minutes at 1000 rpm and the pellet resuspended in 1 mL of Paraformaldehyde (PFA) 2% (v/v) in Phosphate-Buffered Saline (PBS) and stored at 4ºC, to later perform flow cytometry.

This protocol is depicted in **Figure 3.2**.

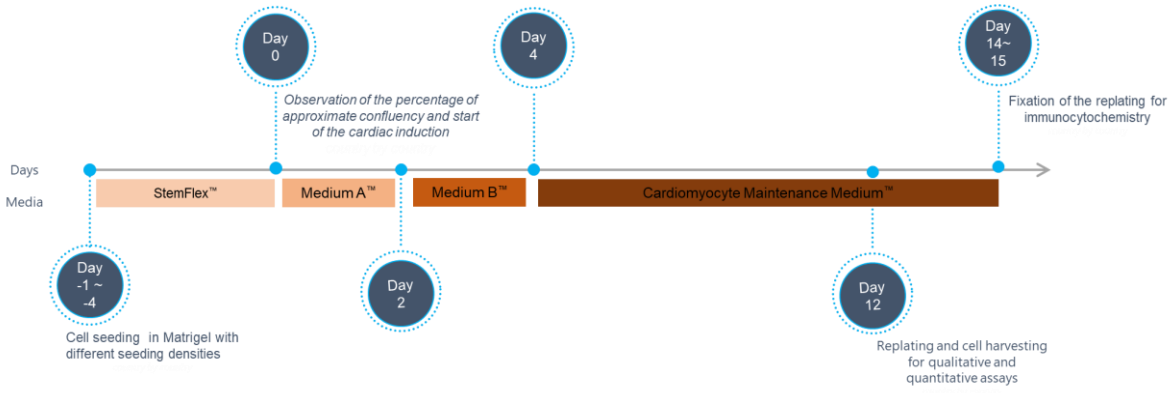

Figure 3.2 Schematic representation of the chemically defined cardiac differentiation in monolayer. Cells in monolayer were expanded between 1 and 4 days in StemFlex™. Afterwards, it was observed the approximate confluency and started the cardiac induction using Medium A. After 2 days, medium was changed to Medium B. At day 4 of differentiation, medium was changed to Cardiomyocyte Maintenance Medium and changed every-other-day until day 12 of differentiation. At day 12, cells were collected for flow cytometry analysis and immunocytochemistry. Also, some cells were replated and expanded between 2 and 3 more days to perform immunocytochemistry.

3.2.2 Cardiac induction of hPSC in aggregates

The aggregates obtained with different seeding densities were expanded between 2 and 7 days in StemFlex™. During this expansion, it was measured the evolution of the average aggregate diameter for each initial condition. Fiji software for ImageJ [120] was used to measure the aggregates area and Microsoft ® Excel to calculate the average diameter.

According to **Figure 3.3**, after the expansion, the medium was changed to Cardiomyocyte Differentiation Medium A. After 2 days, the medium was changed to Cardiomyocyte Differentiation Medium B. At day 4, the medium was changed to CMM and changed every-other-day until day 12 of differentiation. At day 12, the cells were collected and replated to be qualitatively and quantitively analysed.

To perform the replating of the aggregates, they were collected to a Falcon ® tube. Subsequently, the ultra-low- attachment wells were washed with 2 mL of washing medium, in order to ensure that all the aggregates were collected. The cells within the Falcon ® tube were centrifuged during 5 minutes at 1000 rpm. The supernatant was discarded, and the cells resuspended in 3 mL of EDTA. Then the cells were centrifuged during 5 minutes at 1000 rpm. The supernatant was discarded, and the cells resuspended in CMM. A sample of cells was plated in previous Matrigel- coated 24 wells plate (Falcon ®) and expanded between 2 and 3 days, being later used for immunocytochemistry. The downstream process to prepare the cells for flow cytometry is the same that was already mentioned for aggregates in section **3.2.1 Cardiac induction of hPSC in monolayer**. Also, the percentage of aggregates that demonstrate spontaneous contraction in the first day of the spontaneous beating and in the last day of differentiation (day 12) was calculated. In order to perform that, a grid with nine squares was designed in the bottom of the ultra-low attachment wells. Afterwards, the number of beating aggregates and the total number of aggregates were counted.

This protocol is represented in **Figure 3.3**.

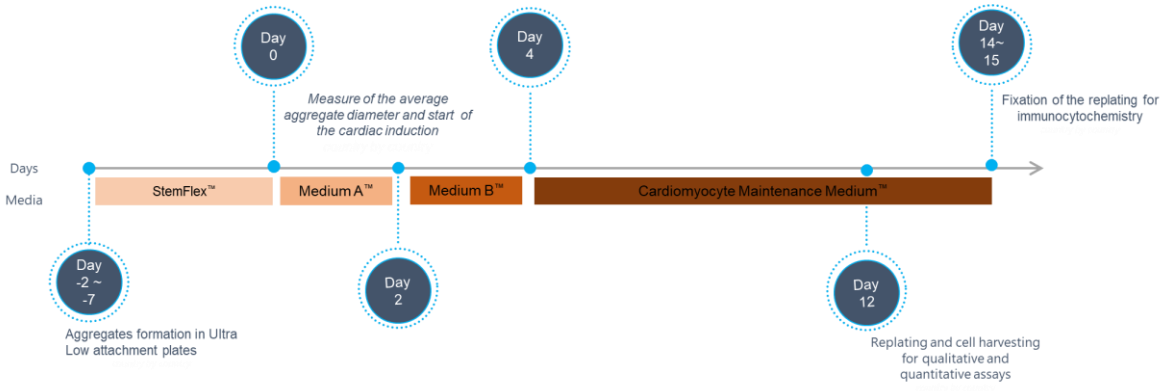

Figure 3.3 Schematic representation of the chemically defined cardiac differentiation in aggregates. Aggregates were formed in 6 well ultra-low-attachment plates were expanded between 2 and 7 days in StemFlex™ ™). Afterwards, it was measured the average aggregate diameter and started the cardiac induction using Medium A. After 2 days, medium was changed to Medium B. At day 4 of differentiation, medium was changed to Cardiomyocyte Maintenance Medium and changed every-other-day until day 12 of differentiation. At day 12, cells were collected for flow cytometry analysis and immunocytochemistry. Also, some aggregates were dissociated, replated and expanded between 2 and 3 more days to perform immunocytochemistry.

3.3 Immunocytochemistry

3.3.1 Surface markers

Cells were washed with PBS and incubated with the primary antibody diluted in washing medium for 30 minutes at room temperature. Cells were washed with washing medium and incubated with the secondary antibody diluted in washing medium for 30 minutes at room temperature, in the dark. Cells were washed to remove the excess of secondary antibody and left with washing medium. The cells were observed under fluorescence optical microscope (Leica Microsystems CMS GmbH, model DMI3000 B).

3.3.2 Intracellular staining

The cells were washed with PBS and were fixed with PFA 4% (v/v) for 10 minutes, in the case of hPSC, or for 30 minutes in the case of differentiated cells. After that, cells were incubated with blocking solution (PBS with 10% (v/v) Normal goat serum (NGS) and 1% (v/v) Triton-X100 (Sigma - Aldrich)) for 30-60 minutes at room temperature. Primary antibodies were diluted in staining solution (PBS with 5% (v/v) NGS and 0.1% (v/v) Triton-X-100) and the cells were incubated overnight at 4ºC. Then, cells were washed with PBS and incubated with secondary antibodies diluted in staining solution for 1 hour, in the dark. In order to remove the excess of secondary antibody, cells were washed with PBS and the incubated with 4',6-diamidino-2-phenylindole (DAPI diluted 1:10000 in $NaCO_3$ – Sigma Aldrich) for 2 minutes at room temperature. Afterwards, cells were washed and left in PBS. Finally, cells were observed under fluorescence optical microscope (Leica Microsystems CMS GmbH, model DMI3000 B) or confocal microscopy (Zeiss Laser Scanning Microscope 710).

In the case of hPSC derived cardiomyocytes, the Human Cardiomyocyte Immunocytochemistry kit (ThermoFisher Scientific™) was also used. In this case, the culture cells were incubated with Fixative Solution (4% formaldehyde in PBS) for 15 minutes at room temperature. After that, the cells were incubated with Permeabilization Solution (1% Saponin in PBS) for 15 minutes at room temperature. Then, the cells were incubated with Blocking Solution (3% BSA in PBS) 30 minutes at room temperature. The primary antibody was directly added to the blocking solution covering the cells and left incubated for 3 hours at room temperature (or overnight at 4ºC). Afterwards, the cells were washed with Wash Buffer and then incubated with the secondary antibody diluted in Blocking Solution for 1 hour at room temperature. Then, the cells were washed with Wash Buffer and incubated with NucBlue ® Fixed Cell Stain (DAPI – 1-2 drops/mL) for 5 minutes at room temperature. Cells were washed and observed under fluorescence optical microscope (Leica Microsystems CMS GmbH, model DMI3000 B).

3.3.3 Antibodies for immunocytochemistry staining

Table 3.3 – **Antibodies used for immunocytochemistry.** cTnT – cardiac troponin T, OCT4 – octamer-binding transcription factor, SMA – smooth muscle actin, Sox - sex determining region Y-box, SSEA – stage-specific embryonic antigen, TRA – tumour rejection antigen Tuj1 – B-III-tubulin. (*) represents the antibodies that were components of Human Cardiomyocyte Immunocytochemistry kit (ThermoFisher Scientific™)

	Primary Antibody				Secondary Antibody		
	Marker	Isotype	Dilution	Brand	Antibody	Dilution	Brand
Intracellular	OCT4	Mouse igG	1:750	Merck Millipore	Goat anti-mouse IgG	1:500	Invitrogen ™
	Sox2	Mouse igG	1:500	R&D Systems	Goat anti-mouse IgG	1:500	Invitrogen ™
	cTnT	Mouse igG	1:200	ThermoFisher Scientific™	Goat anti-mouse IgG	1:400	Invitrogen ™
	cTnT*	Mouse igG	1:1000	ThermoFisher Scientific	Donkey-anti-mouse	1:250	ThermoFisher Scientific
	NKX2.5*	Rabbit igG	1:1000	ThermoFisher Scientific	Donkey-anti- rabbit	1:250	ThermoFisher Scientific
	Tuj1	Mouse igG	1:1000	Covance	Goat anti-mouse IgG	1:500	Invirtogen ™
	α - SMA	Mouse igG	1:1000	Dako	Goat anti-mouse IgG	1:500	Invitrogen ™
	Sox17	Mouse igG	1:1000	R&D Systems	Goat anti-mouse IgG	1:500	Invitrogen ™
Surface	Tra-1-60	Mouse igM	1:135	Invitrogen	Goat anti-mouse IgM	1:1000	Invitrogen ™
	SSEA-4	Mouse igG	1:135	Stemgent	Goat anti mouse IgG	1:1000	Invitr2ogen ™

3.3.4 Confocal microscopy

Images of differentiated embryoid bodies were obtained using Zeiss Laser Scanning Microscope 710. Cell were cultured in cover slips and using moviol, for preserving stained cells, they were assembled on microscopic slides. Alexa Fluor 546 excitation was performed using 514 nm line of an Argon laser. DAPI excitation was performed by using 405 nm line of a Diode laser. Fluorescence emission was collected at selected wavelengths, namely fluorescence emission of Alexa Fluor 546 was collected at 570-640 nm and DAPI at 420-470 nm. Images were obtained with resolution of 1024x1024 or 2048x2014 pixels. The image treatment and merge were developed with Fiji software for ImageJ.

3.4 Flow cytometry

3.4.1 Intracellular staining of PSC

All samples were collected to a Falcon ® tube and singularized due to incubation with Accutase for 7 minutes at 37ºC. Accutase was inactivated by the addition of washing medium. Then, cells were centrifuged at 1000 rpm for 3 minutes. The supernatant was discarded, and the pellet resuspended in 1 mL of PFA 2% in PBS and stored at 4ºC.

Cells stored in PFA 2% were centrifuged for 3 minutes at 1000 rpm and washed twice with 1% normal goat serum (NGS, Sigma Aldrich) in PBS. Eppendorf tubes were previously coated with 1% (v/v) of BSA (Invitrogen) in PBS for 15 minutes. Afterwards, cells were resuspended in 3% NGS and transferred to the previously coated with 1% (v/v) BSA in PBS eppendorfs. Then, cells were centrifuged at 1000 rpm for 3 minutes. The supernatant was discarded, and cells were permeabilized using with (1:1) 3%NGS and 1% saponin (Sigma-Aldrich), during 15 minutes at room temperature. Cells were centrifuged for 3 minutes at 1000 rpm. Afterwards, the supernatant was discarded, and cells resuspended in 3% NGS and incubated at room temperature for 15 minutes. Then, cells were washed with 3% NGS and pellets of negative controls were resuspended only in 3% NGS and the others were resuspended with the appropriate dilution of the primary antibody in 3% NGS and incubated during 90 minutes at room temperature. Afterwards, cells were centrifuged 3 minutes at 1000 rpm and washed twice with 1% NGS and incubated in the dark, for 45 minutes, with the appropriate dilution of the secondary antibody. Then, cells were washed twice with 1% NGS and in the last wash cells were resuspended in PBS, transferred for FACS tubes (Falcon®) and analyzed in FACSalibur ™ flow cytometer (BS Biosciences ®). The results were analyzed using Flowing Software 2.0 (Turku Centre for Biotechnology).

3.4.2 Intracellular staining of hPSC-derived cardiomyocytes

All samples were collected to a Falcon ® tube and singularized through the process previously described in **3.4.1 Intracellular staining of PSC**. Although, in this case, it was used 0.5% Trypsin -EDTA for up 15 minutes at 37ºC.

Cells stored in PFA 2% were centrifuged for 3 minutes at 1000 rpm and resuspended in 90% (v/v) cold methanol, to permeabilize and fixate the cells, and incubated 15 minutes at 4ºC. Following incubation, the suspension was centrifuged for 3 minutes at 1000 rpm, the supernatant was discarded, and cells were washed three times with flow cytometry buffer (FCB) 1 (0.5% BSA in PBS). Afterwards, negative controls were resuspended in FCB 2 (0.5% BSA, 0.1% of Triton X-100 in PBS)) and the other cells were resuspended in the appropriate dilution of primary antibody in FCB2 and incubated during 1 hour at room temperature or at 4ºC overnight. Then, cells were washed once with FCB2 and the cell pellet was resuspended with the appropriate dilution of secondary antibody in FCB2 and left incubate for 30 minutes at room temperature in the dark. Cells were then washed three times with FCB 2, resuspended in FCB1 and transferred to FACS tubes. Samples were analyzed in FACSalibur ™ flow cytometer (BS Biosciences ®). The results were analyzed using Flowing Software 2.0 (Turku Centre for Biotechnology).

3.4.3 Antibodies for flow cytometry

Intracellular staining of PSC: OCT4 (Merck Millipore, 1:300), Goat anti-mouse IgG Alexa Fluor 488 (Invitrogen, 1:1000)

Intracellular staining of hPSC-derived cardiomyocytes: cTnT (ThermoFisher Scientific,1:200), Goat anti-mouse IgG Alexa Fluor 488 (Invitrogen, 1:1000)

3.5 Quantitative real-time polymerase chain reaction analysis (qRT-PCR)

The real-time PCR analysis was performed in order to assess the expression of pluripotency and cardiac markers through the induction of the cardiac differentiation of the suspension aggregates. Samples were collected at different time points of the cardiac induction: 0,1,3,5,7,9 and 12.

The RNA was extracted from the samples using High Pure RNA Isolation Kit (Sigma-Aldrich ®). RNA amount for each sample was quantified using NanoVue™ Plus spectrophotometer (GE Healthcare ®). Complementary deoxyribonucleic acid (cDNA) was synthetized from 100 ng of RNA through the usage of High-Capacity cDNA Reverse Transcription Kit (Applied Biosystems ®). The qRT-PCR was performed in 384-wells plate, in which cDNA samples were placed with TaqMan ® Gene Expression Master Mix (Applied Biosystems) and with the Taqman probes. The housekeeping gene used was glyceraldehyde-3-phosphate dehydrogenase (GAPDH, Hs02758991_g1) and the primers were NANOG (Hs02387400_g1) and TNNT2 (Hs00165960_m1). The plate was analyzed in ViiA 7 ™ Real-Time PCR Instrument.

Threshold cycles (C_T) were compared with the housekeeping gene C_T originating ΔC_T. Also, the previous mentioned values were normalized using the day 0 C_T resulting in $\Delta\Delta C_T$. At last, the final results of gene expression were presented as $2^{-\Delta\Delta CT}$.

3.6 Statistical analysis

When was considered suitable, a statistical analysis was performed using an ordinary two-way ANOVA, that determines how a response is affected by two factors. The statistical analysis was performed in the software GraphPad Prim 6. For ordinary two-way ANOVA, the software computes a column factor *p-value* and a row factor *p-value*. These two *p-values* are calculated in an independent way and represent the probability of the differences in means obtained between columns (column *p-value*) and rows (row *p-value*) are obtained by chance. A *p-value* inferior at 0.05 was considered statistically significant. Error bars in graphs represent the standard error of the mean (SEM).

4 Results and Discussion

4.1 Expansion and characterization of hiPSC in StemFlex™ culture medium as a monolayer

4.1.1 Immunocytochemistry characterization

To access the pluripotency of hiPSC, tests are usually performed, *in vivo,* as teratomas formation and, *in vitro,* with the assessment of pluripotency markers or with the formation of EB. The pluripotency markers can be surface markers, such as TRA-1-60 and SSEA-4 and intracellular, such as OCT4 and Sox2 [9]. In this work, cells were expanded in adherent culture in StemFlex medium and were stained with two surface pluripotency markers: TRA-1-60 and SSEA-4 (**Figure 4.1**) and two intracellular pluripotency markers: Sox2 and OCT4 (**Figure 4.2**), accordingly to the protocol depicted in the materials and methods.

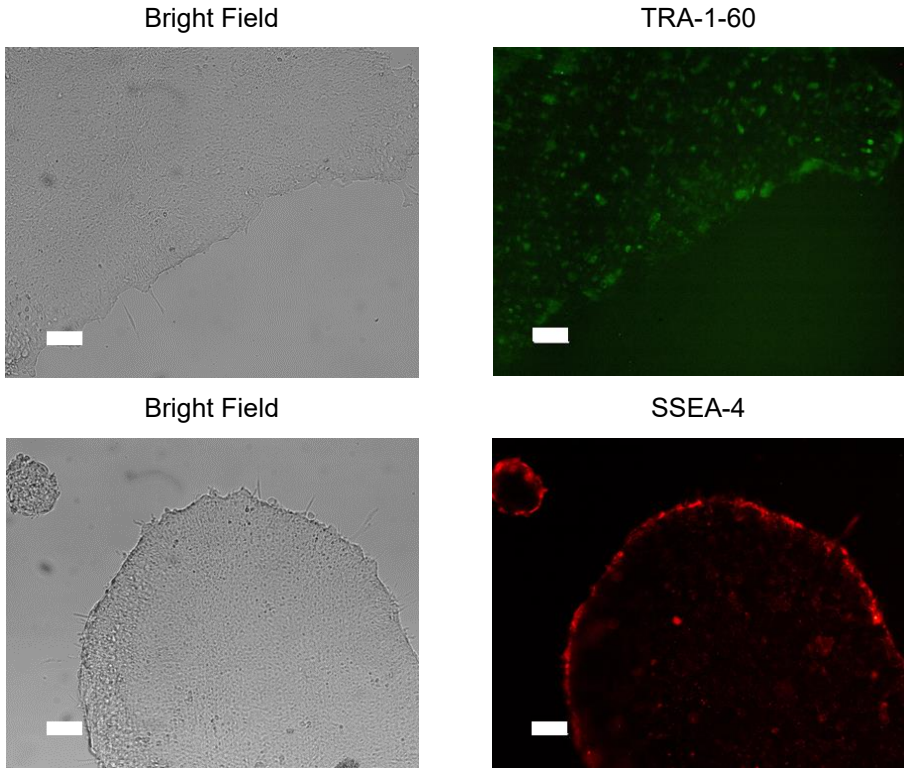

Figure 4.1 Surface markers in pluripotent cells expanded as monolayer in StemFlex. Cells were stained for two markers: TRA-1-60 in green and SSEA-4 in red. Both stained images are at right of their bright field couterparts. This experiment was performed with Gibco cell line. Scale bars 50 µm.

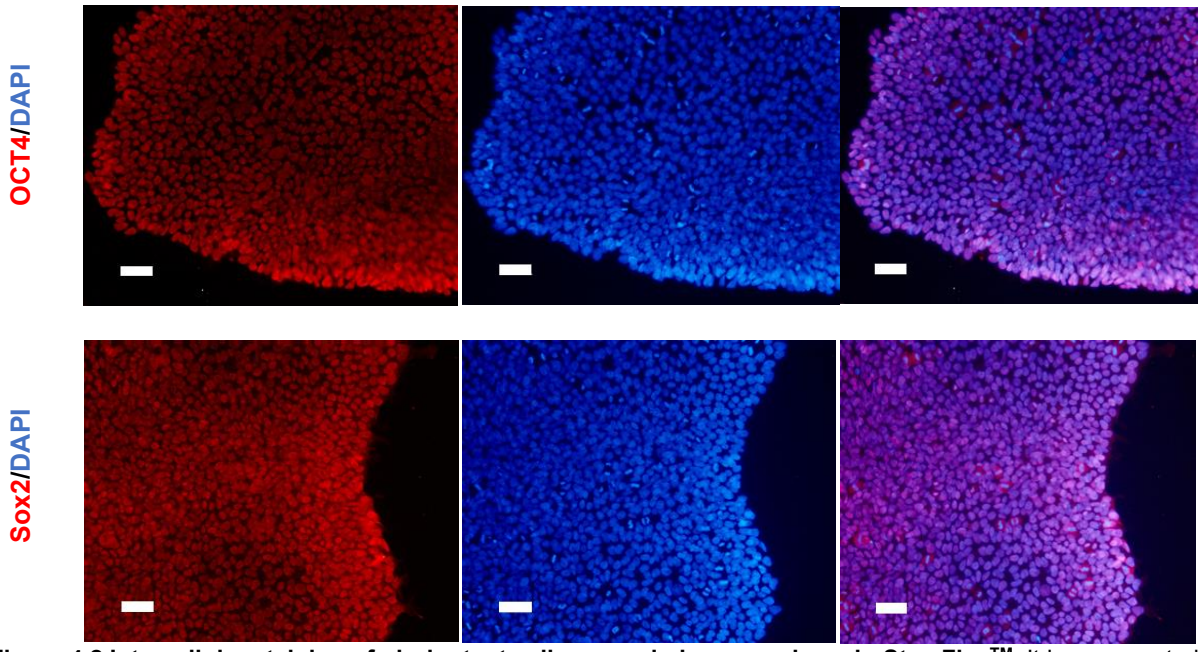

Figure 4.2 Intracellular staining of pluripotent cells expanded as monolayer in StemFlex™. It is represented the OCT4 and Sox2 staining (**left**), the DAPI staining (**middle**) and the overlappping images (**right**). This experiment was performed with Gibco cell line. Scale bars 50 µm

In **Figure 4.1** it is possible to see that the cells expressed the expected surface markers (TRA-1-60 and SSEA-4) and as it is depicted in **Figure 4.2** cells also expressed the intracellular pluripotency markers (OCT4 and Sox2) [5, 9]. These results may indicate that cells could be expanded in StemFlex medium while maintaining the expression of pluripotency markers. Since these results are only qualitative, some quantitative analyses were performed to validate them. Those quantitative analyses are depicted in the sections below.

4.1.2 hiPSC growth as a monolayer

After 3 days of expansion in StemFlex, the fold increase in cellular number was calculated using equation (2) that considers the initial and final number of cells. A fold increase of 2 indicates that after the expansion the amount of pluripotent stem cells that were collected was two times the seeded cells.

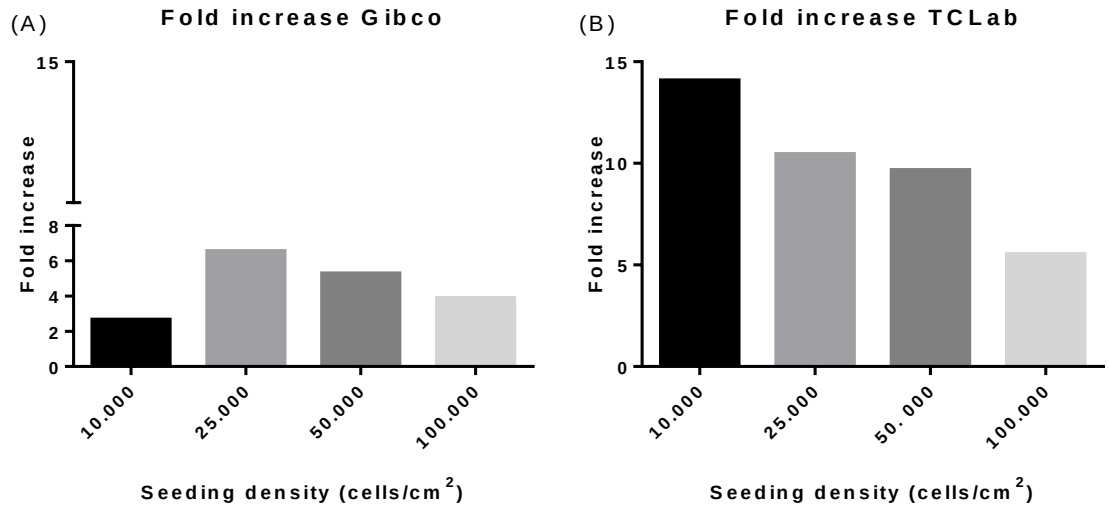

Figure 4.3 Fold increase in cell number after hiPSC expansion in monolayer. It was calculated the cellular yield after 3 days in expansion as a monolayer. It is depicted the yield for the different seeding densities for the Gibco cell line (**A**) and TCLab cell line (**B**) (n=1).

Table 4.1 hiPSC growth as adherent culture represented by the fold increase value. There are represented the two cell lines used and the different seeding densities values (cells/cm^2)

Cell line	Seeding density (cells/cm^2)			
	10.000	25.000	50.000	100.000
Gibco	2.7	6.5	5.3	3.9
TCLab	14.1	10.4	9.7	5.5

In all cases the fold increase was higher than 2 (**Figure 4.3** and **Table 4.1**). This may indicate that the StemFlex medium is appropriate to expand cells. The fold increase for TCLab cell line, for the same seeding densities, was considerably superior than for Gibco cell line, which may indicate that the proliferative capability for TCLab is bigger than for Gibco cell line. Also, apart from Gibco cell line with a seeding density of 10.000 cells/cm^2, lower seeding densities lead to higher fold increase values (**Figure 4.3** and **Table 4.1**). This may be explained by the fact that the expansion was performed in an adherent system being the space for expansion limited. Also, a previous work in which was evaluated the expansion of hPSC (hiPSC and hESC) in mTeSR media revealed that the cellular growth decreased after reaching a certain cellular density, in that case 50.000 cells/cm^2, confirming a slower proliferation after reaching a certain density level (cells/cm^2) [122]. The lower value for the Gibco cell line when seeded at 10.000 cells/cm^2 could be due to losses of cells in the collection after the expansion or due to a higher cellular death in this condition.

4.1.3 Flow cytometry characterization of hiPSC expanded as monolayer

The flow cytometry analysis was performed after 3 days of cellular expansion of cells seeded with different seeding densities (cells/cm^2), in adherent culture. This analysis had one major objective: to ensure that cells remain pluripotent before the induction of the cardiac differentiation. The used marker was OCT4 and the results are depicted in **Figure 4.4**.

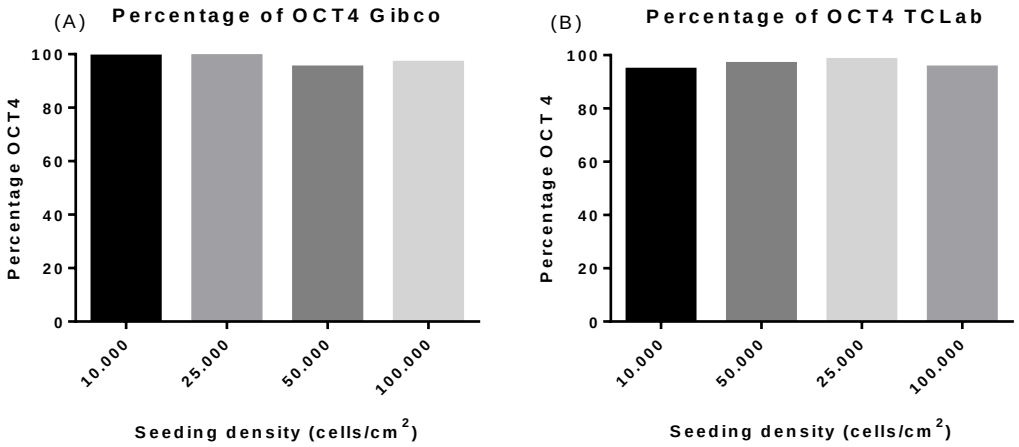

Figure 4.4 Percentage of OCT4 positive cells after expansion as adherent culture. (A) Gibco **and (B)** TCLab cell line. Cells were seeded with different densities (10.000, 25.000, 50.000, 100.000 cells/cm^2) and expanded in adherent culture for 3 days using StemFlex^{TM} medium. Afterwards, a flow cytometry analysis was performed, to assess pluripotency of the cells (n=1).

Table 4.2 Percentage of OCT4 positive cells after expansion as adherent culture. There are represented the two cell lines used and the different seeding densities values (cells/cm^2)

Cell line	Seeding density (cells/cm^2)			
	10.000	25.000	50.000	100.000
Gibco	99.1%	99.6%	95.0%	96.8%
TCLab	94.5%	98.2%	96.7%	95.4%

Through the observation of **Figure 4.4** and **Table 4.2** it is possible to infer that the cells cultured in adherent substrate for 3 days conserved the pluripotent state, being the percentage of cells OCT4 positive always higher than 94%. For the Gibco cell line (**Figure 4.4 A**) the average value of OCT4 positive cells concerning all the different seeding densities was 97.6% and in the TCLab cell line (**Figure 4.4 B**) 96.2%. Apparently, the different seeding densities do not have a considerable impact in the pluripotent state after three days of expansion in adherent culture. This may indicate that the StemFlex medium is appropriate to expand cells, maintaining their pluripotent state (as it was possible to access in **4.1.2 hiPSC growth as a monolayer**). Chen and co-workers, evaluated the expression of pluripotency markers of hESC and hiPSC after their expansion, as adherent culture on Matrigel, in a newly developed medium called Essential 8™ [123]. In the previous protocol, a high expression of the pluripotency marker was obtained (>90%) [123]. The results obtained by Chen and co-workers were

very similar to the results obtained in this work. This may indicate that the cells can be expanded using StemFlex medium and conserve their pluripotency, being able to be posteriorly differentiated.

4.2 Expansion and characterization of hiPSC in StemFlex™ culture medium as 3D aggregates

4.2.1 Efficiency of the aggregation process

In order to unveil the efficiency of the hiPSC aggregation process, cell counting was performed, 24 hours after the aggregates formation. The efficiency of the aggregation process was assessed in the two cells lines with two different seeding densities. The aggregates were formed accordingly with the protocol described in **3.1.8 hPSC aggregates formation with EDTA and expansion**. The cell counting was performed 24 hours after the seeding since at that time point, the first medium change is performed, being removed all the cells that did not form aggregates.

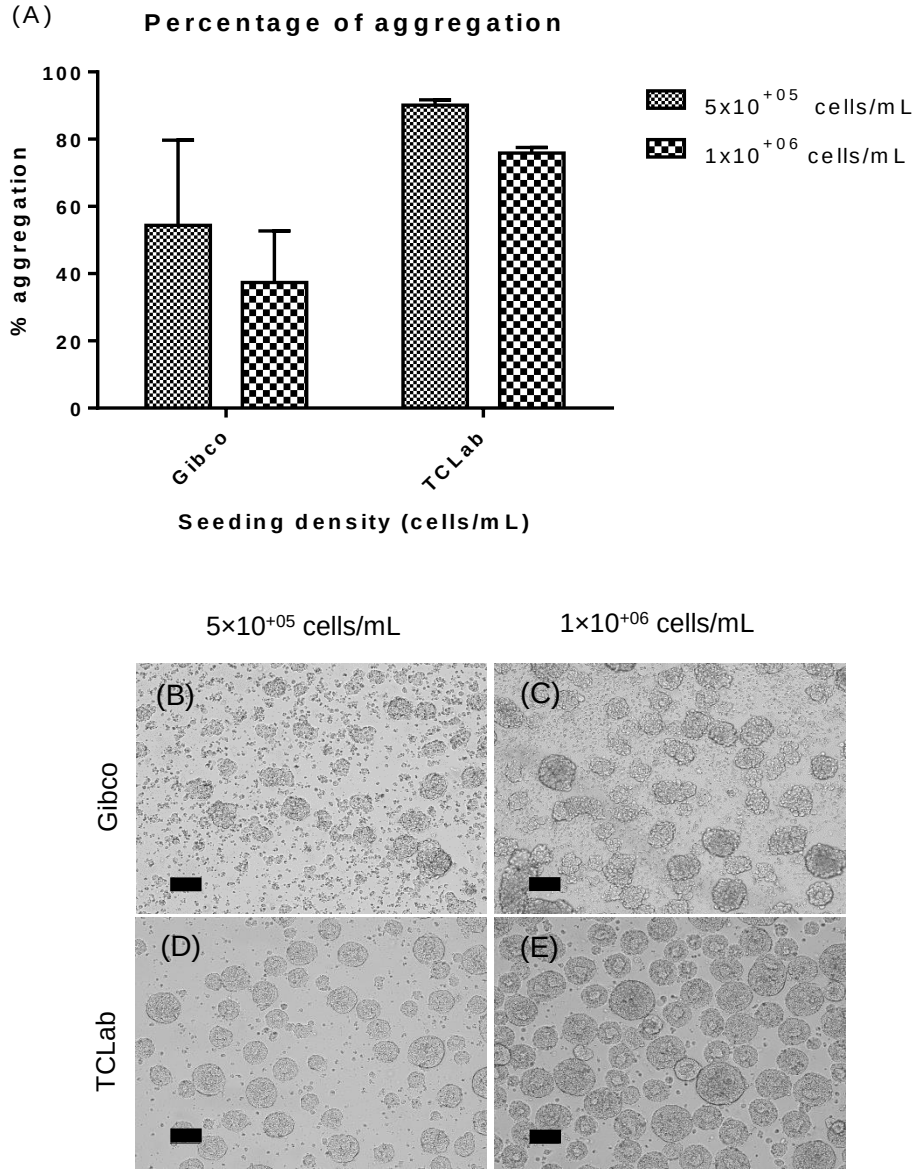

Figure 4.5 Efficiency of the hiPSC aggregation process. (A) The percentage of aggregation was calculated for the two cells lines, Gibco at **left** (n=3), and TCLab at **right** (n=2), for two seeding densities ($5\times10^{+05}$ and $1\times10^{+06}$ cells/mL). It is represented the mean value and the error bars represent the SEM value. **(B-E)** Image of the aggregates 24 hours after the aggregates formation **(B)** Gibco aggregates with the seeding density of $5\times10^{+05}$ **(C)** Gibco aggregates with the seeding density of $1\times10^{+06}$ **(D)** TCLab aggregates with the seeding density of $5\times10^{+05}$ **(E)** TCLab aggregates with the seeding density of $1\times10^{+06}$. Scale bars: 100 µm.

This test was performed to compare the aggregation process in the two cell lines with two different seeding densities. The percentage of aggregation obtained for TCLab cell line was higher than for Gibco cell line, and the percentage of aggregation for the seeding density of $5\times10^{+05}$ was higher than for $1\times10^{+06}$, as well (**Figure 4.5 A**). In conclusion, it seems that the aggregation process in StemFlex medium is more efficient for the TCLab cell line (**Figure 4.5 (D and E)**), than for Gibco cell line (**Figure 4.5 (B and C))**, and that higher seeding densities (**Figure 4.5 (C and E)**), are associated to a higher loss of cells that did not aggregate in the first 24 hours. This could be due to the fact than in that time range only is possible to occur the aggregation of a certain quantity of cells being that all the "extra" cells remain as single cells, being removed with the medium change. This is corroborated by experiments

performed by Dang *et al.*, in which with the increase of murine ESC density, the efficiency of aggregation decreased [124]. This may indicate that considering a certain range of cellular density may be preferable to use a lower cellular number, since most of the cells will have time to aggregate and the number of viable cells that will be "discarded" in the first medium change will be lower. To improve the aggregation percentage cells could be cultured in a rotary system, such as an orbital shaker. Carpenedo *et al.* compared the efficiency of aggregates formation, using murine ESC, in static and rotary conditions. They conclude that the efficiency was much higher in rotary system than in static, obtaining, 12 hours after the aggregates formation, 4.5% of aggregation in static culture and 88.4% in dynamic culture [125]. So, a rotary system could be used in order to improve the efficiency of the aggregation process.

4.2.2 hiPSC growth as 3D aggregates

In order to assess hiPSC expansion when cultured as 3D aggregates, the fold increase values in cellular number were calculated using equation (2). The results are depicted in **Figure 4.6**.

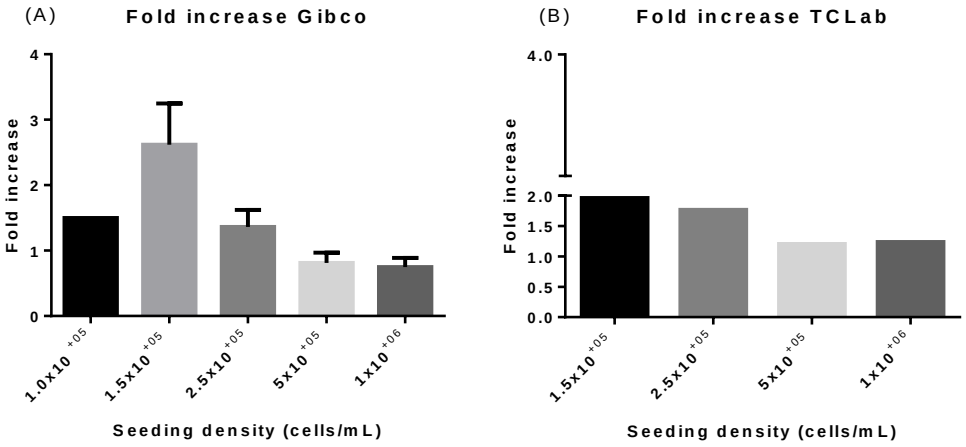

Figure 4.6 Fold increase after expansion as aggregates in StemFlex medium for (A) Gibco cell line (B) and TCLab cell line. (A) The fold increase values were calculated after the culture for up to 6 days in hiPSC Gibco cell line aggregates. It is depicted the fold increase (vertical axis) for the different seeding densities (cells/mL) $1\times10^{+05}$ (n=1), $1.5\times10^{+05}$, $2.5\times10^{+05}$, $5\times10^{+05}$ and $1\times10^{+06}$ (n=2, horizontal axis). **(B)** Aggregates formed with TCLab cell line were expanded for 3 days (n=1). Error bars represent the SEM value.

Table 4.3 hiPSC growth as 3D aggregates represented by the fold increase value. There are represented the two cell lines used and the different seeding densities values (cells/mL)

Cell line	Seeding density (cells/mL)				
	$1\times10^{+05}$	$1.5\times10^{+05}$	$2.5\times10^{+05}$	$5\times10^{+05}$	$1\times10^{+06}$
Gibco	1.5	2.7±0.6	1.4±0.3	0.8±0.2	0.8±0.2
TCLab	-	2.0	1.8	1.2	1.2

Gibco aggregates were expanded for up to 6 days. A fold increase of 2 would indicate that the number of collected cells, after the expansion, was two times the number of seeded cells. Nevertheless, for the Gibco cell line (**Figure 4.6 A** and **Table 4.3**) only three of the seeding densities lead to a fold increase higher than one ($1\times10^{+05}$+, $1.5\times10^{+05}$ and $2.5\times10^{+05}$ cells/mL). These densities appear to be the most

prone to cellular expansion for Gibco cell line aggregates cultured in StemFlex medium. Regarding the TCLab cell line, the fold increase was higher than for the Gibco cell line (**Figure 4.6 B** and **Table 4.3**). These results are corroborated by the obtained results in the expansion as adherent culture, in which the cells from TCLab cell line demonstrate a higher proliferative capacity.

In general, with the increase of the number of cells seeded per volume, the fold increases diminished, indicating that when less cells are originally seeded, a higher cell growth can occur. This could be due to only be possible for each aggregate to achieve a certain cellular number (cells/aggregate), being that when that number is achieved, the aggregates reduce the overall cellular yield [124]. However, this did not occur for the seeding density $1.0\times10^{+05}$ cells/mL that revels a fold increase lower than $1.5\times10^{+05}$ cells/mL and $2.5\times10^{+05}$ cells/mL. This could be due to a loss of cells on the collection step or due to an abnormal cellular death during the expansion.

4.2.3 Flow cytometry characterization of hiPSC expanded as 3D aggregates

After expanding the cells as suspension aggregates for up to 6 days in StemFlex medium, their pluripotent state was assessed by analysing the expression of the intracellular pluripotency marker OCT4 by flow cytometry. The percentage of OCT4 positive cells is represented in **Figure 4.7**.

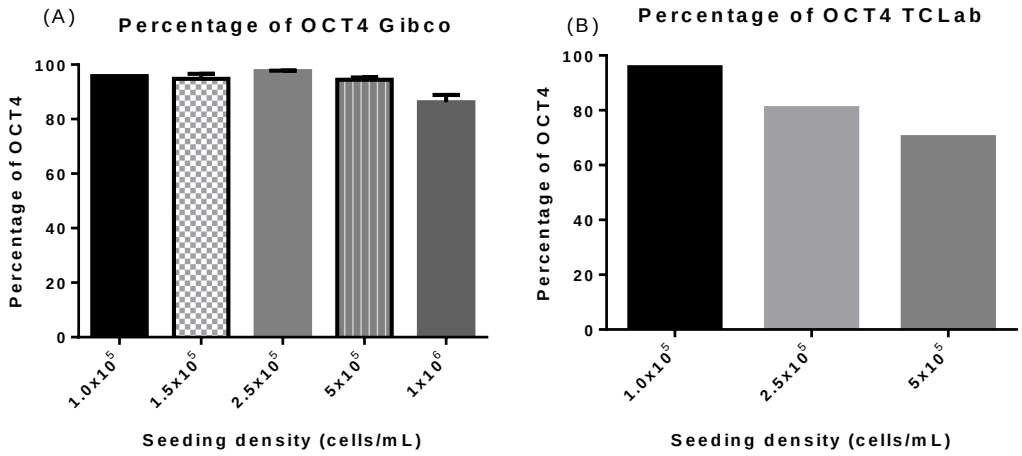

Figure 4.7 Percentage of OCT4 positive cells after expansion of the (A) Gibco **and (B)** TCLab cell line. Cells were seeded with different densities and expanded as aggregates for up to 6 days in StemFlex™ medium. In the horizontal axis are depicted the different seeding densities used (cells/mL) and in the vertical axis the correspondent percentage of OCT4 positive cells. **(A)** Aggregates of hiPSC Gibco cell line were expanded for up to 6 days (n=1 for $1\times10^{+05}$ and n=2 for the other seeding densities). **(B)** Aggregates of TCLab cell line were expanded for 3 days (n=1). The mean values are presented, and error bars depict the SEM value.

Table 4.4 Percentage of OCT4 positive cells after expansion as 3D suspension aggregates. There are represented the two cell lines used and the different seeding densities values (cells/mL).

Cell line	Seeding density (cells/mL)				
	$1\times10^{+05}$	$1.5\times10^{+05}$	$2.5\times10^{+05}$	$5\times10^{+05}$	$1\times10^{+06}$
Gibco	95.8%	94.8±1.8%,	97.6±0.3%,	94.5±0.9%	86.2±2.7%
TCLab	95.7%	-	80.8%	70.2%	-

The results for Gibco cell line vary from 86.20% to 97.60% and for TCLab from 70.22% to 95.70% (**Figure 4.7** and **Table 4.4**). The values obtained were very similar to the ones obtained by Chen and co-workers, that registered a percentage of OCT4 positive cells of over 90% for cells expanded in aggregates with seeding densities between 3-3.5×10^{+05} cells/mL [119]. Comparing Gibco and TCLab cell lines, for two of the three seeding densities (2.5×10^{+05} and 5×10^{+05}) the percentage of OCT4 positive cells was much higher for Gibco than for TCLab cell line. This can possibly indicate that the Gibco cells maintain more easily the pluripotent state when expanded as 3D aggregates in StemFlex than the TCLab cells. Also, in all the seeding densities of all the experiments, the lower value of expression of OCT4 was associated with the higher seeding densities (5×10^{+05} and 1×10^{+06} cells/mL), whereas lower seeding densities (1×10^{+05}, 1.5×10^{+05} and 2.5×10^{+05} cells/mL) are associated to a higher percentage of pluripotent stem cells (**Figure 4.7** and **Table 4.4**). This may indicate that higher seeding densities in the aggregates will lead to more spontaneous differentiation, reducing the number of cells in a pluripotent state, prior diminishing the percentage of differentiated cells in the population of interest. In the higher seeding densities, the number of aggregates that "merge" with each other is more prominent, leading to bigger aggregates with distort shapes. As mentioned by Chen and co-workers, this causes more difficulties for cytokines and nutrients to penetrate the aggregates, which may result in a decreased proliferation and an increased spontaneous differentiation [126]. A previous expansion of hESC in ultra-low-attachment plates accomplish percentages higher than 90% of OCT4 positive cells after the expansion [127]. The results here obtained were always higher than 70% being the OCT4 percentage higher than 90% for most of the seeding densities regarding the Gibco cell line. Therefore, despite some values obtained were lower than the ones presented in a previous work, the overall results were similar.

4.2.4 Kinetics of 3D aggregates diameter

During the expansion in StemFlex™ medium the diameter of the aggregates obtained with different seeding densities were registered day-by-day. To accomplish that, daily photographs (between 10 and 30) were taken in order to measure the diameter of at least 50 aggregates per day and per condition. Seeding densities (cells/mL) ranging from 1.0x10^{5} to 2x10^{6} cells/mL were analyzed. The overall results are depicted in **Figure 4.8** for Gibco cell line and in **Figure 4.9** for TCLab cell line. Also, in **Table 8.1** (**Supplementary Informat**ion) is represented in detail the values of the day-by-day evolution of the average aggregate diameters for all seeding densities. The coefficient of variation (Cv) for the aggregates diameters was also calculated through equation (3) and represented in ***Figure 4.10***.

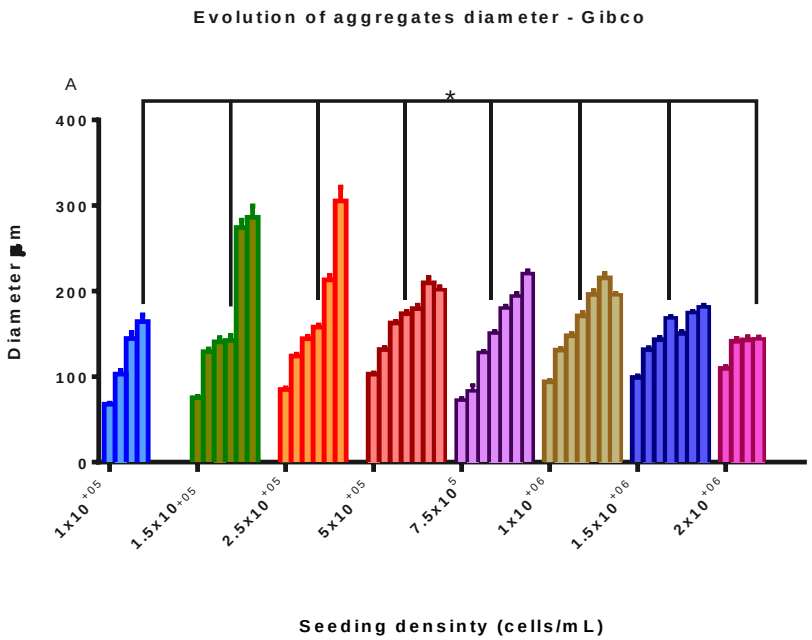

Figure 4.8 Day by day evolution of hiPSC aggregates diameter (day 1 to day 6) for seeding densities (cells/mL) of $1x10^5$ (n=3 for day 1-3 and n=2 for day 4), $1.5x10^5$ (n= 4, for day 1-3, n=3 for day 4 and n=1 for day 5 and 6), $2.5x10^5$, $5x10^5$, (n=6 for day 1-3, n=5 for day 4, n=2 for day 5-6 and n=1 for day 7), $7.5x10^5$ (n=1), $1x10^6$ (n=5 for day 1-3, n=4 for day 4 n=2 for day 5-6 and n=1 for day 7), $1.5x10^6$ (n=2 for day 1-3 and n=1 for day 4). The results are represented as diameter mean value of each seeding density for each day of expansion. In the horizontal axis each group of graphs represent a seeding density and each column a day of expansion. This experiment comprises the Gibco cell line. The error bars represent the SEM value. The * denotes statistical significance ($p<0.0001$) between all seeding densities in day 4 of expansion.

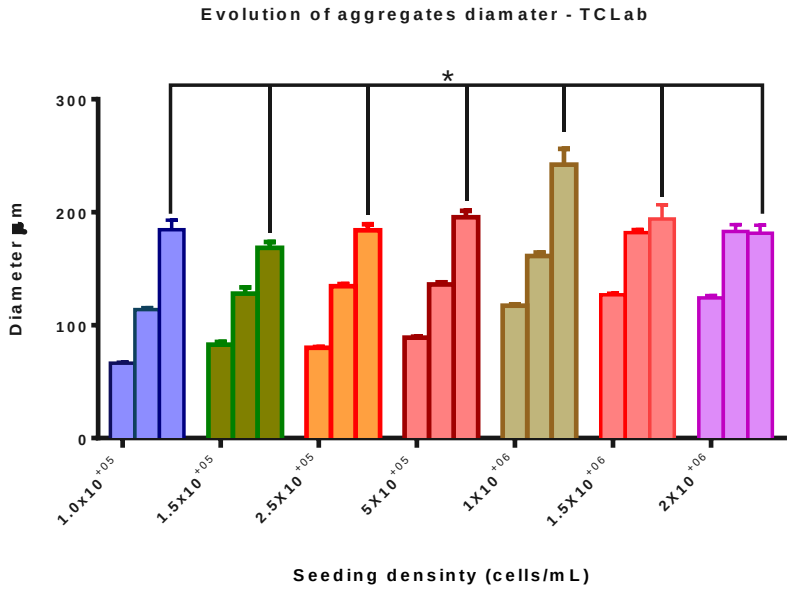

Figure 4.9 Day by day evolution of aggregates diameter (day 1 to day 3) for seeding densities (cells/mL) of $1.0x10^5$ (n=3 for day 1-2 and n=1 for day 3), $1.5x10^5$ (n=2), $2.5x10^5$, $5x10^5$ (n=5 for day 1 and 2 and n=3 for day 3, $1x10^6$(n=4 for day 1 and 2 and n=2 for day 3), $1.5x10^6$ (n=3 for day 1-2 and n=1 for day 3) and $2x10^6$ (n=2 for day 1-2 and n=1 for day 3). The results are represented as diameter mean value of each seeding density for each day of expansion. In the horizontal axis each group of graphs represent a seeding density and each column a day of expansion. This experiment comprises the TCLab cell line. The error bars represent the SEM value. The * denotes statistical significance ($p<0.0001$) between all seeding densities in day 3 of expansion

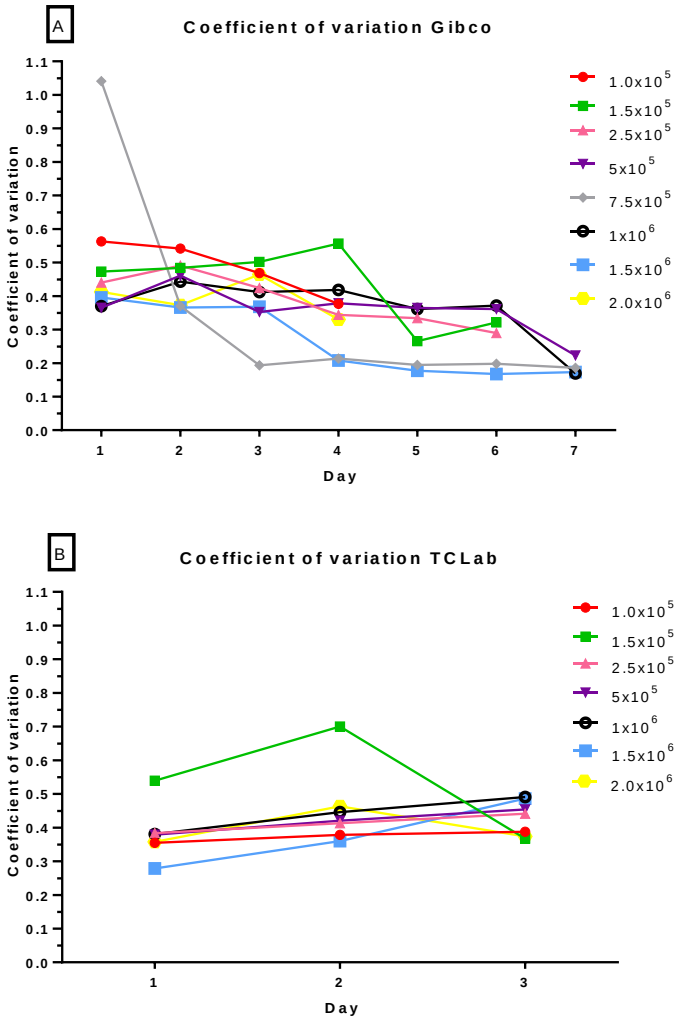

Figure 4.10 Coefficient of variation (Cv) of the aggregates diameter in each day of expansion of hiPSC for seeding densities comprised between $1\times10^{+05}$ and $2\times10^{+06}$ cells/mL for the Gibco cell line (A) and TCLab cell line (B).

As it is possible to conclude from **Figure 4.8** and **Figure 4.9**, in general, day-by-day it occurs an increase of the average aggregate diameter. Also, in most of the cases using lower seeding densities (cells/mL) it is obtained lower values for the aggregates diameter and with higher seeding densities were formed aggregates with slightly bigger diameters. Despite of that, the maximum difference on the aggregate diameter between the lower and the higher seeding density ($1.0\times10^{+05}$ and $2.0\times10^{+06}$ cells/mL) for Gibco aggregates is 41.8 µm and for TCLab aggregates is 57.8 µm. Thus, an increase of almost 20 times in the number of seeded cells only leads to an increase, in the average aggregates diameter, of 41.8 µm for Gibco and 57.8 µm for TCLab aggregates. This may indicate that with an increase of the seeded cells the number of aggregates increases, and the aggregates diameter does not change drastically. Also, these results can be due to a bigger death rate or non-aggregation in the aggregate formation in higher seeding densities than in the lower ones. This finding corroborates the previously discussed results (**4.2.1 Efficiency of the aggregation process**) that appear to indicate that with higher seeding densities are obtained lower efficiencies in the aggregation process, meaning that with a higher number

of seeded cells, the number of live cells that remain non-aggregated is much more representative than with a lower number of seeded cells.

Through the observation of **Figure 4.10**, it is possible to evaluate the dispersion of the aggregates diameter for each seeding density of the two cell lines. In a perfect scenario the obtained value would be 0. The Cv values obtained for the Gibco cell line, in the last day of expansion, assume values in the range of 0.16-0.37 and between 0.37-0.48, for TCLab cell line. These results reveal a considerable heterogeneity in the aggregates diameters obtained. This heterogeneity could lead to harmful consequences in the cardiac differentiation of the aggregates, that will be later discussed in section **4.4 Differentiation of hPSC into cardiomyocytes in aggregates.** It was previously reported for suspension culture a Cv of 0.49 (with a seeding of $0.5x10^5$ cells/mL) for aggregates of murine iPSC expanded for 3 days [40]. The results obtained in this work using hiPSC, concerning the last day of expansion, were always lower than 0.49. It is important to note, that for the Gibco cell line the dispersion within aggregates diameter reduces throughout the expansion and for the TCLab cell line, in most of the seeding densities, the coefficient of variation increases. This indicates than despite being obtained a lower heterogeneity in the aggregates formation using the TCLab cell line, in the end of the expansion, the heterogeneity in these diameters was similar for both cell lines. The decrease in the Cv value, in Gibco cell line, could be a consequence of, in the first days, the aggregates with higher diameters be measured contributing to the Cv, but in the following days, these aggregates start to assume distort shapes, not being possible to measure their diameter, leading to an “apparent” improvement in the Cv. This problem could be overcome by using a seeding method that generates more homogenous aggregates, such as using an orbital rotary system.

4.2.5 Pluripotency assessment of hiPSC

After expansion as 3D aggregates in StemFlex medium, hiPSC were evaluated concerning their pluripotency. If the cells retained the ability to differentiate in cells from all the three germ layers, then they are considered pluripotent [1, 5]. Aggregates/Embryoid bodies (EB) were formed and expanded for 2 days in StemFlex medium. Afterwards, the EB were cultured in a medium to induct the differentiation into the three germ layers (endoderm, mesoderm and ectoderm). At day 26 of differentiation, the EB were replated and cultured for more 7 days. Subsequently, it was performed an immunocytochemistry analysis using markers for endoderm (Sox17), mesoderm (α – SMA) and ectoderm (Tuj1) cells. The images were acquired in a confocal microscope and are represented in **Figure 4.11**.

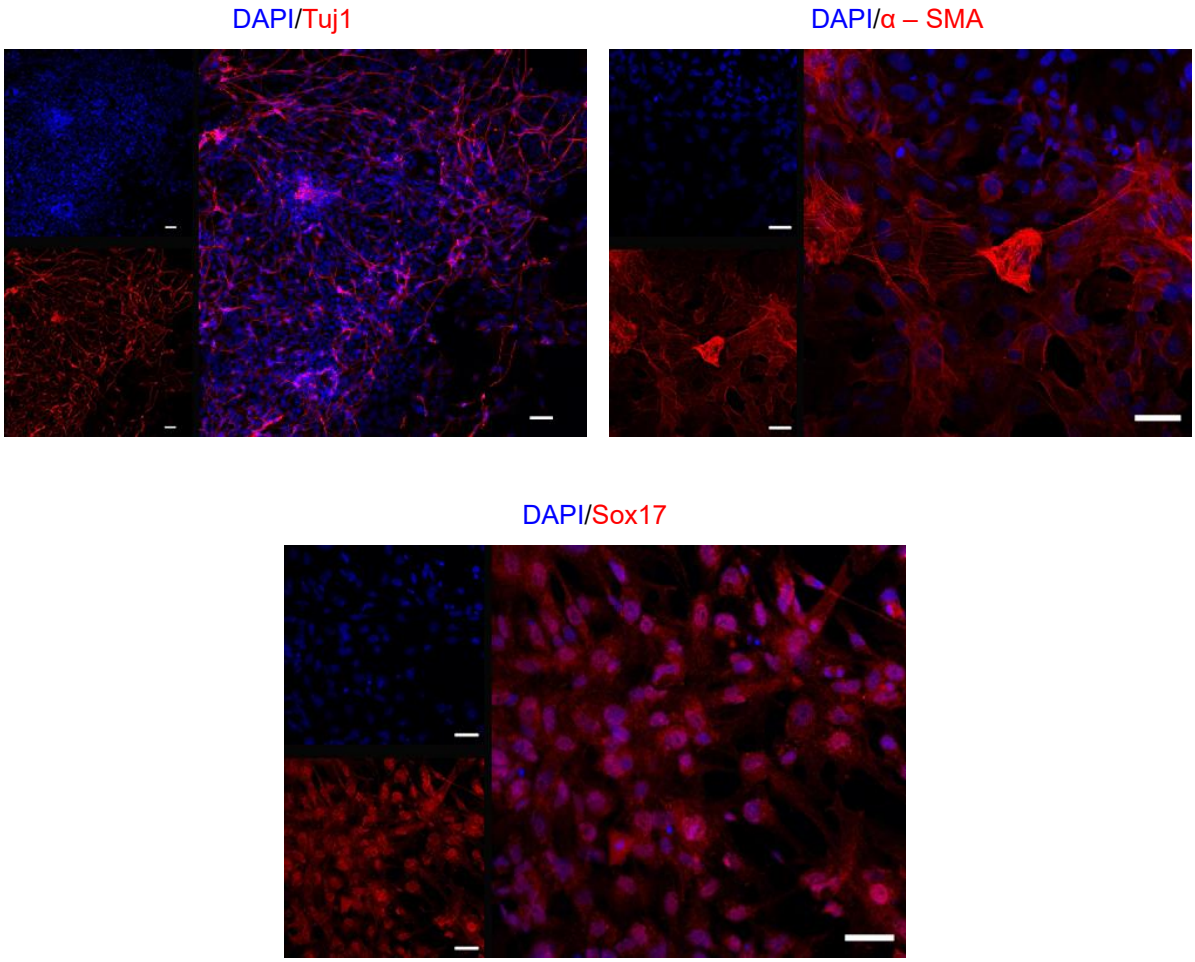

Figure 4.11 Intracellular staining of the replated hiPSC-derived EB. In the upper right is represented the ectoderm marker (Tuj1) in the upper left the mesoderm marker (α – SMA) and in the bottom the endoderm marker (Sox17). The images were obtained using Zeiss Laser Scanning Microscope 710 with a resolution of 1024x1024 for α – SMA and Sox17 and 2048x2048 for Tuj1 staining. Scale bars: 50 μm. This experiment was performed using the Gibco cell line.

In **Figure 4.11** is it possible to see the staining of the cells with the three germ layer markers. The results represented in **Figure 4.11** seem to indicate, once again, that cells cultured in StemFlex medium remain in a pluripotent state and consequently can be differentiated into any cellular type.

4.3 Differentiation of hiPSC into cardiomyocytes as a 2D monolayer

After the expansion in monolayer for up to 4 days, the approximate confluency for each seeding density was registered and the differentiation was initiated afterwards. The confluency could be obtained with more precision by measuring the area occupied by cells in a previously took photograph. The approximate percentage of confluency for all experiments and all seeding densities is presented in **Table 8.2** (**Supplementary Information**) and the number of times that each approximate confluency was obtained is depicted in **Figure 8.1.** (**Supplementary Information**). The morphology of cells differentiated in adherent culture is presented (**Figure 4.12**), before the beginning of the cardiac

induction (day 0) and in the last day of differentiation, when already presented spontaneous contraction (day 12).

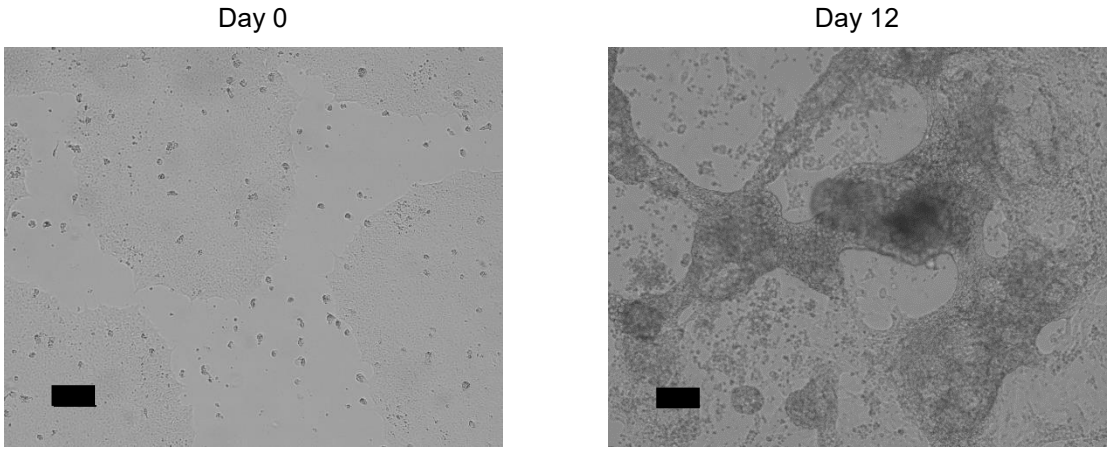

Figure 4.12 Morphology of hiPSC differentiated in adherent culture at day 0 (left) and day 12 (right). It is represented an approximate confluency of 60-70% before cardiac differentiation. Scale bars: 100 µm.

The initial seeding density, together with the time of expansion before initiation of the differentiation are the critical parameters to consider an efficient cardiac differentiation [41, 95]. This indicates that cell-cell contacts and the concentration of paracrine factors are directly related with the percentage of cTnT positive cells obtained [41, 95]. In an efficient differentiation, in adherent culture, contracting elongated sheets of hiPSC-CM are originated, as it is represented in **Figure 4.12**.

For each experiment, the first day that the cells started to show spontaneous beating was registered. The results are represented in **Figure 4.13**. It is important to mention that only the approximate confluences that showed a spontaneous beating are presented in the graph. It is also presented the morphology of the cells in the first day of the spontaneous contraction (**Figure 4.13 C**).

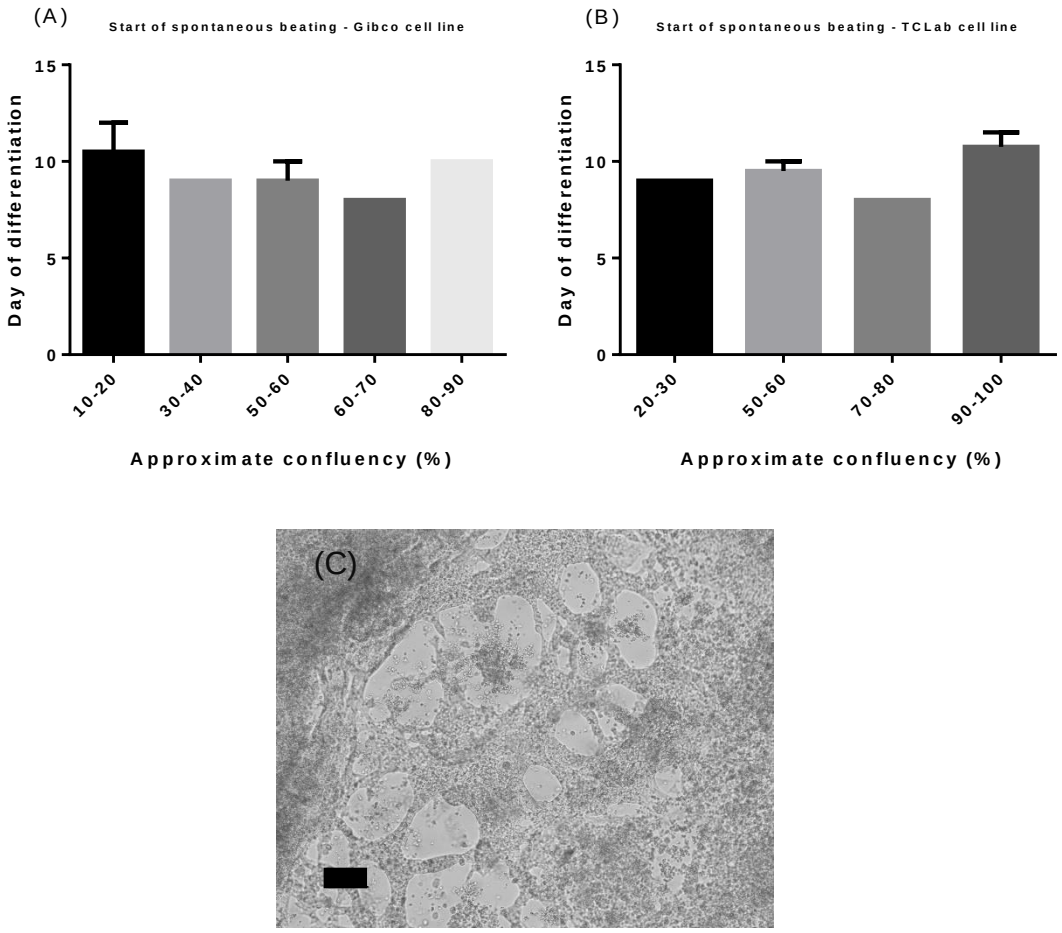

Figure 4.13 (A-B) First day of spontaneous beating of hiPSC differentiated in monolayer for Gibco (A) and **(B) TCLab cell line.** It was registered for each approximate confluency and for each cellular line the first day of the spontaneous beating. **(A)** Gibco cell line: 10-20% (n=2), 30-40% (n=1), 50-60% (n=2), 60-70% (n=1), 80-90% (n=1). **(A)** TCLab cell line: 20-30% (n=1), 50-60% (n=2), 70-80% (n=1), 90-100% (n=2). It is presented the mean value ± SEM. **(C) Morphology of hiPSC-CM in the first day of spontaneous contraction.** In this image is represented Gibco cell line. Scale bar: 100 µm.

Table 4.5 Start of the spontaneous contraction for cells differentiated in 2D. It is represented the different approximate confluences (%) and cell lines (Gibco and TCLab). The approximate confluency to correspond to a n>1 is presented the mean value ± SEM value.

Cell line	Approximate confluency (%)							
	10-20	20-30	30-40	50-60	60-70	70-80	80-90	90-100
Gibco	10.5±1.5	-	9.0±0	9.0±0	8	-	10.0±0	-
TCLab	-	9	-	9.5±0.5	-	8	-	10.8±0.8

Gibco and TCLab cells started to contract between day 8 and 12. In previous experiments it was reported that hPSC differentiation into the cardiac lineage as monolayer started to contract spontaneously between day 7 – 9, and here we observe that the start of the spontaneous beating was relatively delayed [96]. It is important to note that, for the Gibco cell line an approximate confluency superior at 90% before cardiac induction did not display spontaneous beating, which also occurred when using the TCLab cell line with confluences below 20%.

Interestingly, the approximate confluences that showed an earlier spontaneous beating, are the same ones that have a higher percentage of cTnT-positive cells. In the case of the Gibco cell line, cells with an approximate confluency of 60-70% before cardiac induction started to beat at day 8 and had 42.1% of cTnT-positive cells. On the other hand, TCLab cells that began the cardiac induction with an approximate confluency of 70-80%, started to show spontaneous beating at day 8 and had a 36.7% of cTnT positive cells. This might indicate a direct relation between the first day that the cells demonstrate spontaneous beating and the percentage of cTnT that will be obtained.

At day 12 of cardiac differentiation, cells were recovered and tested for the expression of intracellular cardiomyocyte-specific markers (**Figure 4.14**) or replated into Matrigel-coated plates and cultured an additional 2-3 days in CMM before initiating the staining procedure (**Figure 4.15**).

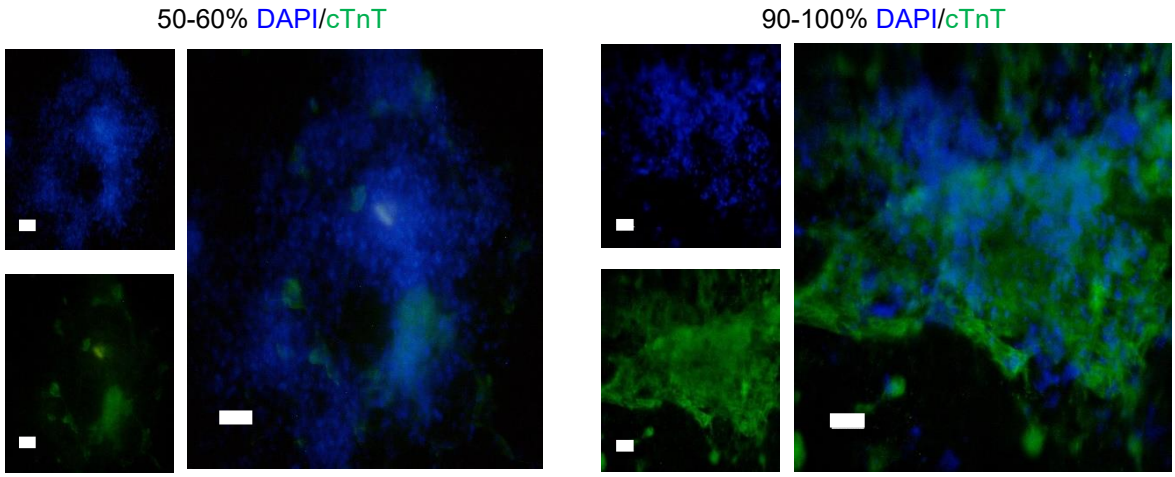

Figure 4.14 Intracellular staining of hiPSC-CM differentiated in monolayer. Above each group of images, it is mentioned the approximate percentage of confluence before the cardiac induction. DAPI staining is represented in blue, and cTnT in green. This experiment was performed with TCLab cell line. Scale bars: 50 μm

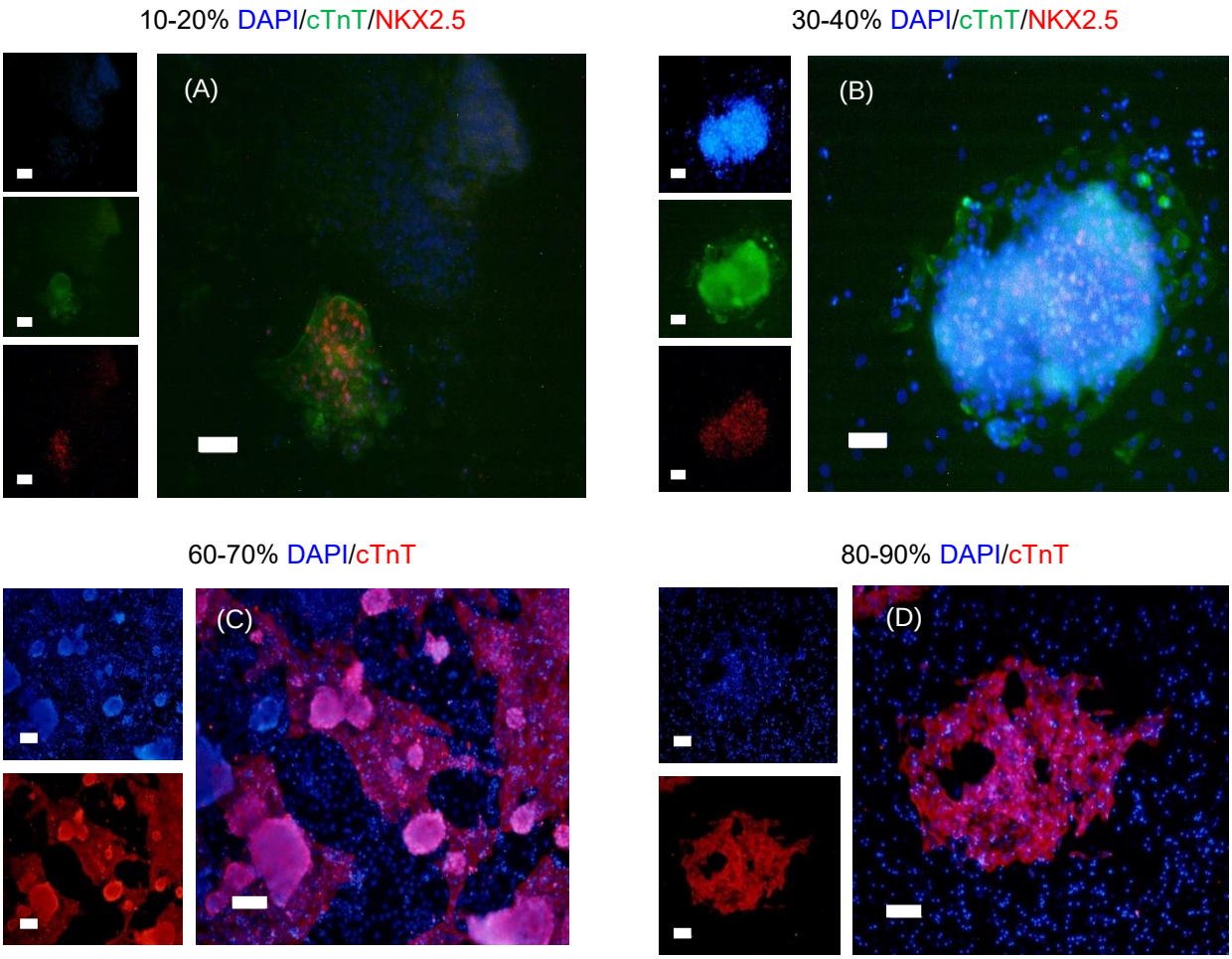

Figure 4.15 Intracellular staining of hiPSC-CM differentiated in monolayer. Above each group of images, it is mentioned the approximate percentage of confluence before the cardiac induction. This experiment was performed with Gibco cell line. **(A-B)** DAPI staining is represented in blue, cTnT in green and NKX2.5 in red in. Scale bars 50 µm **(C-D)** DAPI staining is represented in blue and cTnT in red in**.** Celle were not stained with NKX2.5. Scale bars: 100 µm.

In **Figure 4.14** hiPSC-CM were marked with NKX2.5, cTnT and DAPI, but only DAPI and cTnT had a positive staining. The NKX2.5 is a cardiac progenitor marker expressed before cTnT. [67, 81, 96] This may indicate that at day 12 of differentiation there is a lower expression of the NKX2.5 gene, not being possible to access its expression by immunocytochemistry. Nevertheless, the hiPSC-CM expressed the cTnT marker, which may indicate a successful differentiation [96].

In **Figure 4.15** were used three different markers (NKX2.5, cTnT and DAPI) in **(A)** and **(B)** and only two different markers (cTnT and DAPI) in **(C)** and **(D)**. The replated cells expressed all the cardiac markers which appears to indicate an efficient differentiation into cardiomyocytes. In replated hiPSC-CM the staining for NKX2.5 was positive. This marker expression could be due the expansion of replated cells in the new Matrigel coated wells.

Overall, these results might suggest a successful cardiac differentiation in adherent culture of hiPSC [96]. However, immunocytochemistry characterization is only a quantitative analysis, being needed quantitative analysis to corroborate the obtained results. One quantitative analysis performed was flow

cytometry using the cardiomyocyte marker cTnT. The results are depicted in **Figure 4.16**, that represent the percentage of cTnT positive cells according to approximate confluency before initiating the cardiac induction of hiPSC (**Figure 4.16 A** and **B**). Also, using equation (4) the cardiomyocyte yields were calculated (***Figure 4.16*** **C** and **D**).

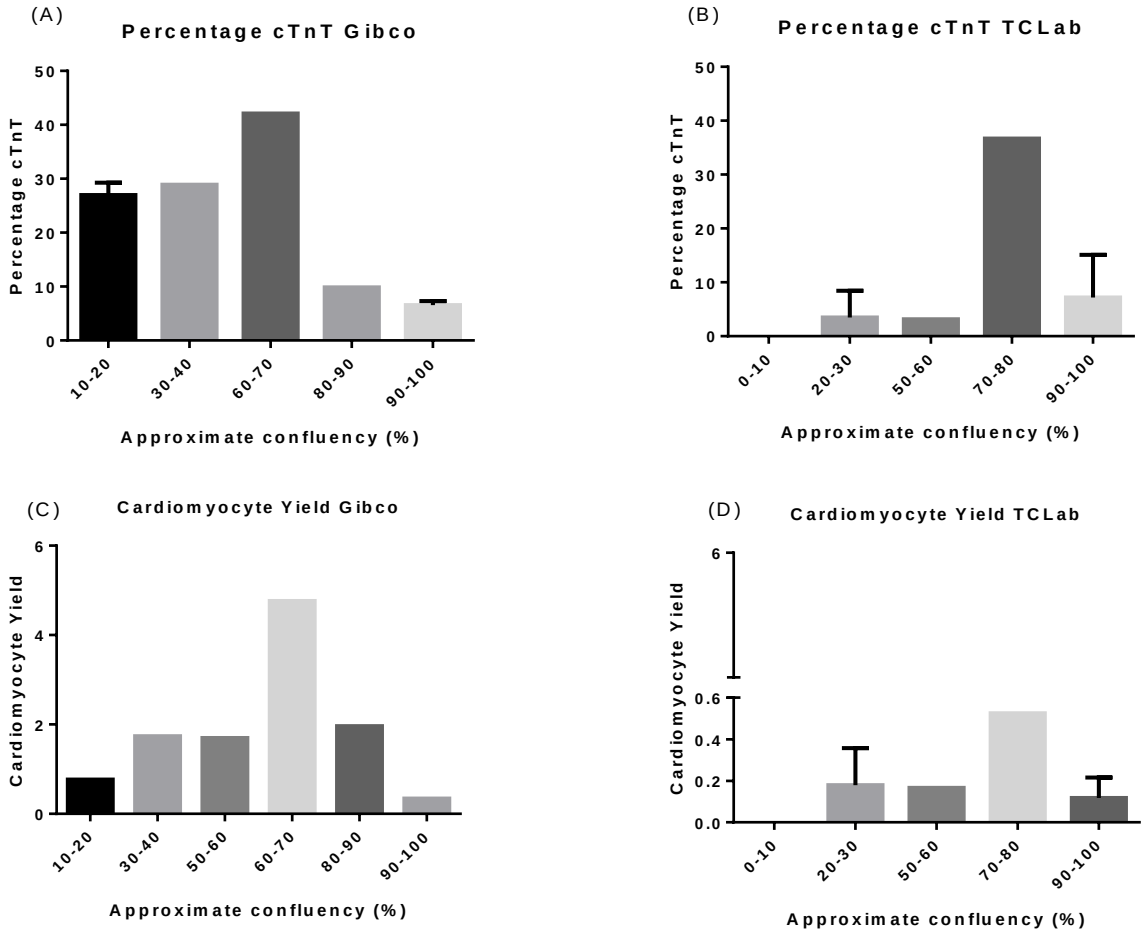

Figure 4.16 (A-B) Percentage of cTnT positive cells according to the approximate confluency before cardiac induction for Gibco cell line (A) and for TCLab cell line (B).) The differentiation process was initiated at different approximate confluences in monolayer and the percentage of cTnT at day 12 of differentiation is represented in function of the initial approximate confluency. For Gibco cell line: 30-40%, 60-70% and 80-90% (n=1), 10-20% and 90-100% (n=2). For TCLab cell line: 50-60% and 70-80% (n=1), 0-10, 20-30% and 90-100% (n=2) **(C-D) Cardiomyocyte Yield obtained in monolayer for Gibco cell line (C) and for TCLab cell line (D).** The cardiomyocyte yield in monolayer was calculated using equation (4) for the different approximate confluences. n=1 for Gibco cell line and for TCLAb cell line: 50-60%, 70-80% (n=1), 0-10%, 20-30% and 90-100% (n=2). Error bars represent the SEM value.

Table 4.6 Percentage of cTnT positive cells for the different approximate confluences (%) for both cell lines. For the confluences in which the n>1 are presented the mean value ± SEM value.

Cell line	Approximate confluency (%)							
	10-20	20-30	30-40	50-60	60-70	70-80	80-90	90-100
Gibco	30.0±2.3%	-	28.9%	-	42.1%	-	9.8%	6.5±0.8%
TCLab	-	7.0%	-	3.1%	-	36.7%		7.2±5.6%

As is depicted in **Figure 4.16 A** and **B** and **Table 4.6** the most suitable approximate confluency for the cardiac differentiation is between an average confluence of 60 and 70% for Gibco and between 70 and 80% for TCLab cell line. For both the cell lines the higher confluences did not lead to a successful differentiation (approximate confluency 90-100%). This fact is corroborated by the work of Burridge and co-workers that highlight the fact that the prevention of over confluence is determinant for a successful cardiac differentiation [96]. At the same time, Lian *et al* described the need of generating confluent monolayers in order to perform efficient differentiations [95]. This may indicate that average cell confluence before cardiac induction plays a role in the efficiency of the differentiation towards the concentration of the paracrine factors.

The cTnT positive cells in the two cell lines for the same approximate confluency portrays different percentages. This could be caused by different rates and conditions at which different hiPSC lines differentiate into cardiomyocytes, being necessary to further optimize the differentiation conditions for the different cell lines [128, 129]. In addition, for the Gibco cell line it was possible to obtain higher values of cTnT positive cells for a wider range of approximate confluences than for the TCLab cell line. It is known that hiPSC lines display some epigenetic diversity being more prone to be differentiated in some cellular lineages that others [101]. This can explain the wider range of approximate confluences for the Gibco cell line, in which it was possible to obtain higher percentages of cTnT positive cells. Also, the lower percentage of cTnT positive cells that we obtained, comparatively to the article in which our protocol is based, could be explained by the usage of cell lines less prone to cardiac differentiation [96].

In addition, in most of the protocols cardiomyocytes were differentiated at least for 15 days [94-96]. So, if cardiac induction was prolonged, probably it would be possible to achieve higher percentages of cTnT.

Also, an "*off-the-shelf*" culture medium that has a constant concentration of the molecules to induce and to inhibit the Wnt signalling pathway was used. These concentrations could be not adequate to the culture system that we are testing. Namely, the concentration of CHIR included in Cardiomyocyte Medium Differentiation A was 6 µM but has been reported that the optimal CHIR concentration for 2D culture is different than for 3D culture [41]. Namely, for 2D culture the optimal concentration was mentioned to be 10 µM of CHIR and for 3D only 7.5 µM suggesting a differential activity of GSK3 in 2D and 3D [41].These results were obtained for an ESC and later confirmed by hiPSC lines. Probably for an efficient monolayer differentiation would be necessary a higher CHIR concentration than the one used in aggregates [41]. These conclusions were corroborated by posterior works from the same researchers, although the CHIR concentrations that lead to better results were not the same as previously mentioned [130].

To enhance the cardiomyocytes percentage, it is also possible to use a purification method. Kadari *et al*. [131] tried to develop a robust protocol for the generation of cardiomyocytes through the differentiation in monolayer for several iPSC lines and obtained yields from 33 to 92% of cTnT positive cells of different iPSC cell lines, before purification. This high range of cTnT positive cells sustains the high line-to-line variability. Nevertheless, they demonstrate that even the lowest percentages of cTnT positive cells could be optimized up to 74% using the lactate purification method [109, 131]. Moreover, Nguyen [108] *et al.* were able to achieve percentages of ~90% of cTnT from initial populations of 10-

40% of cardiomyocytes by generating 3D cardiospheres from adherent cultures of cardiomyocytes, using microwells. Thus, both methods could also be used to improve the cTnT percentage obtained by our protocol under adherent culture conditions.

Concerning the cardiomyocytes yield (**Figure 4.16 C**), the Gibco cell line revealed results higher than 1 using approximate confluences between 30 and 90%, implying that in the end of the differentiation, the number of obtained cardiomyocytes was at least the same as the number of seeded hiPSC. The TCLab cell line did not demonstrate results higher than 1, despite the approximate confluency of 70-80% had associated a value of 36.7% of cTnT-positive cells. The lower value of the cardiac yield in this case, was due to a low number of cells collected in the end of the cardiac differentiation. These low numbers could be due to the death and loss of cells during the enzymatic dissociation and collection of the cells.

4.4 Differentiation of hiPSC into cardiomyocytes as 3D suspension aggregates

Previously formed aggregates in StemFlex culture medium were expanded for up to 7 days before the beginning of the cardiac differentiation. In **Table 8.3** (**Supplementary Information**) are presented the average aggregate diameters for each seeding density before the start of the cardiac induction and the number of times that different average diameters were obtained in **Figure 8.2** (**Supplementary Information**). The morphology of the hiPSC aggregates was different from the one presented by hiPSC-CM as it is represented in **Figure 4.17**.

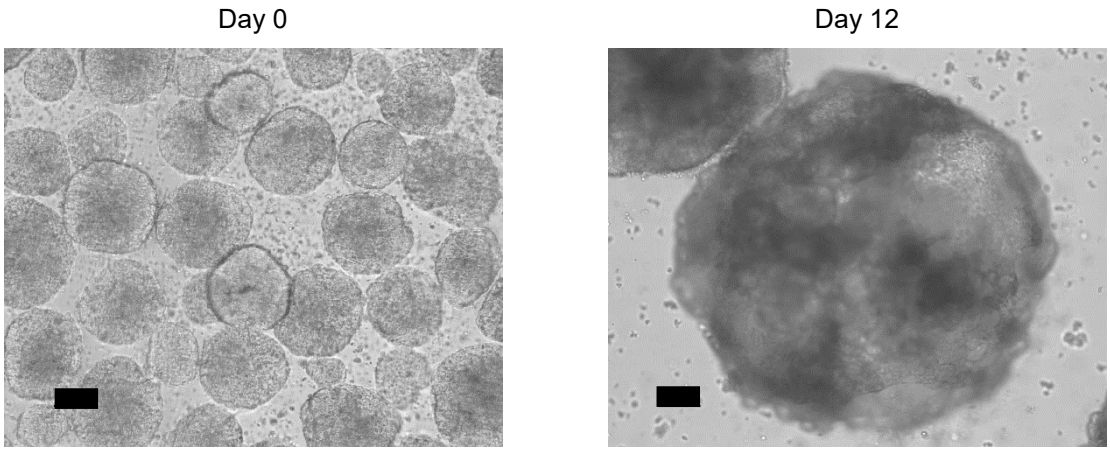

Figure 4.17 Morphology of hiPSC differentiated as suspension aggregates at day 0 (left) and day 12 (right) of differentiation. It is represented an average diameter of 195-205 µm, obtained with a seeding density of $5.0\times10^{+05}$ cells/mL. Scale bars: 100 µm.

In an efficient differentiation, the round shape aggregates from day 0 originated contracting and denser aggregates, with vast diameters (**Figure 4.17** C).

Despite the importance of the initial aggregates diameter for the success of the cardiac differentiation, some slight differences in the diameter did not lead to significative differences in the efficiency of cardiac differentiation [41]. As it was mentioned before in the section **4.2.3 Day by Day diameter aggregates evolution** the obtained aggregates in one seeding density were heterogenous in size and in shape, as

well. This could lead to variations of cardiac differentiation efficiency, being more difficult to identify the appropriate aggregates diameter before the cardiac induction. To overcome this problem, a suspension culture system (e.g. a spinner flask) could be used to promote aggregate homogeneity [129]. Also, homogeneity could be accomplished through the usage of a microwell system to form the aggregates, and then the aggregates could be transferred to a free suspension culture system [39, 40]. As mentioned before, the average diameter does not change drastically between different seeding densities, being possible to compare the impact of the seeding density in the efficiency of the cardiac differentiation.

To evaluate the effect of the initial hiPSC density towards the efficiency of cardiac differentiation, the first day of spontaneous beating of the hiPSC-CM aggregates was monitored (***Figure 4.18***). Also, the percentage of aggregates that were contracting spontaneously in the first day of spontaneous contraction and in the last day of differentiation was calculated (***Figure 4.18*** **C**). The diameter and the morphology of the both cell lines in the day that started beating and in the last day of differentiation (**Figure 8.3** and **Figure 8.4** – **Supplementary Information**).

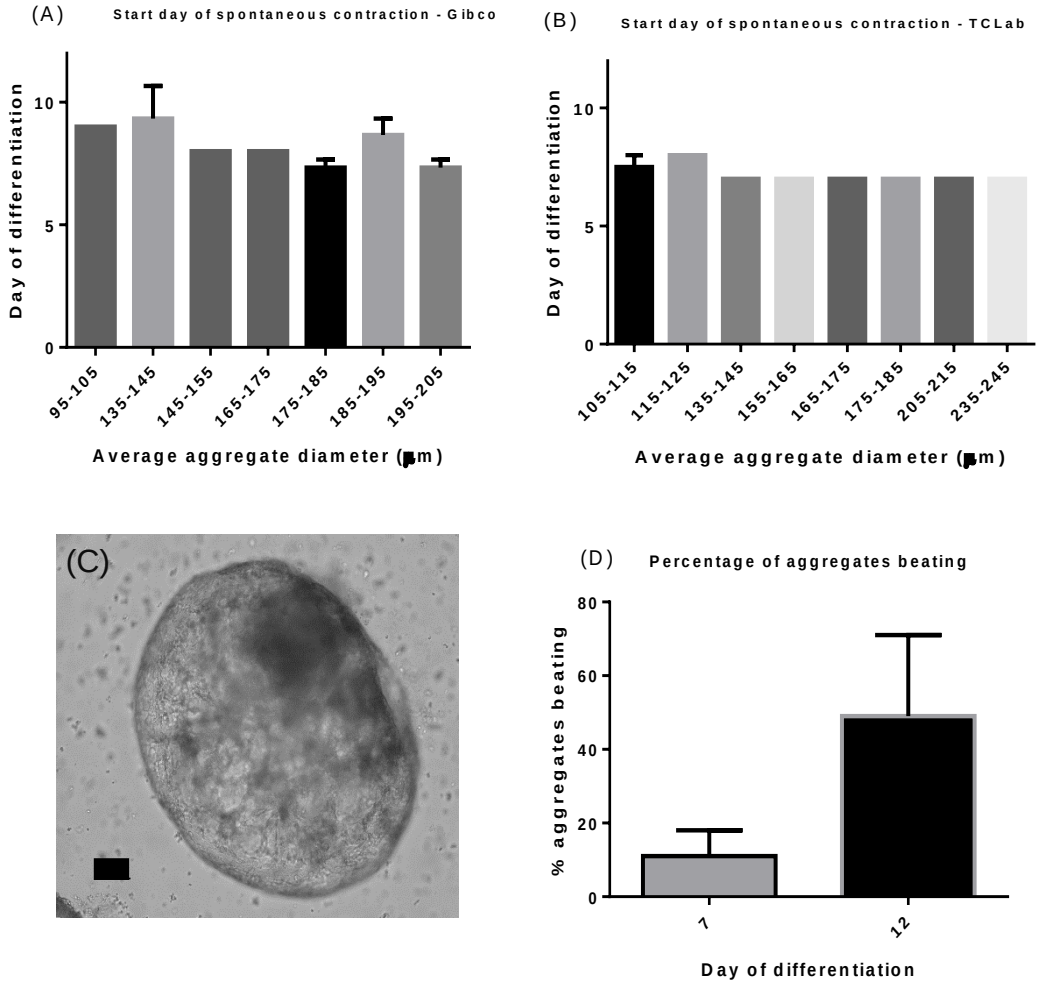

Figure 4.18 (A-B) First day of spontaneous beating of hiPSC differentiated as aggregates according to the average diameter before cardiac induction for Gibco (A) and TCLab (B) aggregates. (A) Gibco aggregates: 95-105 µm, 165-175 µm, 195-205 µm (n=1), 145-155 µm (n=2) and 135-145 µm, 175-185 µm, 185-195 µm (n=3), 195-205 µm (n=3). **(B)** TCLab aggregates: 115-125 µm, 135-145 µm, 165-175 µm, 235-245 µm (n=1), 105-115 µm, 155-165 µm (n=2) and 175-185 µm (n=3)**. (C) Morphology of hiPSC-CM in the first day of spontaneous aggregates contraction.** Scale bar: 100 µm **(D) Percentage of beating aggregates in the first day of the spontaneous beating (day 7) and at day 12** (n=2)**.** This experiment was performed with Gibco cell line with an average aggregate diameter between 195-205 µm. Error bars represent the SEM value when n>1.

Table 4.7 Start of the spontaneous contraction for cell differentiated in 3D. It is represented the different approximate confluences (%) and cell lines (Gibco and TCLab). The average diameters to correspond to a n>1 is presented the mean value ± SEM value.

Cell line	Approximate confluency (%)											
	95-105	105-115	115-125	135-145	145-155	155-165	165-175	175-185	185-195	195-205	205-215	235-245
Gibco	9±0	-	-	8.0±0	8.67± 1.67	-	8.0±0	7.33± 0.33	8.67± 0.67	8±0	-	-
TCLab	-	7.5± 0.5	8±0	7±0	-	7±0	-	7±0	-	-	7±0	7±0

Gibco cell line aggregates with an average diameter of 175-185 µm and 195-205 µm presented spontaneous beating at day 7.33±0.33 (**Figure 4.18 A** and **Table 4.7**). TCLab aggregates with an

average diameter of higher than 135 µm before cardiac induction, started to contract spontaneously at day 7 (**Figure 4.18 B** and **Table 4.7**). The earliest day that the aggregates demonstrate spontaneous beating was day 7 of differentiation for both the cell lines (***Figure 4.18*** **A** and **B**).

Concerning the Gibco cell line aggregates there is no clear division for which diameters lead to an early spontaneous beating. Apparently the more suitable diameter for an early spontaneous beating is 175-185 µm or 195-205 µm. The average diameter that leads to a higher value of cTnT is between 195-205 µm with an average value of 36.81±20.84%. This seems to indicate, that there is a correlation between the early beginning of the spontaneous beating and higher percentages of cTnT positive cells. In the case of TCLab aggregates, an average diameter lower than 125 started to show spontaneous beating later than the bigger average diameters: 125-235 µm. In the case of TCLab cell line, is difficult to choose a range for the aggregates diameter that leads to an earlier start of the spontaneous beating. Although, for diameters lower than 125 µm the average percentage of cTnT positive cells is 6.80% and for diameters higher than 125 µm is 13.3%. Once again, appears than with the early start of the spontaneous beating are associated higher percentages of cTnT.

Fonoudi *et al.* [132], also performed experiments with the goal of differentiating aggregates of hPSC (both hESC and hiPSC) into cardiomyocytes [132]. They used a more complex protocol, in which besides modelling the canonical Wnt signaling pathway, they used a cocktail of small molecules to modulate other signaling pathways. However, the earliest spontaneous beating was at day 7 of cardiac differentiation [132]. Using our protocol that only modulates the Wnt pathway, it was possible to achieve similar results, concerning the initiation of the spontaneous beating. In ***Figure 4.18*** **D**, the percentage of aggregates beating at day 7 was 11.0±7.0% and at day 12 of differentiation was 49.0±22.0%. Both experiments were performed using Gibco cell line. Through the analysis of these results it seems that the value of the initial percentage of beating aggregates will directly influence the beating percentage at day 12. Interestingly the results for flow cytometry, that were performed at day 12 of differentiation, revealed very similar values to the ones obtained by counting the beating aggregates. Namely, it was obtained an average value of 49.3±28.9% by flow cytometry (**Figure 8.5 – Supplementary Information**).

hiPSC-CM were recovered at day 12 of differentiation, replated upon Matrigel-coated plates, and cultured up to 3 more days under adherent conditions using CMM medium. The replating was performed to allow a better visualization of the staining from the different markers. At this point, replated cells from the two hPSC lines were analyzed for the expression of cardiac markers namely cTnT and NKX2.5 (**Figure 4.19** for Gibco cell line and **Figure 4.20** for TCLab cell line).

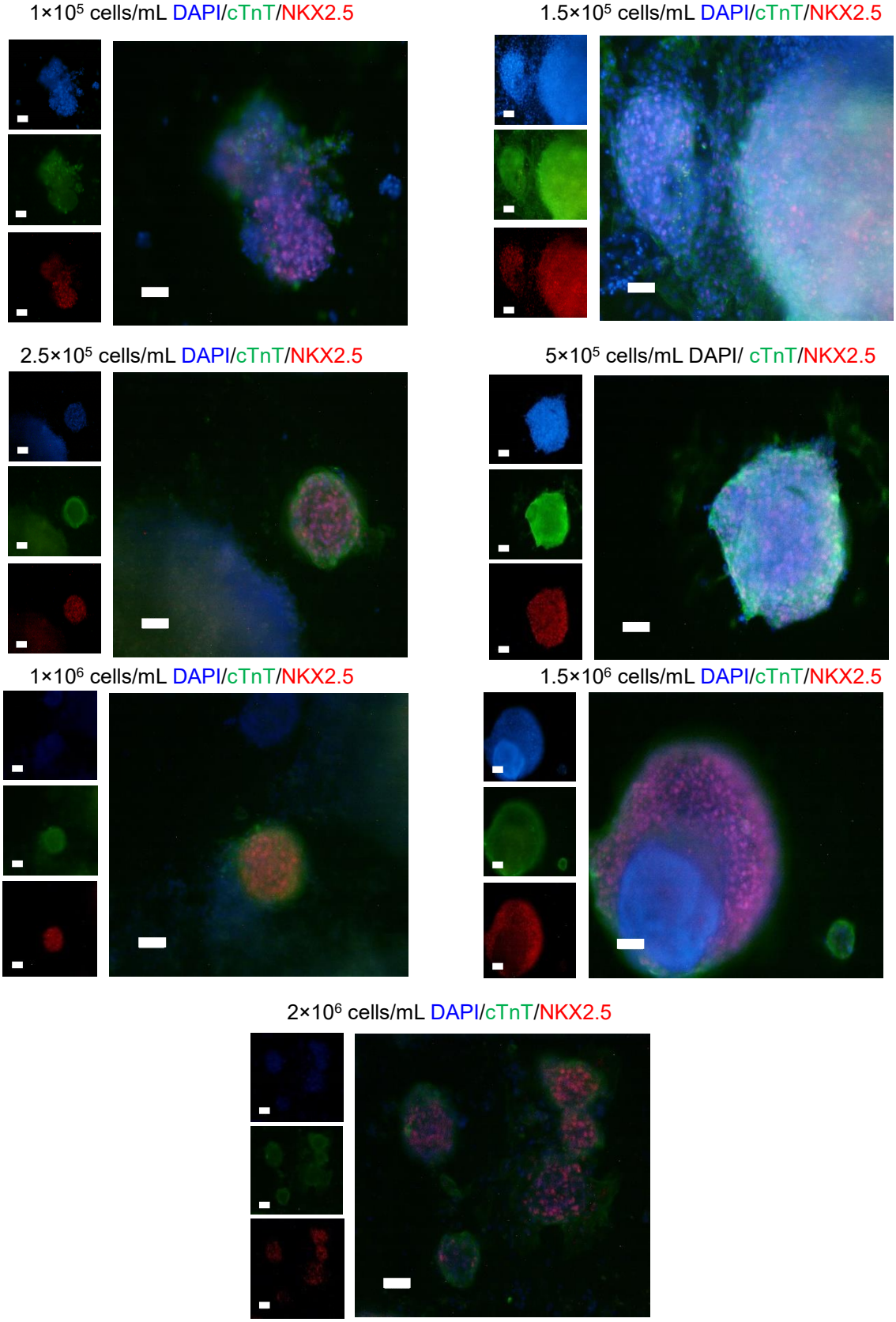

Figure 4.19 Intracellular staining of hiPSC-CM differentiated as suspension aggregates, for Gibco cell line. Above each image it is mentioned the initial seeding density (cells/mL). DAPI staining is represented in blue, cTnT in green and NKX2.5 in red. Scale bars: 50 μm.

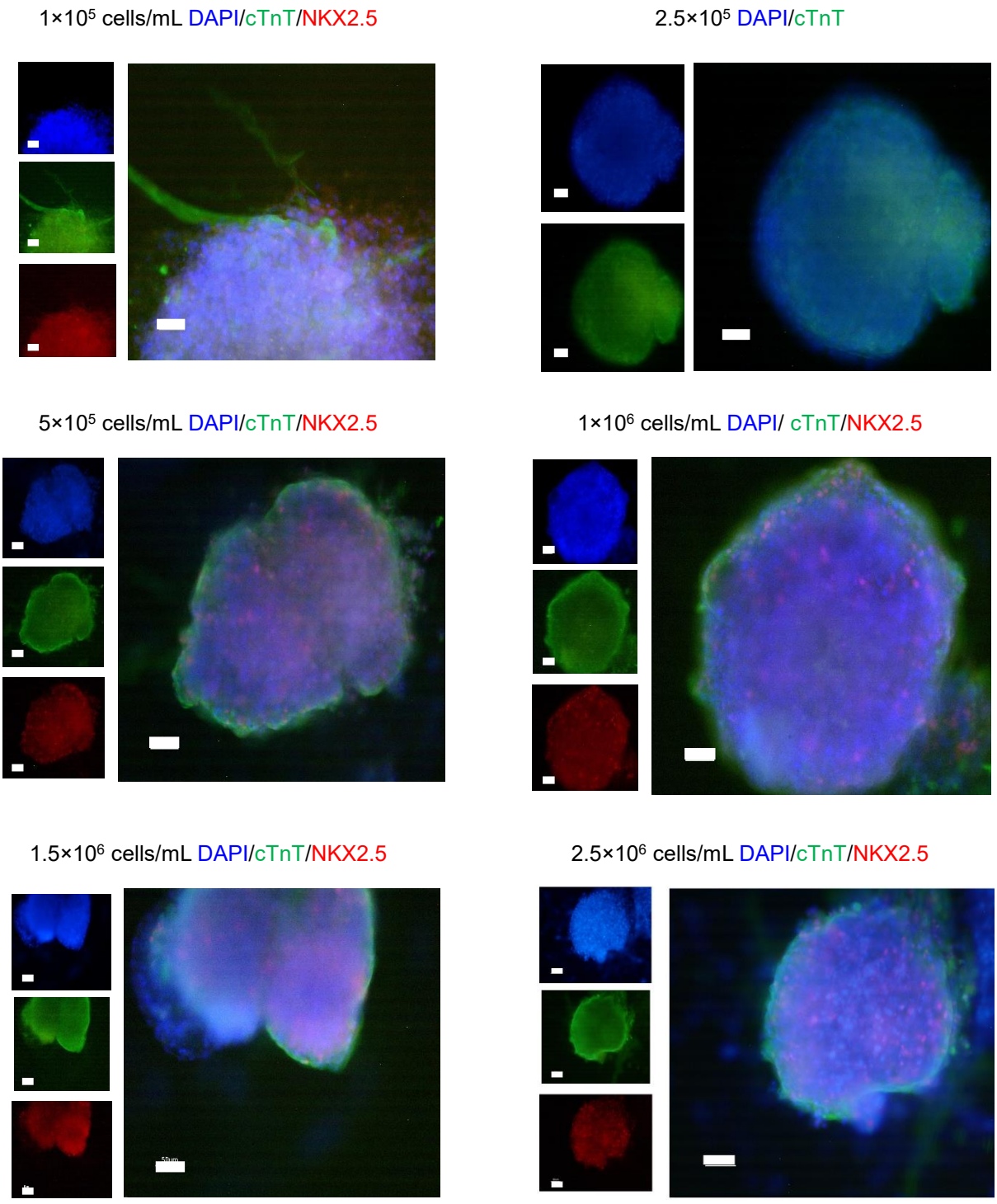

Figure 4.20 Intracellular staining of hiPSC-CM differentiated as suspension aggregates, for TCLab cell line Above each image it is mentioned the initial seeding density (cells/mL). DAPI staining is represented in blue, cTnT in green and NKX2.5 in red. Scale bars: 50 μm

The immunocytochemistry appears to indicate a successful differentiation of the hiPSC (for Gibco and TCLab cell line) into cardiomyocytes [41, 96]. It is possible to visualize the three markers in aggregates from all seeding densities in the Gibco cell line. For the TCLab cell line, it was only visible the cTnT and DAPI staining in the seeding density 2.5×10^5 cell/mL. The absence of this marker may indicate cardiomyocytes in a more mature state, since the NKX2-5 gene expression occur before the TNNT2 [96]. Altogether, these results appear to indicate a successful differentiation. However, these analyses are only qualitative, being needed quantitative results to validate them.

To better evaluate the effect of the seeding density upon the efficiency of the cardiac differentiation of hPSC, the percentage of cTnT-positive cells at day 12 of differentiation was assessed by flow cytometry (**Figure 4.21 A**-**D**). Also, the yield of cardiomyocytes differentiated from hPSC was calculated using equation (4) (**Figure 4.21 E** and **F**).

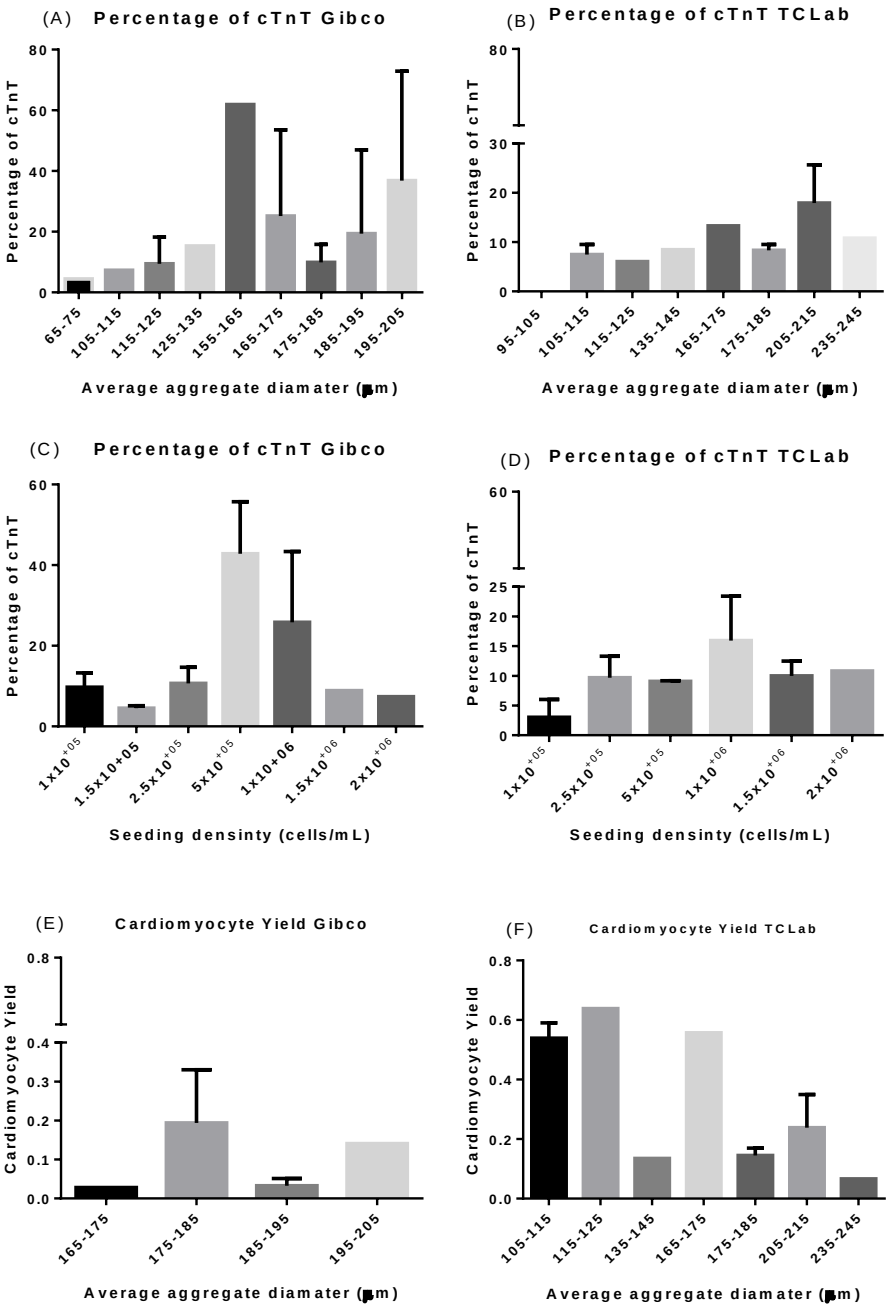

Figure 4.21 (A) % cTnT positive cells before cardiac induction for Gibco aggregates according to the average aggregate diameter: 65-75 (n=1), 105-115 (n=1), 115-125 (n=3), 125-135 (n=1), 155-165 (n=1), 165-175 (n=2), 175-185 (n=3), 185-195 (n=4), 195-205 (n=3) µm. **(B) % cTnT positive cells before cardiac induction for TCLab aggregates according to the average aggregate diameter:** 95-105 (n=1), 105-115 (n=2), 115-125 (n=1), 135-145 (n=1), 165-175 (n=1), 175-185 (n=2), 205-215 (n=2), 235-245 (n=1) µm. **(C) % cTnT positive cells before cardiac induction for Gibco aggregates according to the seeding density:** $1\times10^{+05}$ (n=3), $1.5\times10^{+05}$ (n=3), $2.5\times10^{+05}$ (n=4), $5\times10^{+05}$ (n=5), $1\times10^{+06}$ (n=3), $1.5\times10^{+06}$ (n=1), $2\times10^{+06}$ (n=1) cells/mL **(D) % cTnT positive cells before cardiac induction for TCLab aggregates according to the seeding density:** $1\times10^{+05}$ (n=2), $2.5\times10^{+05}$ (n=2), $5\times10^{+05}$ (n=2), $1\times10^{+06}$ (n=2), $1.5\times10^{+06}$ (n=2) and $2\times10^{+06}$ (n=1) cells/mL **(E) Cardiomyocyte Yield obtained for Gibco aggregates according to the average aggregate diameter before cardiac induction:** 165-175 (n=1), 175-185 (n=3), 185-195 (n=3), 195-205 (n=1) µm. **(F) Cardiomyocyte Yield obtained for TCLab aggregates according to the average aggregate diameter before cardiac induction:** 105-115 (n=2), 115-125 (n=1), 135-145 (n=1), 165-175 (n=1), 175-185 (n=3), 205-215 (n=2), 235-245 (n=1) µm. The error bars represent the SEM value.

The percentage of cTnT positive cells obtained for Gibco cell line with an average diameter of 155-165 µm was 61.93%, 165-175 µm was 25.15±20.09%, 175-185 µm was 9.90±3.44%, 185-195 µm was 19.36±13.82%, 195-205 µm was 36.81±20.84% (**Figure 4.21** A). In the case of the TCLab cells differentiated as aggregates, the percentage of cTnT positive cells obtained for average diameter of 165-175 µm was 13.3%, 175-185 µm was 8.34±0.83%, 205-215 µm was 17.95±5.45% and 235-215 µm was 10.8% (**Figure 4.21** B). In the average diameters that correspond to a n>1, it is presented the mean value ± SEM value.

Through **Figure 4.21 A** it is possible to observe that the better results for the Gibco cell line were obtained between the diameters of 155-205 µm with an overall average value of 30.6%. The highest value obtained in one experiment was 78.18% and it was obtained with an average diameter before cardiac induction of 195-205 µm. Also, Gibco aggregates with an average diameter lower than 135 µm expressed a very low percentage of cTnT. Etoc *et al.* [133] micropatterned hESC colonies that recapitulate the spatial arrangement of the germ layers, in order to unveil the earliest aspects of human embryogenesis [133]. They discovered that cells establish their fate by measuring their distance from the edge and that the reduction of the diameter eliminates the mesodermal fates, which can explain the fact that with diameters lower than 135 µm the percentage of cTnT positive cells is below 15%. Also, Fonoudi *et al.* [132], when performed experiments to discover the best aggregate diameter to cardiac induction realized that for smaller diameters (between 60-120 µm) occurred the disruption and the dispersion of the aggregates, after the CHIR treatment [132]. This, once again can explain the low values for cTnT obtained with diameters lower than 135 µm.

On the other hand, in **Figure 4.21 B**, is possible to observe that the percentage of cTnT-positive cells for the TCLab cell line is very similar for all the diameters. Nevertheless, a slightly higher percentage of cTnT is attained for an average diameter of 205-215 µm and highest result obtained was 23.4%. These results appear to indicate that the optimal hPSC diameter for the initiation of the cardiac induction has line-to-line variability [131].

Considering both cell lines, it was possible to achieve higher results for wider ranges of aggregate diameters for the Gibco cell line than for the TCLab cell line. This could indicate that the Gibco cell line is more prone to cardiac differentiation than the TCLab cell line, that could be related with the epigenetic memory of hiPSC cell lines [101]. This is corroborated by the results obtained in the 2D differentiation.

Fonoudi and co-workers [132] when establishing a protocol for cardiac differentiation in aggregates, identified the better diameters for the beginning of the cardiac differentiation between 150-200 µm for several hESC and hiPSC cell lines [132] .These results are very similar to the ones obtained in this work: 155-205 µm (considering the two cells lines that were used). Therefore, this seems to indicate that the aggregates diameters before cardiac induction is an important parameter to the differentiation efficiency into cardiomyocytes that must be optimized.

In **Figure 4.21 C** and **D** the percentage of cTnT positive cells is presented accordingly to the seeding density. It seems that the best seeding densities for the cardiac induction are $5.0\times10^{+05}$ and $1.0\times10^{+06}$ cells/mL for Gibco cell line (**Figure 4.21 C**). The results obtained for TCLab were not very conclusive

seeming that the best seeding density is $1.0\times10^{+06}$ cells/mL (**Figure 4.21 D**). Once again, higher percentages of cTnT-positive cells were achieved using the Gibco cell line for a wider range of seeding densities rather than using the TCLab cell line. Kempf *et al.* previously conclude that the initial density was relevant mainly due to the concentration of paracrine factors that are released from the cells to the culture medium, appearing to be important to the initial cells survival and a correct aggregate formation [41].

The cardiomyocyte yield concerning the aggregates, despite being higher for the TCLab cell line, is relatively low for both cell lines, as it is depicted in **Figure 4.21 E and F.** If the cardiomyocyte yield was equal 1, the number of cTnT-positive cells was equal to the number of seeded cells, in this differentiation all values were lower than 1. This indicates that the number of cardiomyocytes obtained in the end of the differentiation was lower that the cellular number of hiPSC in the beginning. Therefore, it was not possible to obtain a positive cardiomyocyte yield in this part of the work.

The percentage of cTnT positive hPSC-CM that was obtained was relatively low, but this percentage could be easily enhanced by cardiomyocyte purification after differentiation. Hemmi *et al.* [129] obtained a percentage of 99.5% post-purification cardiomyocytes from an initial population of 25.0% using the lactate method [129]. So, after the day 12 of differentiation aggregates can be purified using the lactate method to be obtained a higher percentage of cTnT positive cells. As mentioned before in section **4.2 Differentiation of hPSC into cardiomyocytes in adherent culture**, it was used a medium that already had in their composition the molecules to induce and to inhibit the Wnt signalling pathway, and the used concentrations could be not adequate for the differentiation as aggregates. Also, the aggregates were only differentiated for 12 days, with an increase of the days of differentiation, probably would be possible to achieve higher percentages of hiPSC-CM [41, 96].

Finally, qRT-PCR was performed using samples collected from aggregates generated with a seeding density of $5\times10^{+05}$ cells/mL. Cells from Gibco cell line were expanded until reaching an average aggregate diameter of 195-205 µm. This seeding and this diameter were used, since it was previously perceptible that they lead to more efficient differentiations. It was assessed the expression of pluripotency gene NANOG at days 0, 1,3, 5, 6, 7, 9 and 12, cardiomyocyte gene TNNT2 at days 0, 5, 6, 7, 9 and 12 of differentiation, normalized against expression at day 0 and expression of housekeeping gene GAPDH. The relative expression of these genes during cardiac differentiation is represented in **Figure 4.22**.+

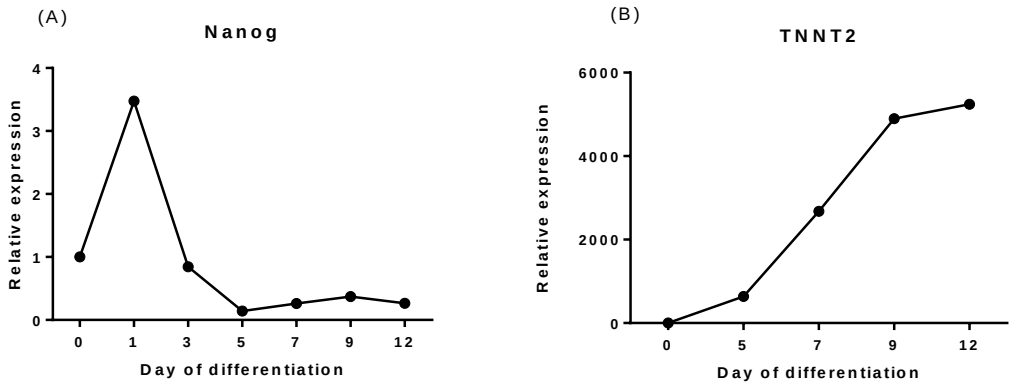

Figure 4.22 Relative expression profiles of pluripotency and cardiac marker during cardiac differentiation of induced pluripotent stem cells. (A) Nanog expression at day 0,1,3,5,7,9, and 12 of cardiac differentiation. **(B)** TNNT2 expression at day 0, 5, 7, 9 and 12 of cardiac differentiation.

Along the differentiation, in general, the expression of the pluripotency gene Nanog decreases, which is expectable since the cells are progressively being committed to the cardiac lineage. Although, at day 1, the value obtained for the relative expression of Nanog is higher than at day 0. As in this work, it was previously reported, in cardiac differentiation as suspension aggregates, that the relative expression of Nanog remained almost constant and very low from day 5 onward [41].

In contrast, gene expression of the cardiomyocyte marker TNNT2 gradually increased over time exponentially. This increase is more pronounced at day 5 of differentiation (vast difference in the relative expression between day 5 and day 7). Interestingly, these aggregates started the spontaneous contraction at day 7. It was previously reported the upregulation of TNNT2 gene from day 5 onward, in aggregates that started contract from day 6 and 7 onward [41].

5 Conclusions

Since the first derivation of hPSC and more specifically the derivation of hiPSC several researchers tried to establish protocols to ensure their correct expansion in order to be possible to differentiate these cells into almost every cellular type. This holds great promises in the field of disease modelling, drug screening, toxicity assays, personalized medicine and even regenerative medicine. So, through the years protocols and media have been developed for the expansion of hPSC that tried to ensure the cellular yield while maintaining the undifferentiated state, in order to later induce the differentiation in a certain cellular type. Cardiomyocyte differentiation attracts special attention, since cardiovascular diseases are the leading cause of death worldwide [71]. So, there is an urge to establish a reliable platform to unveil the mechanisms that are in the origin of these diseases and that at the same time, can generate a big quantity of cardiomyocytes and other cardiac cells that could be used in treatments to ameliorate the quality and quantity of patient's lifetime. Namely, hiPSC can be considered an unlimited source of cardiomyocytes [132]. Several differentiation protocols into cardiomyocytes have been developed throughout the years and some obtained impressive percentages of cTnT positive cells. Although, in most of them all the concentrations of small molecules had to be tuned between different cell lines/culture systems maybe due to their epigenetic memory [101].

This work had two major objectives. The first one was to characterize the expansion of hPSC in adherent culture and as suspension aggregates, in StemFlex medium. The second one, was to establish the best approximate confluence to initiate the cardiac induction, in the case of adherent culture and in the case of suspension aggregates to establish a range of average aggregates diameters to initiate the cardiac induction after hiPSC expansion. It was also included in this second objective to characterize cells during the process of cardiac differentiation through the modulation of the Wnt signaling pathway, to obtain spontaneously beating cTnT positive cells.

Regarding the expansion as adherent culture and also as suspension aggregates the StemFlex medium seems to achieve, in overall, satisfactory results. Immunocytochemistry analysis performed after the expansion revealed the maintenance of the pluripotency markers. Concerning the expansion as aggregates, it was also performed a pluripotency assay in which was observable by immunocytochemistry the differentiation of the hiPSC into the three germ layers, after being expanded as aggregates. Both analysis confirm the pluripotent state of the cells. The fold increase obtained for hiPSC growth in adherent culture seems to indicate that the capacity of proliferation for TCLab cell line is higher than for Gibco cell line. Also, in general with lower seeding densities was possible to achieve higher fold increases. Concerning the aggregates, the fold increase values are lower than the ones obtained in monolayer and once again higher for the TCLab cell line. Additionally, other quantitative analysis was performed at the same time, namely flow cytometry. For cellular culture in monolayer, pluripotency marker levels were always up to 99.6% for Gibco cell line and up to 98.2% for TCLab cell line. Concerning the suspension aggregates it was obtained results off up to 97.6% for Gibco aggregates and up to 95.7 % for TCLab aggregates. Nevertheless, in aggregate culture, it is possible to observe that higher seeding densities lead to a loss of the pluripotency throughout expansion. It was only

obtained 80.3% for the highest seeding density ($1\times10^{+06}$ cells/mL) for the Gibco cells and 70.2% for highest seeding density ($5\times10^{+05}$) for TCLab cells. The evaluation of the efficiency of the aggregation process, during the aggregates formation, revealed that with higher seeding densities the efficiency diminishes. By measuring the day-by-day evolution of the aggregates diameter, it was possibly to conjecture the daily augment of the average diameter and through the Cv calculation was possible to quantify and perceive the heterogeneity of the aggregates diameter. In general, the obtained results seem to indicate that the StemFlex medium could be used successfully for the expansion of hiPSC in adherent culture and as suspension aggregates, as well.

The differentiation protocol was considerably heterogeneous in the originated results. Concerning the cardiac induction in adherent culture, the best results through cytometric analysis, performed at day 12 of cardiac induction, were obtained with Gibco cell line in an approximate confluency of 60-70% before cardiac induction, with 42.1% of cTnT positive cells. For TCLab cell line, the best result was obtained with an approximate confluency of 70-80% with 36.7 % of cTnT positive cells. For both cell lines the percentage of cTnT positive cells for higher and lower confluences was considerably diminished, despite being possible to achieve relatively higher percentages of cTnT positive cells for wider ranges of approximate confluences for the Gibco cell line. These results indicate that cells need to reach a certain level of confluence to result in a good cardiac differentiation, but the over confluence needs to be avoided, as well. [95, 96] The early spontaneous contraction of cells was registered at day 8 of cardiac induction. Interestingly, the approximate confluences that display higher cTnT results were the ones that show an earlier spontaneous contraction for both cell lines. Also, the best approximate confluence was different for Gibco and TCLab cell line. Considering all range of approximate confluences before cardiac induction the percentage of cTnT positive cells obtained for the Gibco cell line was considerably higher than for the TCLab cell line. This could be caused by the different capability that different cell lines hold of differentiating into a specific type of cells. Despite of that, the maximum value obtained was very similar for both cell lines. Also, the concentration of small molecules that was used could be more optimized for a 3D culture system. Concerning the cardiomyocyte yield, only with the Gibco cell line was achieved a yield higher than 1 and not in all the approximate confluences. The best cardiomyocyte yield was obtained to the approximate confluence of 60-70% and for Gibco cell line.

Regarding the cardiac differentiation in a 3D system: it was obtained percentage of cTnT positive cells, at day 12 of cardiac induction, up to 78.2% for Gibco cell line and up to 23.4% for TCLab aggregates. The average aggregates diameters that lead to higher percentages of cTnT cells were between 155-205 µm for Gibco cell line. For the TCLab aggregates the percentage of cTnT positive cells was very similar for all the aggregates diameter, being obtained a slightly higher percentage for an average diameter of 205-215 µm. It was possible to achieve higher cTnT percentages for wider ranges of aggregates diameter for the Gibco cell line that for the TCLab cell line. Concerning the initial seeding density (cells/mL) the ones that lead to better results for Gibco cell line were $5\times10^{+05}$ and $1\times10^{+06}$. For TCLab cell line aggregates was more difficult to define the best seeding density but it appears to be 1×10^{06} cells/mL. The earliest aggregates to present spontaneous beating for both cell lines was at day 7 of cardiac induction, being that the cardiomyocytes in aggregates demonstrate spontaneous beating

before the aggregates cultured in monolayer. Remarkably, the percentages of beating aggregates counted at day 12 were very similar to the percentage of cTnT obtained by flow cytometry. The qRT-PCR confirmed that through the differentiation the expression of pluripotency markers gradually decreases, and the expression of cardiac markers progressively increases. The cardiomyocyte yield for both cell lines in all the different averages diameter was lower than 1. This may indicate that the cardiomyocyte yield in 6 well ultra-low attachment plates is not considerable, being needed to use other type of suspension cultures to improve the cardiac yield.

Comparing the differentiation in 2D and 3D, the 3D system was more robust, since in this system the cardiomyocytes started to contract earlier, and it was obtained higher percentages of cTnT positive cells. This could be due to the 3D system enable the cellular interaction with each other and with the surrounding environment. Also, the cells in vivo are displayed in a 3D layout being this culture system more similar to the in vivo reality. Although, cardiomyocyte yield was higher in monolayer, but it is necessary to considerate that the number of seeded cells was lower and that in a 2D system the yield capability is severely limited by the available space. Also, the best results for cardiac induction, both in 2D and 3D were achieved with Gibco cell line.

To validate all the presented results there is a need to replicate most of the experiments, since exists a lack of replicates, that only were possible to obtain with more available time.

Altogether, in this work we tried to expand hPSC in a recent commercially available medium, in adherent culture and also as suspension aggregates to posteriorly differentiate the cells into cardiomyocytes using a differentiation kit. The results revealed that the StemFlex medium was appropriate and reliable to expand hPSC cells. It was also possible to obtain through the Cardiomyocyte differentiation kit spontaneously beating cells that through different analysis were identified as cardiomyocytes. Although the differentiation protocol did not lead to high percentage of cTnT positive cells, it was possible to assess which are the most suitable approximate confluences, in the case of adherent culture and the most suitable aggregates diameters to induce the cardiac differentiation, in the case of suspension aggregates. So, the combination of the expansion in StemFlex medium with the posterior usage of the Cardiomyocyte differentiation kit holds potential, but still requires further optimization in order to be possible to achieve higher percentages of cTnT positive cells.

6 Future perspectives

Considering the initial objectives of this work, that were to characterize the expansion in StemFlex medium and the differentiation of hPSC into cardiomyocytes using a Cardiomyocyte Differentiation kit, in 2D and 3D, there is a long way to explore in order to optimize this protocol.

As mentioned before one shortcoming of this work is the small number of replicates. Considering the expansion in monolayer, in order to validate the more suitable approximate confluences for the beginning of the cardiac induction there is a need to perform more replicates. For the expansion in aggregates, in order to access the most suitable diameters for the cardiac differentiation, for both cell lines, there is a need to obtain more homogenous aggregates. This could be accomplished by the usage of a rotary orbital shaker [125]. A microwell system, such as AggreWells,® could also be used [39]. Nevertheless, the last option may result in an increase of processing costs, rendering it difficult for bioprocessing development. Also, to ensure the maintenance of pluripotency after the expansion in StemFlex complementary assays could be performed using the pluripotency markers, namely qRT-PCR using OCT4, SOX2 or Nanog or even teratoma formation. These assays will improve the confidence in the pluripotency maintenance after the expansion.

Also, in the next flow cytometry analyses it should be assessed what type of cells are the cTnT negative cells present in culture. It is important to understand if these cells remain pluripotent or if they initiate their differentiation in other cellular type rather than cardiomyocytes, being significant to know if they differentiate into other heart specific cells or just into a different cellular type. In addition, to better understand the differentiation process from hiPSC to cardiomyocytes the expression of other genes than Nanog and TNNT2, such as T/ Brachyury, ISL1 and NKX2.5 should be assessed by qRT-PCR. Also, to enhance the percentage of cTnT positive cells, the days of differentiation should be augmented for at least 15 days, since most of the differentiation protocols have a differentiation period equal or higher than 15 days [96, 119]. Since the percentage of beating aggregates at day 12, was so similar with the percentage of cTnT positive cells obtained, beating aggregates should be counted in more time points, in order to be possible to see the evolution of the percentage of beating aggregates through the days of differentiation. In addition, since all the results for the cardiac yield were very low an apoptosis assay, such as Anexin staining, could be done for different time points, to assess the extent of cellular death during differentiation

The hiPSC derived cardiomyocytes electrophysiological properties should be characterized as well, and this could be performed by patch clamp or nanopillar electroporation [41, 96]. Cells should be classified according to their action potentials in nodal, atrial and ventricular like cardiomyocytes. Also, it should be tested the pharmacological response to drugs with known effects, in order to ensure that the differentiation protocol leads to the formation of bona fide human cardiomyocytes that display the typical properties of early derived cardiomyocytes [41, 100].

After aggregate diameter optimizations before cardiac induction, the culture system should be scaled-up. The aggregates should be expanded and differentiated, for example in rotary spinners flasks in order

to be possible to achieve higher cardiac yields and consequently bigger quantities of cardiomyocytes [41, 119]. After the scale-up, since for some applications there is a need of totally pure population of cardiomyocytes it could be applied some purification method to enhance the percentage of cTnT positive cells and also to ensure that there is no contamination with other types of cells.

In addition, it is important to mention that the medium used for cellular expansion (StemFlex) contains BSA that has animal origin, so for clinical purposes the usage of this medium should be avoided. The use of xeno-free medium for expansion, such as Essential 8, may be considered an alternative to avoid the usage of components with animal origin.

Altogether these alterations will lead to a xeno-free, therefore clinical safe protocol to generate pure and non-tumorigenic populations of cardiovascular progenitor cells, that could lead to cardiomyocytes, endothelial cells and smooth muscle cells. These cells will be produced in large scale with the silver lining of being used in drug screening, disease modelling, personalized and regenerative medicine.

7 References

[1] R. Lanza, J. Gearhart, B. Hogan, D. Melton, E. Pedersen, D. Thomas*, et al.*, *Essentials of stem cell biology* 2nd Edition ed., 2009.

[2] A. J. Becker, C. E. Mc, and J. E. Till, "Cytological demonstration of the clonal nature of spleen colonies derived from transplanted mouse marrow cells," *Nature,* vol. 197, pp. 452-4, Feb 02 1963.

[3] A. Bongso and M. Richards, "History and perspective of stem cell research," *Best Pract Res Clin Obstet Gynaecol,* vol. 18, pp. 827-42, Dec 2004.

[4] M. Hayes, G. Curley, B. Ansari, and J. G. Laffey, "Clinical review: Stem cell therapies for acute lung injury/acute respiratory distress syndrome - hope or hype?," *Crit Care,* vol. 16, p. 205, Dec 12 2012.

[5] T. e. a. Fernandes, *Stem Cell Bioprocessing: For Cellular Therapy, Diagnostics and Drug Development*: Woodhead publishing, 2013.

[6] K. O'Donoghue and N. M. Fisk, "Fetal stem cells," *Best Pract Res Clin Obstet Gynaecol,* vol. 18, pp. 853-75, Dec 2004.

[7] A. Bongso and E. H. Lee, *Stem cells : from bench to bedside*. Singapore ; Hackensack, NJ ; London: World Scientific, 2005.

[8] H. J. Rippon and A. E. Bishop, "Embryonic stem cells," *Cell Prolif,* vol. 37, pp. 23-34, Feb 2004.

[9] K. Takahashi, K. Tanabe, M. Ohnuki, M. Narita, T. Ichisaka, K. Tomoda*, et al.*, "Induction of pluripotent stem cells from adult human fibroblasts by defined factors," *Cell,* vol. 131, pp. 861-72, Nov 30 2007.

[10] M. J. Evans and M. H. Kaufman, "Establishment in culture of pluripotential cells from mouse embryos," *Nature,* vol. 292, pp. 154-6, Jul 09 1981.

[11] G. R. Martin, "Isolation of a pluripotent cell line from early mouse embryos cultured in medium conditioned by teratocarcinoma stem cells," *Proc Natl Acad Sci U S A,* vol. 78, pp. 7634-8, Dec 1981.

[12] J. A. Thomson, J. Itskovitz-Eldor, S. S. Shapiro, M. A. Waknitz, J. J. Swiergiel, V. S. Marshall*, et al.*, "Embryonic stem cell lines derived from human blastocysts," *Science,* vol. 282, pp. 1145-7, Nov 06 1998.

[13] G. de Wert and C. Mummery, "Human embryonic stem cells: research, ethics and policy," *Hum Reprod,* vol. 18, pp. 672-82, Apr 2003.

[14] J. S. Draper, C. Pigott, J. A. Thomson, and P. W. Andrews, "Surface antigens of human embryonic stem cells: changes upon differentiation in culture," *J Anat,* vol. 200, pp. 249-58, Mar 2002.

[15] M. Amit, M. K. Carpenter, M. S. Inokuma, C. P. Chiu, C. P. Harris, M. A. Waknitz*, et al.*, "Clonally derived human embryonic stem cell lines maintain pluripotency and proliferative potential for prolonged periods of culture," *Dev Biol,* vol. 227, pp. 271-8, Nov 15 2000.

[16] K. Takahashi and S. Yamanaka, "Induction of pluripotent stem cells from mouse embryonic and adult fibroblast cultures by defined factors," *Cell,* vol. 126, pp. 663-76, Aug 25 2006.

[17] J. Yu, M. A. Vodyanik, K. Smuga-Otto, J. Antosiewicz-Bourget, J. L. Frane, S. Tian*, et al.*, "Induced pluripotent stem cell lines derived from human somatic cells," *Science,* vol. 318, pp. 1917-20, Dec 21 2007.

[18] N. M. Mordwinkin, P. W. Burridge, and J. C. Wu, "A review of human pluripotent stem cell-derived cardiomyocytes for high-throughput drug discovery, cardiotoxicity screening, and publication standards," *J Cardiovasc Transl Res,* vol. 6, pp. 22-30, Feb 2013.

[19] M. H. Chin, M. J. Mason, W. Xie, S. Volinia, M. Singer, C. Peterson*, et al.*, "Induced pluripotent stem cells and embryonic stem cells are distinguished by gene expression signatures," *Cell Stem Cell,* vol. 5, pp. 111-23, Jul 02 2009.

[20] M. C. Marchetto, G. W. Yeo, O. Kainohana, M. Marsala, F. H. Gage, and A. R. Muotri, "Transcriptional signature and memory retention of human-induced pluripotent stem cells," *PLoS One,* vol. 4, p. e7076, Sep 18 2009.

[21] J. Deng, R. Shoemaker, B. Xie, A. Gore, E. M. LeProust, J. Antosiewicz-Bourget*, et al.*, "Targeted bisulfite sequencing reveals changes in DNA methylation associated with nuclear reprogramming," *Nat Biotechnol,* vol. 27, pp. 353-60, Apr 2009.

[22] M. G. Guenther, G. M. Frampton, F. Soldner, D. Hockemeyer, M. Mitalipova, R. Jaenisch*, et al.*, "Chromatin structure and gene expression programs of human embryonic and induced pluripotent stem cells," *Cell Stem Cell,* vol. 7, pp. 249-57, Aug 06 2010.

[23] A. M. Newman and J. B. Cooper, "Lab-specific gene expression signatures in pluripotent stem cells," *Cell Stem Cell,* vol. 7, pp. 258-62, Aug 06 2010.
[24] N. Malik and M. S. Rao, "A review of the methods for human iPSC derivation," *Methods Mol Biol,* vol. 997, pp. 23-33, 2013.
[25] S. Yamanaka, "Induced pluripotent stem cells: past, present, and future," *Cell Stem Cell,* vol. 10, pp. 678-84, Jun 14 2012.
[26] A. D. Celiz, J. G. Smith, R. Langer, D. G. Anderson, D. A. Winkler, D. A. Barrett*, et al.*, "Materials for stem cell factories of the future," *Nat Mater,* vol. 13, pp. 570-9, Jun 2014.
[27] L. G. Villa-Diaz, A. M. Ross, J. Lahann, and P. H. Krebsbach, "Concise review: The evolution of human pluripotent stem cell culture: from feeder cells to synthetic coatings," *Stem Cells,* vol. 31, pp. 1-7, Jan 2013.
[28] C. Xu, M. S. Inokuma, J. Denham, K. Golds, P. Kundu, J. D. Gold*, et al.*, "Feeder-free growth of undifferentiated human embryonic stem cells," *Nat Biotechnol,* vol. 19, pp. 971-4, Oct 2001.
[29] H. K. Kleinman, M. L. McGarvey, L. A. Liotta, P. G. Robey, K. Tryggvason, and G. R. Martin, "Isolation and characterization of type IV procollagen, laminin, and heparan sulfate proteoglycan from the EHS sarcoma," *Biochemistry,* vol. 21, pp. 6188-93, Nov 23 1982.
[30] S. R. Braam, L. Zeinstra, S. Litjens, D. Ward-van Oostwaard, S. van den Brink, L. van Laake*, et al.*, "Recombinant vitronectin is a functionally defined substrate that supports human embryonic stem cell self-renewal via alphavbeta5 integrin," *Stem Cells,* vol. 26, pp. 2257-65, Sep 2008.
[31] T. Miyazaki, S. Futaki, K. Hasegawa, M. Kawasaki, N. Sanzen, M. Hayashi*, et al.*, "Recombinant human laminin isoforms can support the undifferentiated growth of human embryonic stem cells," *Biochem Biophys Res Commun,* vol. 375, pp. 27-32, Oct 10 2008.
[32] Z. Melkoumian, J. L. Weber, D. M. Weber, A. G. Fadeev, Y. Zhou, P. Dolley-Sonneville*, et al.*, "Synthetic peptide-acrylate surfaces for long-term self-renewal and cardiomyocyte differentiation of human embryonic stem cells," *Nat Biotechnol,* vol. 28, pp. 606-10, Jun 2010.
[33] M. Nagaoka, K. Si-Tayeb, T. Akaike, and S. A. Duncan, "Culture of human pluripotent stem cells using completely defined conditions on a recombinant E-cadherin substratum," *BMC Dev Biol,* vol. 10, p. 60, Jun 02 2010.
[34] K. Watanabe, M. Ueno, D. Kamiya, A. Nishiyama, M. Matsumura, T. Wataya*, et al.*, "A ROCK inhibitor permits survival of dissociated human embryonic stem cells," *Nat Biotechnol,* vol. 25, pp. 681-6, Jun 2007.
[35] L. Li, S. A. Bennett, and L. Wang, "Role of E-cadherin and other cell adhesion molecules in survival and differentiation of human pluripotent stem cells," *Cell Adh Migr,* vol. 6, pp. 59-70, Jan-Feb 2012.
[36] J. Beers, D. R. Gulbranson, N. George, L. I. Siniscalchi, J. Jones, J. A. Thomson*, et al.*, "Passaging and colony expansion of human pluripotent stem cells by enzyme-free dissociation in chemically defined culture conditions," *Nat Protoc,* vol. 7, pp. 2029-40, Nov 2012.
[37] K. Zhang and J. Chen, "The regulation of integrin function by divalent cations," *Cell Adh Migr,* vol. 6, pp. 20-9, Jan-Feb 2012.
[38] R. Edmondson, J. J. Broglie, A. F. Adcock, and L. Yang, "Three-dimensional cell culture systems and their applications in drug discovery and cell-based biosensors," *Assay Drug Dev Technol,* vol. 12, pp. 207-18, May 2014.
[39] S. Rungarunlert, M. Techakumphu, M. K. Pirity, and A. Dinnyes, "Embryoid body formation from embryonic and induced pluripotent stem cells: Benefits of bioreactors," *World J Stem Cells,* vol. 1, pp. 11-21, Dec 31 2009.
[40] J. Dahlmann, G. Kensah, H. Kempf, D. Skvorc, A. Gawol, D. A. Elliott*, et al.*, "The use of agarose microwells for scalable embryoid body formation and cardiac differentiation of human and murine pluripotent stem cells," *Biomaterials,* vol. 34, pp. 2463-71, Mar 2013.
[41] H. Kempf, R. Olmer, C. Kropp, M. Ruckert, M. Jara-Avaca, D. Robles-Diaz*, et al.*, "Controlling expansion and cardiomyogenic differentiation of human pluripotent stem cells in scalable suspension culture," *Stem Cell Reports,* vol. 3, pp. 1132-46, Dec 09 2014.
[42] M. Amit, I. Laevsky, Y. Miropolsky, K. Shariki, M. Peri, and J. Itskovitz-Eldor, "Dynamic suspension culture for scalable expansion of undifferentiated human pluripotent stem cells," *Nat Protoc,* vol. 6, pp. 572-9, May 2011.
[43] S. M. Badenes, T. G. Fernandes, C. A. Rodrigues, M. M. Diogo, and J. M. Cabral, "Scalable expansion of human-induced pluripotent stem cells in xeno-free microcarriers," *Methods Mol Biol,* vol. 1283, pp. 23-9, 2015.

[44] B. W. Phillips, R. Horne, T. S. Lay, W. L. Rust, T. T. Teck, and J. M. Crook, "Attachment and growth of human embryonic stem cells on microcarriers," *J Biotechnol,* vol. 138, pp. 24-32, Nov 06 2008.
[45] M. Amit, J. Chebath, V. Margulets, I. Laevsky, Y. Miropolsky, K. Shariki*, et al.*, "Suspension culture of undifferentiated human embryonic and induced pluripotent stem cells," *Stem Cell Rev,* vol. 6, pp. 248-59, Jun 2010.
[46] R. Zweigerdt, R. Olmer, H. Singh, A. Haverich, and U. Martin, "Scalable expansion of human pluripotent stem cells in suspension culture," *Nat Protoc,* vol. 6, pp. 689-700, May 2011.
[47] C. K. Kwok, Y. Ueda, A. Kadari, K. Gunther, A. Heron, A. C. Schnitzler*, et al.*, "Scalable stirred suspension culture for the generation of billions of human induced pluripotent stem cells using single-use bioreactors," *J Tissue Eng Regen Med,* Apr 06 2017.
[48] Y. Lei, D. Jeong, J. Xiao, and D. V. Schaffer, "Developing Defined and Scalable 3D Culture Systems for Culturing Human Pluripotent Stem Cells at High Densities," *Cell Mol Bioeng,* vol. 7, pp. 172-183, Jun 2014.
[49] C. Kropp, D. Massai, and R. Zweigerd, "Progress and Challenges in Large-Scale Expansion of Pluripotent Stem Cells," *Process Biochemistry,* 2016.
[50] G. Q. Daley and D. T. Scadden, "Prospects for stem cell-based therapy," *Cell,* vol. 132, pp. 544-8, Feb 22 2008.
[51] A. Polymeri, W. V. Giannobile, and D. Kaigler, "Bone Marrow Stromal Stem Cells in Tissue Engineering and Regenerative Medicine," *Horm Metab Res,* vol. 48, pp. 700-713, Nov 2016.
[52] M. Grskovic, A. Javaherian, B. Strulovici, and G. Q. Daley, "Induced pluripotent stem cells--opportunities for disease modelling and drug discovery," *Nat Rev Drug Discov,* vol. 10, pp. 915-29, Nov 11 2011.
[53] X. Carvajal-Vergara, A. Sevilla, S. L. D'Souza, Y. S. Ang, C. Schaniel, D. F. Lee*, et al.*, "Patient-specific induced pluripotent stem-cell-derived models of LEOPARD syndrome," *Nature,* vol. 465, pp. 808-12, Jun 10 2010.
[54] M. C. Marchetto, C. Carromeu, A. Acab, D. Yu, G. W. Yeo, Y. Mu*, et al.*, "A model for neural development and treatment of Rett syndrome using human induced pluripotent stem cells," *Cell,* vol. 143, pp. 527-39, Nov 12 2010.
[55] A. Moretti, M. Bellin, A. Welling, C. B. Jung, J. T. Lam, L. Bott-Flugel*, et al.*, "Patient-specific induced pluripotent stem-cell models for long-QT syndrome," *N Engl J Med,* vol. 363, pp. 1397-409, Oct 07 2010.
[56] P. Beauchamp, W. Moritz, J. M. Kelm, N. D. Ullrich, I. Agarkova, B. D. Anson*, et al.*, "Development and Characterization of a Scaffold-Free 3D Spheroid Model of Induced Pluripotent Stem Cell-Derived Human Cardiomyocytes," *Tissue Eng Part C Methods,* vol. 21, pp. 852-61, Aug 2015.
[57] Y. Shi, H. Inoue, J. C. Wu, and S. Yamanaka, "Induced pluripotent stem cell technology: a decade of progress," *Nat Rev Drug Discov,* vol. 16, pp. 115-130, Feb 2017.
[58] A. Trounson and N. D. DeWitt, "Pluripotent stem cells progressing to the clinic," *Nat Rev Mol Cell Biol,* vol. 17, pp. 194-200, Mar 2016.
[59] M. Bellin, M. C. Marchetto, F. H. Gage, and C. L. Mummery, "Induced pluripotent stem cells: the new patient?," *Nat Rev Mol Cell Biol,* vol. 13, pp. 713-26, Nov 2012.
[60] J. H. van Weerd, K. Koshiba-Takeuchi, C. Kwon, and J. K. Takeuchi, "Epigenetic factors and cardiac development," *Cardiovasc Res,* vol. 91, pp. 203-11, Jul 15 2011.
[61] P. W. Burridge, A. Sharma, and J. C. Wu, "Genetic and Epigenetic Regulation of Human Cardiac Reprogramming and Differentiation in Regenerative Medicine," *Annu Rev Genet,* vol. 49, pp. 461-84, 2015.
[62] P. A. Iaizzo, *Handbook of cardiac anatomy, physiology, and devices*. Totowa, N.J.: Humana Press, 2005.
[63] A. Krishnan, R. Samtani, P. Dhanantwari, E. Lee, S. Yamada, K. Shiota*, et al.*, "A detailed comparison of mouse and human cardiac development," *Pediatr Res,* vol. 76, pp. 500-7, Dec 2014.
[64] K. K. Niakan and K. Eggan, "Analysis of human embryos from zygote to blastocyst reveals distinct gene expression patterns relative to the mouse," *Dev Biol,* vol. 375, pp. 54-64, Mar 01 2013.
[65] J. Nichols and A. Smith, "Pluripotency in the embryo and in culture," *Cold Spring Harb Perspect Biol,* vol. 4, p. a008128, Aug 01 2012.
[66] J. Rossant, "Human embryology: Implantation barrier overcome," *Nature,* vol. 533, pp. 182-3, May 12 2016.

[67] I. Bulatovic, A. Mansson-Broberg, C. Sylven, and K. H. Grinnemo, "Human fetal cardiac progenitors: The role of stem cells and progenitors in the fetal and adult heart," *Best Pract Res Clin Obstet Gynaecol,* vol. 31, pp. 58-68, Feb 2016.
[68] C. L. Mummery, J. Zhang, E. S. Ng, D. A. Elliott, A. G. Elefanty, and T. J. Kamp, "Differentiation of human embryonic stem cells and induced pluripotent stem cells to cardiomyocytes: a methods overview," *Circ Res,* vol. 111, pp. 344-58, Jul 20 2012.
[69] D. Srivastava, "Making or breaking the heart: from lineage determination to morphogenesis," *Cell,* vol. 126, pp. 1037-48, Sep 22 2006.
[70] A. C. Sturzu and S. M. Wu, "Developmental and regenerative biology of multipotent cardiovascular progenitor cells," *Circ Res,* vol. 108, pp. 353-64, Feb 04 2011.
[71] E. J. Benjamin, M. J. Blaha, S. E. Chiuve, M. Cushman, S. R. Das, R. Deo*, et al.*, "Heart Disease and Stroke Statistics-2017 Update: A Report From the American Heart Association," *Circulation,* vol. 135, pp. e146-e603, Mar 07 2017.
[72] N. Cao, H. Liang, J. Huang, J. Wang, Y. Chen, Z. Chen*, et al.*, "Highly efficient induction and long-term maintenance of multipotent cardiovascular progenitors from human pluripotent stem cells under defined conditions," *Cell Res,* vol. 23, pp. 1119-32, Sep 2013.
[73] P. W. Burridge, G. Keller, J. D. Gold, and J. C. Wu, "Production of de novo cardiomyocytes: human pluripotent stem cell differentiation and direct reprogramming," *Cell Stem Cell,* vol. 10, pp. 16-28, Jan 06 2012.
[74] J. J. McMurray, S. Adamopoulos, S. D. Anker, A. Auricchio, M. Bohm, K. Dickstein*, et al.*, "ESC Guidelines for the diagnosis and treatment of acute and chronic heart failure 2012: The Task Force for the Diagnosis and Treatment of Acute and Chronic Heart Failure 2012 of the European Society of Cardiology. Developed in collaboration with the Heart Failure Association (HFA) of the ESC," *Eur Heart J,* vol. 33, pp. 1787-847, Jul 2012.
[75] P. W. Serruys, P. de Jaegere, F. Kiemeneij, C. Macaya, W. Rutsch, G. Heyndrickx*, et al.*, "A comparison of balloon-expandable-stent implantation with balloon angioplasty in patients with coronary artery disease. Benestent Study Group," *N Engl J Med,* vol. 331, pp. 489-95, Aug 25 1994.
[76] D. Rosenstrauch, G. Poglajen, N. Zidar, and I. D. Gregoric, "Stem celltherapy for ischemic heart failure," *Tex Heart Inst J,* vol. 32, pp. 339-47, 2005.
[77] I. Batalov and A. W. Feinberg, "Differentiation of Cardiomyocytes from Human Pluripotent Stem Cells Using Monolayer Culture," *Biomark Insights,* vol. 10, pp. 71-6, 2015.
[78] A. J. Moss, W. Zareba, W. J. Hall, H. Klein, D. J. Wilber, D. S. Cannom*, et al.*, "Prophylactic implantation of a defibrillator in patients with myocardial infarction and reduced ejection fraction," *N Engl J Med,* vol. 346, pp. 877-83, Mar 21 2002.
[79] A. Boyle, "Current status of cardiac transplantation and mechanical circulatory support," *Curr Heart Fail Rep,* vol. 6, pp. 28-33, Mar 2009.
[80] A. Beniaminovitz, S. Itescu, K. Lietz, M. Donovan, E. M. Burke, B. D. Groff*, et al.*, "Prevention of rejection in cardiac transplantation by blockade of the interleukin-2 receptor with a monoclonal antibody," *N Engl J Med,* vol. 342, pp. 613-9, Mar 02 2000.
[81] M. J. Birket and C. L. Mummery, "Pluripotent stem cell derived cardiovascular progenitors--a developmental perspective," *Dev Biol,* vol. 400, pp. 169-79, Apr 15 2015.
[82] C. Bearzi, M. Rota, T. Hosoda, J. Tillmanns, A. Nascimbene, A. De Angelis*, et al.*, "Human cardiac stem cells," *Proc Natl Acad Sci U S A,* vol. 104, pp. 14068-73, Aug 28 2007.
[83] L. Yang, M. H. Soonpaa, E. D. Adler, T. K. Roepke, S. J. Kattman, M. Kennedy*, et al.*, "Human cardiovascular progenitor cells develop from a KDR+ embryonic-stem-cell-derived population," *Nature,* vol. 453, pp. 524-8, May 22 2008.
[84] S. M. Wu, K. R. Chien, and C. Mummery, "Origins and fates of cardiovascular progenitor cells," *Cell,* vol. 132, pp. 537-43, Feb 22 2008.
[85] F. Lescroart, S. Chabab, X. Lin, S. Rulands, C. Paulissen, A. Rodolosse*, et al.*, "Early lineage restriction in temporally distinct populations of Mesp1 progenitors during mammalian heart development," *Nat Cell Biol,* vol. 16, pp. 829-40, Sep 2014.
[86] L. Bu, X. Jiang, S. Martin-Puig, L. Caron, S. Zhu, Y. Shao*, et al.*, "Human ISL1 heart progenitors generate diverse multipotent cardiovascular cell lineages," *Nature,* vol. 460, pp. 113-7, Jul 02 2009.
[87] S. Sharma, P. G. Jackson, and J. Makan, "Cardiac troponins," *J Clin Pathol,* vol. 57, pp. 1025-6, Oct 2004.
[88] I. Kehat, D. Kenyagin-Karsenti, M. Snir, H. Segev, M. Amit, A. Gepstein*, et al.*, "Human embryonic stem cells can differentiate into myocytes with structural and functional properties of cardiomyocytes," *J Clin Invest,* vol. 108, pp. 407-14, Aug 2001.

[89] S. M. Frisch and R. A. Screaton, "Anoikis mechanisms," *Curr Opin Cell Biol,* vol. 13, pp. 555-62, Oct 2001.
[90] E. Bettiol, L. Sartiani, L. Chicha, K. H. Krause, E. Cerbai, and M. E. Jaconi, "Fetal bovine serum enables cardiac differentiation of human embryonic stem cells," *Differentiation,* vol. 75, pp. 669-81, Oct 2007.
[91] M. Kennedy, S. L. D'Souza, M. Lynch-Kattman, S. Schwantz, and G. Keller, "Development of the hemangioblast defines the onset of hematopoiesis in human ES cell differentiation cultures," *Blood,* vol. 109, pp. 2679-87, Apr 01 2007.
[92] M. A. Laflamme, K. Y. Chen, A. V. Naumova, V. Muskheli, J. A. Fugate, S. K. Dupras*, et al.*, "Cardiomyocytes derived from human embryonic stem cells in pro-survival factors enhance function of infarcted rat hearts," *Nat Biotechnol,* vol. 25, pp. 1015-24, Sep 2007.
[93] J. Zhang, M. Klos, G. F. Wilson, A. M. Herman, X. Lian, K. K. Raval*, et al.*, "Extracellular matrix promotes highly efficient cardiac differentiation of human pluripotent stem cells: the matrix sandwich method," *Circ Res,* vol. 111, pp. 1125-36, Oct 12 2012.
[94] X. Lian, C. Hsiao, G. Wilson, K. Zhu, L. B. Hazeltine, S. M. Azarin*, et al.*, "Robust cardiomyocyte differentiation from human pluripotent stem cells via temporal modulation of canonical Wnt signaling," *Proc Natl Acad Sci U S A,* vol. 109, pp. E1848-57, Jul 03 2012.
[95] X. Lian, J. Zhang, S. M. Azarin, K. Zhu, L. B. Hazeltine, X. Bao*, et al.*, "Directed cardiomyocyte differentiation from human pluripotent stem cells by modulating Wnt/beta-catenin signaling under fully defined conditions," *Nat Protoc,* vol. 8, pp. 162-75, Jan 2013.
[96] P. W. Burridge, E. Matsa, P. Shukla, Z. C. Lin, J. M. Churko, A. D. Ebert*, et al.*, "Chemically defined generation of human cardiomyocytes," *Nat Methods,* vol. 11, pp. 855-60, Aug 2014.
[97] B. T. MacDonald, K. Tamai, and X. He, "Wnt/beta-catenin signaling: components, mechanisms, and diseases," *Dev Cell,* vol. 17, pp. 9-26, Jul 2009.
[98] S. Angers and R. T. Moon, "Proximal events in Wnt signal transduction," *Nat Rev Mol Cell Biol,* vol. 10, pp. 468-77, Jul 2009.
[99] X. Lian, X. Bao, M. Zilberter, M. Westman, A. Fisahn, C. Hsiao*, et al.*, "Chemically defined, albumin-free human cardiomyocyte generation," *Nat Methods,* vol. 12, pp. 595-6, Jul 2015.
[100] P. W. Burridge, S. Thompson, M. A. Millrod, S. Weinberg, X. Yuan, A. Peters*, et al.*, "A universal system for highly efficient cardiac differentiation of human induced pluripotent stem cells that eliminates interline variability," *PLoS One,* vol. 6, p. e18293, Apr 08 2011.
[101] K. Kim, A. Doi, B. Wen, K. Ng, R. Zhao, P. Cahan*, et al.*, "Epigenetic memory in induced pluripotent stem cells," *Nature,* vol. 467, pp. 285-90, Sep 16 2010.
[102] R. J. Skelton, M. Costa, D. J. Anderson, F. Bruveris, B. W. Finnin, K. Koutsis*, et al.*, "SIRPA, VCAM1 and CD34 identify discrete lineages during early human cardiovascular development," *Stem Cell Res,* vol. 13, pp. 172-9, Jul 2014.
[103] P. Menasche, V. Vanneaux, J. R. Fabreguettes, A. Bel, L. Tosca, S. Garcia*, et al.*, "Towards a clinical use of human embryonic stem cell-derived cardiac progenitors: a translational experience," *Eur Heart J,* vol. 36, pp. 743-50, Mar 21 2015.
[104] M. G. Klug, M. H. Soonpaa, G. Y. Koh, and L. J. Field, "Genetically selected cardiomyocytes from differentiating embronic stem cells form stable intracardiac grafts," *J Clin Invest,* vol. 98, pp. 216-24, Jul 01 1996.
[105] N. C. Dubois, A. M. Craft, P. Sharma, D. A. Elliott, E. G. Stanley, A. G. Elefanty*, et al.*, "SIRPA is a specific cell-surface marker for isolating cardiomyocytes derived from human pluripotent stem cells," *Nat Biotechnol,* vol. 29, pp. 1011-8, Oct 23 2011.
[106] F. Hattori, H. Chen, H. Yamashita, S. Tohyama, Y. S. Satoh, S. Yuasa*, et al.*, "Nongenetic method for purifying stem cell-derived cardiomyocytes," *Nat Methods,* vol. 7, pp. 61-6, Jan 2010.
[107] H. Uosaki, H. Fukushima, A. Takeuchi, S. Matsuoka, N. Nakatsuji, S. Yamanaka*, et al.*, "Efficient and scalable purification of cardiomyocytes from human embryonic and induced pluripotent stem cells by VCAM1 surface expression," *PLoS One,* vol. 6, p. e23657, 2011.
[108] D. C. Nguyen, T. A. Hookway, Q. Wu, R. Jha, M. K. Preininger, X. Chen*, et al.*, "Microscale generation of cardiospheres promotes robust enrichment of cardiomyocytes derived from human pluripotent stem cells," *Stem Cell Reports,* vol. 3, pp. 260-8, Aug 12 2014.
[109] S. Tohyama, F. Hattori, M. Sano, T. Hishiki, Y. Nagahata, T. Matsuura*, et al.*, "Distinct metabolic flow enables large-scale purification of mouse and human pluripotent stem cell-derived cardiomyocytes," *Cell Stem Cell,* vol. 12, pp. 127-37, Jan 03 2013.
[110] K. Miki, K. Endo, S. Takahashi, S. Funakoshi, I. Takei, S. Katayama*, et al.*, "Efficient Detection and Purification of Cell Populations Using Synthetic MicroRNA Switches," *Cell Stem Cell,* vol. 16, pp. 699-711, Jun 04 2015.

[111] X. Li, L. Yu, J. Li, I. Minami, M. Nakajima, Y. Noda*, et al.*, "On chip purification of hiPSC-derived cardiomyocytes using a fishnet-like microstructure," *Biofabrication,* vol. 8, p. 035017, Sep 08 2016.
[112] P. Menasche, V. Vanneaux, A. Hagege, A. Bel, B. Cholley, I. Cacciapuoti*, et al.*, "Human embryonic stem cell-derived cardiac progenitors for severe heart failure treatment: first clinical case report," *Eur Heart J,* vol. 36, pp. 2011-7, Aug 07 2015.
[113] S. Funakoshi, K. Miki, T. Takaki, C. Okubo, T. Hatani, K. Chonabayashi*, et al.*, "Enhanced engraftment, proliferation, and therapeutic potential in heart using optimized human iPSC-derived cardiomyocytes," *Sci Rep,* vol. 6, p. 19111, Jan 08 2016.
[114] J. S. Wendel, L. Ye, R. Tao, J. Zhang, J. Zhang, T. J. Kamp*, et al.*, "Functional Effects of a Tissue-Engineered Cardiac Patch From Human Induced Pluripotent Stem Cell-Derived Cardiomyocytes in a Rat Infarct Model," *Stem Cells Transl Med,* vol. 4, pp. 1324-32, Nov 2015.
[115] E. Gouadon, T. Moore-Morris, N. W. Smit, L. Chatenoud, R. Coronel, S. E. Harding*, et al.*, "Concise Review: Pluripotent Stem Cell-Derived Cardiac Cells, A Promising Cell Source for Therapy of Heart Failure: Where Do We Stand?," *Stem Cells,* vol. 34, pp. 34-43, Jan 2016.
[116] H. Masumoto, T. Ikuno, M. Takeda, H. Fukushima, A. Marui, S. Katayama*, et al.*, "Human iPS cell-engineered cardiac tissue sheets with cardiomyocytes and vascular cells for cardiac regeneration," *Sci Rep,* vol. 4, p. 6716, Oct 22 2014.
[117] J. J. Chong and C. E. Murry, "Cardiac regeneration using pluripotent stem cells--progression to large animal models," *Stem Cell Res,* vol. 13, pp. 654-65, Nov 2014.
[118] L. Ye, Y. H. Chang, Q. Xiong, P. Zhang, L. Zhang, P. Somasundaram*, et al.*, "Cardiac repair in a porcine model of acute myocardial infarction with human induced pluripotent stem cell-derived cardiovascular cells," *Cell Stem Cell,* vol. 15, pp. 750-61, Dec 04 2014.
[119] V. C. Chen, J. Ye, P. Shukla, G. Hua, D. Chen, Z. Lin*, et al.*, "Development of a scalable suspension culture for cardiac differentiation from human pluripotent stem cells," *Stem Cell Res,* vol. 15, pp. 365-75, Sep 2015.
[120] J. Schindelin, I. Arganda-Carreras, E. Frise, V. Kaynig, M. Longair, T. Pietzsch*, et al.*, "Fiji: an open-source platform for biological-image analysis," *Nat Methods,* vol. 9, pp. 676-82, Jun 28 2012.
[121] C. C. Miranda, T. G. Fernandes, M. M. Diogo, and J. M. Cabral, "Scaling up a chemically-defined aggregate-based suspension culture system for neural commitment of human pluripotent stem cells," *Biotechnol J,* vol. 11, pp. 1628-1638, Dec 2016.
[122] J. Wu, Y. Fan, and E. S. Tzanakakis, "Increased culture density is linked to decelerated proliferation, prolonged G1 phase, and enhanced propensity for differentiation of self-renewing human pluripotent stem cells," *Stem Cells Dev,* vol. 24, pp. 892-903, Apr 01 2015.
[123] G. Chen, D. R. Gulbranson, Z. Hou, J. M. Bolin, V. Ruotti, M. D. Probasco*, et al.*, "Chemically defined conditions for human iPSC derivation and culture," *Nat Methods,* vol. 8, pp. 424-9, May 2011.
[124] S. M. Dang, M. Kyba, R. Perlingeiro, G. Q. Daley, and P. W. Zandstra, "Efficiency of embryoid body formation and hematopoietic development from embryonic stem cells in different culture systems," *Biotechnol Bioeng,* vol. 78, pp. 442-53, May 20 2002.
[125] R. L. Carpenedo, C. Y. Sargent, and T. C. McDevitt, "Rotary suspension culture enhances the efficiency, yield, and homogeneity of embryoid body differentiation," *Stem Cells,* vol. 25, pp. 2224-34, Sep 2007.
[126] V. C. Chen, S. M. Couture, J. Ye, Z. Lin, G. Hua, H. I. Huang*, et al.*, "Scalable GMP compliant suspension culture system for human ES cells," *Stem Cell Res,* vol. 8, pp. 388-402, May 2012.
[127] B. C. Heng, J. Li, A. K. Chen, S. Reuveny, S. M. Cool, W. R. Birch*, et al.*, "Translating human embryonic stem cells from 2-dimensional to 3-dimensional cultures in a defined medium on laminin- and vitronectin-coated surfaces," *Stem Cells Dev,* vol. 21, pp. 1701-15, Jul 01 2012.
[128] S. J. Kattman, A. D. Witty, M. Gagliardi, N. C. Dubois, M. Niapour, A. Hotta*, et al.*, "Stage-specific optimization of activin/nodal and BMP signaling promotes cardiac differentiation of mouse and human pluripotent stem cell lines," *Cell Stem Cell,* vol. 8, pp. 228-40, Feb 04 2011.
[129] N. Hemmi, S. Tohyama, K. Nakajima, H. Kanazawa, T. Suzuki, F. Hattori*, et al.*, "A massive suspension culture system with metabolic purification for human pluripotent stem cell-derived cardiomyocytes," *Stem Cells Transl Med,* vol. 3, pp. 1473-83, Dec 2014.
[130] H. Kempf, R. Olmer, A. Haase, A. Franke, E. Bolesani, K. Schwanke*, et al.*, "Bulk cell density and Wnt/TGFbeta signalling regulate mesendodermal patterning of human pluripotent stem cells," *Nat Commun,* vol. 7, p. 13602, Dec 09 2016.

[131] A. Kadari, S. Mekala, N. Wagner, D. Malan, J. Koth, K. Doll*, et al.*, "Robust Generation of Cardiomyocytes from Human iPS Cells Requires Precise Modulation of BMP and WNT Signaling," *Stem Cell Rev,* vol. 11, pp. 560-9, Aug 2015.

[132] H. Fonoudi, H. Ansari, S. Abbasalizadeh, M. R. Larijani, S. Kiani, S. Hashemizadeh*, et al.*, "A Universal and Robust Integrated Platform for the Scalable Production of Human Cardiomyocytes From Pluripotent Stem Cells," *Stem Cells Transl Med,* vol. 4, pp. 1482-94, Dec 2015.

[133] F. Etoc, J. Metzger, A. Ruzo, C. Kirst, A. Yoney, M. Z. Ozair*, et al.*, "A Balance between Secreted Inhibitors and Edge Sensing Controls Gastruloid Self-Organization," *Dev Cell,* vol. 39, pp. 302-315, Nov 07 2016.

8 Supplementary Information

Table 8.1 Day by day evolution of the aggregates diameter. The aggregates in both cell lines were formed after single cell dissociation using EDTA. Afterwards, aggregates were formed by random aggregation process and were expanded for up 7 days, in the case of Gibco aggregates and for up 3 days, in the case of TCLab aggregates. It is represented the mean value for each seeding density for all the days of expansion ± SEM value.

	Seeding density (cells/mL)	$1.0\times10^{+05}$	$1.5\times10^{+05}$	$2.5\times10^{+05}$	$5\times10^{+05}$	$7.5\times10^{+05}$	$1\times10^{+06}$	$1.5\times10^{+06}$	$2.0\times10^{+06}$
Gibco	Day 1	67.7±1.8	75.3±1.5	85.0±1.5	99.4±1.1	83.3±6.5	94.0±1.1	99.0±1.7	109.5±1.9
	Day 2	102.8±4.2	129.1±3.1	124.0±2.2	120.9±2.4	72.6±2.3	131.0±2.1	131.5±2.0	141.4±2.9
	Day 3	144.5±6.6	140.8±4.5	144.2±2.9	153.2±2.4	128.2±1.9	147.7±2.3	143.1±2.4	143.0±3.3
	Day 4	164.2±7.7	142.4±5.4	157.8±2.5	164.1±3.3	150.9±2.5	171.1±3.5	150.6±1.9	144.1±2.8
	Day 5	-	274.4±8.3	213.0±4.9	179.6±3.8	180.3±2.7	196.0±4.2	168.8±2.0	-
	Day 6	-	266.1±13.1	305.4±16.2	209.7±5.8	194.3±3.4	215.3±5.1	175.0±1.8	-
	Day 7	-	-	-	201.7±3.7	220.5±3.6	195.7±2.3	181.6±2.6	-
TCLab	Day 1	66.3±0.9	82.7±2.4	79.9±0.8	88.9±0.9	-	117.3±1.2	126.9±1.4	124.1±2.0
	Day 2	113.8±1.7	127.9±5.5	134.5±1.8	136.1±1.8	-	161.3±3.0	181.8±2.8	182.9±6.0
	Day 3	184.6±8.4	168.5±5.2	183.9±53	195.6±5.6	-	242.1±14.0	194.0±12.5	181.4±7.0

Table 8.2 Approximate percentage of confluency in monolater after beginning the cardiac induction. Gibco: n=1,2 were expanded 3 days. n=3, 50.000 were expanded 1 day, 10.000 and 25.000 for 4 days. **TCLab:** n=1 were expanded for 3 days. n=2 for 1 day and n=3 for 2 days.

Seeding density (cells/cm²)	Gibco			TCLab		
	n=1	n=2	n=3	n=1	n=2	n=3
10.000	10-20	30-40	10-20	10-20	0-10	0-10
25.000	30-40	50-60	60-70	50-60	20-30	20-30
50.000	90-100	90-100	80-90	90-100	50-60	70-80
100.000	90-100	90-100	-	90-100	90-100	90-100

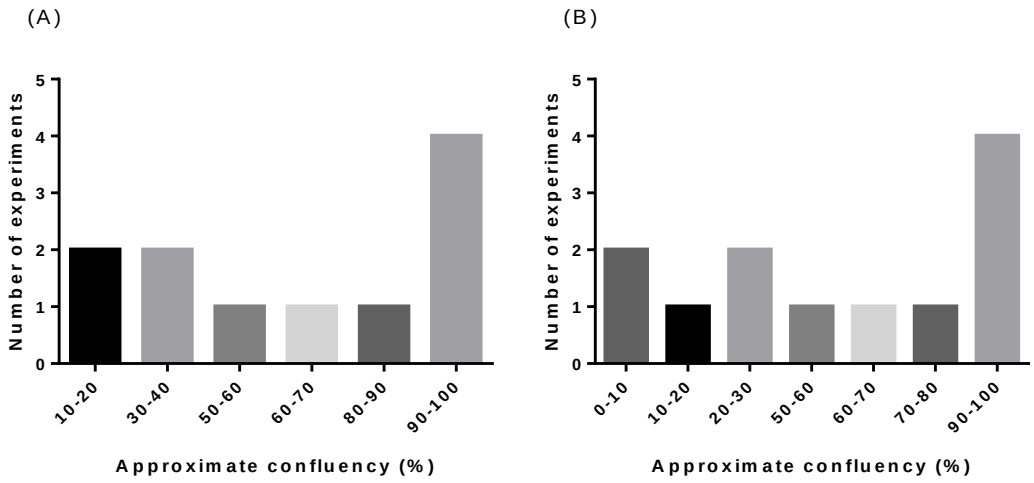

Figure 8.1 Number of times that each approximate confluency was obtained for Gibco cell line (A) and TCLab cell line (B) expanded in adherent culture. In the horizontal axis are represented the approximated confluences and in the vertical axis the number of times that a certain confluence was obtained.

Table 8.3 – Average aggregates diameter before the cardiac induction. Gibco: n=1 were expanded 3 days, n=2 were expanded 4 days and n=3 were expanded 7 days. TCLab: n=1 for 3 days, n=2,3 for 2 days. It is important to note that the diameters are presented within a 10 µm range instead of the real average value that was obtained, since very little variations in the average diameter will not be relevant.

Seeding density (cells/mL)	Gibco							TCLab		
	n=1	n=2	n=3	n=4	n=5	n=6	n=7	n=1	n=2	n=3
$1\times10^{+05}$	175-185	105-115	-	115-125	105-115	-	-	155-165	95-105	105-115
$1.5\times10^{+05}$	175-185	95-105	-	115-125	65-75	-	-	155-165	-	-
$2.5\times10^{+05}$	185-195	125-135	185-195	125-135	115-125	-	-	165-175	115-125	165-175
$5\times10^{+05}$	195-205	135-145	195-205	165-175	155-165	195-205	195-205	-	105-115	175-185
$7.5\times10^{+05}$	-	-	215-225	-	-	-	-	-	-	-
$1\times10^{+06}$	165-175	145-155	195-205	195-205	185-195	-	-	-	135-145	205-215
$1.5\times10^{+06}$	185-195	145-155	175-185	-	-	-	-	-	175-185	205-215
$2\times10^{+06}$	175-185	145-155	-	-	-	-	-	-	-	235-245

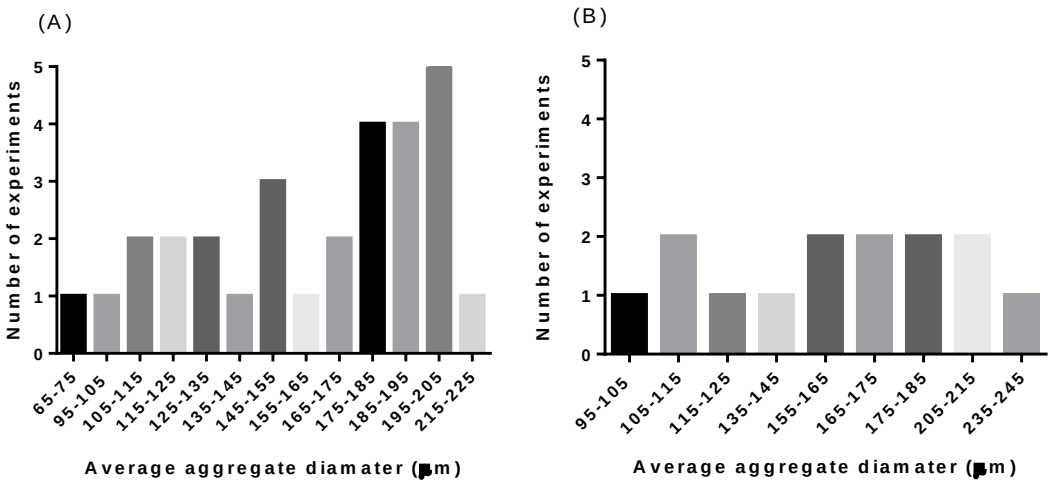

Figure 8.2 Number of times that each average aggregate diameter was obtained for Gibco aggregates (A) and TCLab aggregates (B). In the horizontal axis are represented the average aggregates diameters (µm) and in the vertical axis the number of times that a certain confluence was obtained.

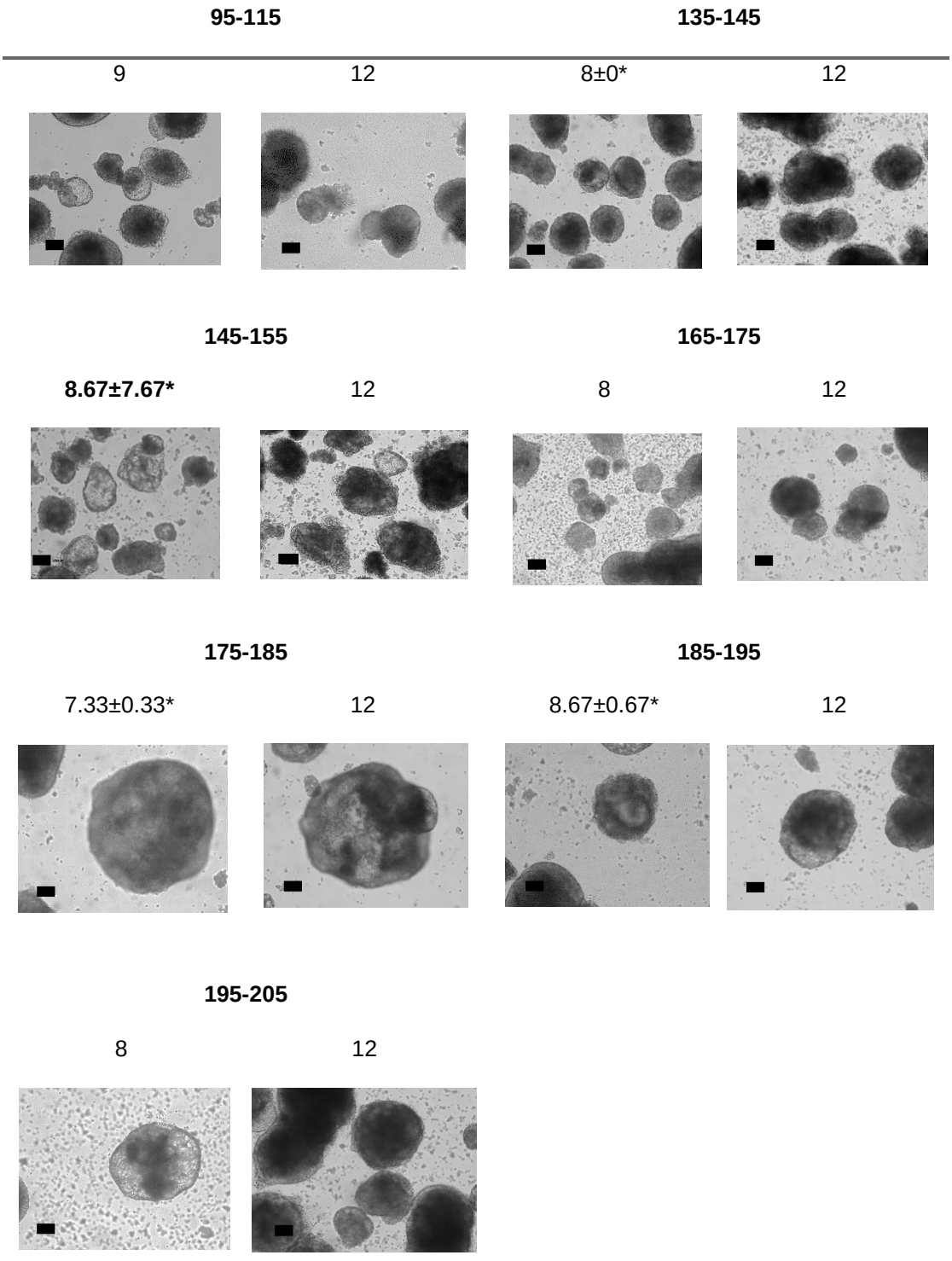

Figure 8.3 Morphology of the Gibco aggregates in the first day of the spontaneous beating and in the last day of differentiation. Above each image is mentioned the average aggregate diameter before the cardiac induction and also, the day of differentiation in each the aggregates start to demonstrate the spontaneous beating. Values with (*) represent a n>1 and it is presented the mean value ± SEM. Scale bars: 100 μm

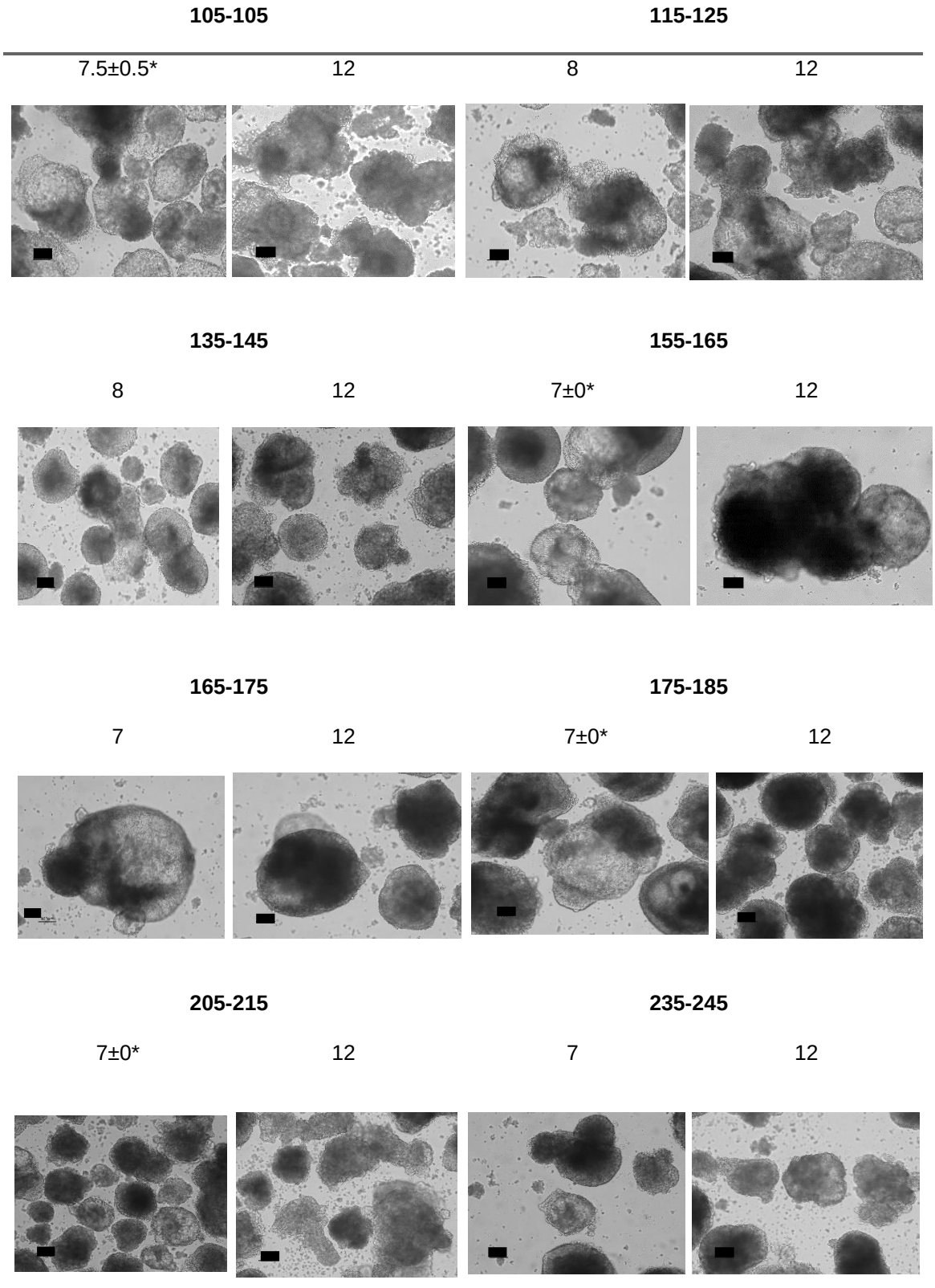

Figure 8.4 Morphology of the TCLab aggregates in the first day of the spontaneous beating and in the last day of differentiation. Above each image is mentioned the average aggregate diameter before the cardiac induction and also, the day of differentiation in each the aggregates start to demonstrate the spontaneous beating. Values with (*) represent a n>1 and it is presented the mean value ± SEM. Scale bars: 100 μm

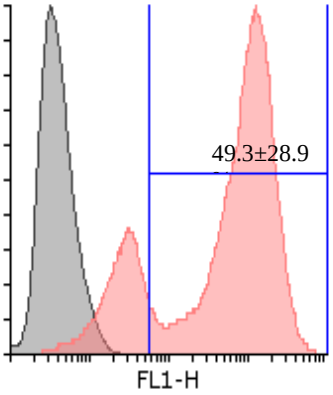

Figure 8.5 Percentage of cTnT positive cells assessed by flow cytometry.